UNIVERSITY OF TROMSØ UIT
Faculty of Health Sciences
Department of Pharmacy

School of Biomedical Sciences
The University of Queensland

DEVELOPMENT OF BIOACTIVE PEPTIDES FROM THE PARASITIC HOOKWORM AS POTENTIAL TREATMENTS FOR AUTOIMMUNE DISEASES

Markus Baumann

Far-3901: Master thesis for the degree Master of Pharmacy

May 2012

Abstract

Hookworms are parasitic nematodes that reside in the intestines of their host, where they feed on host blood. The large number of infected individuals and the long survival time inside the host makes it interesting to study the immunomodulatory activities of the hookworms. The excretory/secretory (ES) products are suspected to be responsible for these effects. One aim of this project was to fractionate the low molecular weight part (< 10 kDa) of ES products from the dog hookworm *Ancylostoma caninum* and test their activity in a mouse colitis model that resembles human Crohn's disease. The results were inconclusive, but trends could be seen and it seems that two fractions might show activity in the future if the tests are scaled up. The second aim was to use Fmoc-SPPS to synthesise two disulfide-rich peptides that were identified in the transcriptome of hookworms. These peptides possess the cysteine framework of the sea anemone toxin ShK, which is able to block voltage-gated potassium channels. One peptide, Name2, was synthesised successfully and as predicted folded into a ShK-like domain as confirmed by NMR spectroscopy. The three dimensional structure of the peptide was determined and it was revealed to contain two helical segments that were braced by the three disulfide bonds. Difficulties were encountered in the synthesis of Acan1 and the correct peptide was not obtained.

Acknowledgements

This project was conducted at the School of Biomedical Sciences, The University of Queensland, Australia, in the period from October 2011 to May 2012.

First of all, I would like to thank Dr Richard Clark for being my supervisor and for letting me work on this exciting project. Thanks are also due to Dr Johan Rosengren for his help on the NMR spectroscopy part of this project.

Special thanks go to Dr Linda Haugaard-Kedström and Jan-Willem van Dijk for their help with the lab equipment, innumerable advices and for always taking time for discussions. I also wish to thank Maryon Jones, Lee Han Siean, Charlie Tran and Randy Aliyanto for making working in this lab an unforgettable experience.

My sincere thanks go to Dr Severine Navarro at the Queensland Tropical Health Alliance for performing the animal experiments and for showing me how to dissect mice.

I also wish to thank Dr Jon Våbenø for making it possible to write this thesis in Australia.

Thanks go to my family for always supporting me and I owe a great dept of gratitude to my parents for their much appreciated advices and for always believing in me.

Finally, I wish to thank my fellow students in Tromsø for five amazing years.

Table of contents

1. Introduction 1
1.1 Peptides and their potential use as drugs 1
1.2 Solid-Phase Peptide Synthesis (SPPS) 2
1.3 Autoimmune diseases 3
1.4 Hookworms 5
1.4.1 Hookworm infection 5
1.4.2 Immunologic aspects to hookworm infections 6
1.4.3 Excretory/secretory products (ES) 7
1.5 Prelimenary data 7
1.6 ShK-like peptide sequences 8
1.7 Experimental TNBS colitis in mice 8
1.7.1 Immunology of TNBS coltitis 8
1.7.2 The Relation between the TNBS model and Crohn's disease 9
1.8 Aims 10

2. Results 11
2.1 Fractionation of low molecular weight components of *A. caninum* ES products (LMW AcES) 11
2.2 Bioactivity testing of fractionated LMW AcES in mice with experimental colitis 12
2.2.1 First batch of LMW AcES fractions 13
2.2.2 Second batch of LMW AcES fractions 15
2.3 LC/MS analysis of fractions C and E 17
2.3.1 Fraction C 17
2.3.2 LC/MS of fraction E 17
2.4 1D ^{1}H NMR spectroscopy of fraction C 19
2.5 Peptide synthesis 20
2.5.1 Synthesis of Name2 20
2.5.1.1 Synthesis of Name2 N-terminus 21
2.5.1.2 Synthesis of Name2 C-terminus 23
2.5.1.3 Native chemical ligation of Name2 N-terminus and C-terminus 25
2.5.1.4 Folding of Name2 27
2.5.1.5 NMR of Name2 29
2.5.2 Synthesis of Acan1 34
2.5.2.1 Synthesis of the Acan1 N-terminus as a peptide hydrazide 36
2.5.2.2 Synthesis of Acan1 C-terminus 38
2.5.2.3 Native chemical ligation of Acan1 using a peptide hydrazide 39
2.5.2.4 Synthesis of Acan1 N-terminus with a Dbz-group 40
2.5.2.5 Native chemical ligation of of Acan1* 43
2.5.2.6 Folding of Acan1* 46
2.5.2.7 NMR of Acan1* 48
2.5.2.8 Ligation of Acan1 49

3. Discussion 49
3.1 Bioactivity testing of fractionated LMW AcES 49
3.2 Synthesis of Name2 51
3.3 Synthesis of Acan1 52

4. Conclusion 54

5. Materials and Methods 55
5.1 Fractionation of low molecular weight components of *A. caninum* ES products (LMW AcES) 55
5.1.1 Origin of LMW AcES material analysed in this project 55
5.1.2 Fractionation of LMW AcES 55
5.2 Bioactivity testing of fractionated LMW AcES in mice with experimental colitis 56

5.2.1 Endotoxin removal with Endo Trap® ... 56
5.2.2 Peptide quantification with Micro BCA™ Protein Assay Kit ... 57
5.2.3 Mouse experiment ... 57
5.2.4 Experimental design ... 58
5.2.5 Material used for mice anaesthesia ... 59
5.2.6 Sample injection ... 60
5.2.7 Colitis induction ... 60
5.2.8 Sacrifice and dissection ... 60
5.2.9 Macroscopic Evaluation ... 60
5.3 LC/MS of fractions C and E ... 61
5.4 NMR spectroscopy of fraction C ... 61
5.5 Peptide synthesis ... 62
5.5.1 Deprotection for Fmoc chemistry ... 62
5.5.2 Peptide bond formation from HBTU- and HCTU-mediated reactions ... 63
5.5.3 The ninhydrin test ... 65
5.5.4 Native chemical ligation via the formation of a C-terminal acylurea moiety ... 67
5.5.5 Native chemical ligation via the formation of a peptide hydrazide ... 69
5.5.6 Synthesis of Name 2 ... 70
5.5.6.1 Synthesis of Name2 N-terminus ... 70
5.5.6.2 Synthesis of Name2 C-terminus ... 71
5.5.6.3 Native chemical ligation of Name2 ... 72
5.5.6.4 Folding of Name2 ... 73
5.5.6.5 NMR spectroscopy of Name2 ... 73
5.5.7 Synthesis of Acan1 ... 74
5.5.7.1 Synthesis of Acan1 N-terminus as a peptide hydrazide ... 74
5.5.7.2 Synthesis of Acan 1 C-terminus ... 75
5.5.7.3 Ligation of Acan 1 using a peptide hydrazide ... 75
5.5.7.4 Synthesis of Acan1 N-terminus with a Dbz group ... 76
5.5.7.5 Ligation of Acan1* ... 77
5.5.7.6 Folding of Acan1* ... 77
5.5.7.7 NMR spectroscopy of Acan1* ... 78
5.5.7.8 Ligation of Acan 1 ... 78
5.5.8 Equipment ... 78
6. References ... 80
7. Appendix ... 84
7.1 Analytical HPLC of fractions ... 84
7.2 LC/MS of fraction E ... 89
7.3 ESI-MS ... 89

List of Abbreviations

BCA	Bicinchonic acid
Boc	*tert*-Butoxycarbonyl
Dbz	Diaminobenzoic acid
DCM	Dichloromethane
DIPEA	*N*,*N*-Diisopropylethylamine
DMF	*N*,*N*-Dimethylformamide
DODT	3,6-Dioxa-1,8-octanedithiol
EtOH	Ethanol
ES	Excretory/secretory products
ESI-MS	Electrospray ionization mass spectrometry
Fmoc	9-Fluorenylmethyloxycarbonyl
Fmoc-Dbz	3-Fmoc-4-diaminobenzoic acid
Gn · HCl	Guanidine hydrochloride
GSH	Reduced glutathione
GSSG	Oxidised glutathion
HBTU	*O*-(6-Benzotriazol-1-yl)-*N*,*N*,*N'*,*N'*-tetramethyluronium hexafluorophosphate
HCl (*aq*)	Hydrochloric acid
HCTU	*O*-(6-Chlorobenzotriazol-1-yl)-*N*,*N*,*N'*,*N'*-tetramethyluronium hexafluorophosphate
HSQC	Heteronuclear single quantum coherence spectroscopy
IFN-γ	Interferon γ
IL	Interleukin
MBHA	4-Methylbenzhydrylamine
MeOH	Methanol
MPAA	4-Mercaptophenylacetic acid
Na_2HPO_4	Disodium hydrogen phosphate
NaOH	Sodium hydroxide
$NaNO_2$	Sodium nitrite
Nbz	*N*-acyl-benzimidazolinone
NCL	Native chemical ligation
NH_4HCO_3	Ammonium bicarbonate
NMR	Nuclear magnetic resonance
NOE	Nuclear Overhauser effect
NOESY	Nuclear Overhauser effect spectroscopy
PBS	Phosphate buffered saline
RP-HPLC	Reverse-phase high-pressure liquid chromatography
SPPS	Solid phase peptide synthesis
TCEP · HCl	Tris(2-carboxyethyl)phosphine hydrochloride
TFA	Trifluoroacetic acid
TIPS	Triisopropylsilane
TNBS	2,4,6-Trinitrobenzenesulfonic acid
TNF-α	Tumour necrosis factor α
TOCSY	Total correlation spectroscopy
Xan	Xanthenyl

1. Introduction

1.1 Peptides and their potential use as drugs

Peptides are made of amino acids, covalently joined together by amide bonds [1]. The size of biologically occurring peptides shows a great variability, ranging from dipeptides to proteins with masses above 10,000 Da [1]. In general, all organisms use the same set of 20 proteinogenic amino acids encoded in the genetic code for their synthesis of peptides and proteins [1]. Exceptions are peptides where uncommon amino acids have been incorporated during the synthesis or certain residues that underwent postsynthetic modifications, like hydroxylation or carboxylation [1]. Peptides and proteins are involved in many different biological processes, such as the regulation of blood glucose after a meal by the hormone insulin, or the conversion of glucose to glucose 6-phosphate by the enzyme hexokinase in the first step of the metabolic pathways to utilize the carbohydrate as fuel. Peptides also transduce signals as neurotransmitters and receptors, are part of the immune defence (as antibodies) or do harm (toxins) [2]. This variety of biological functions makes peptides and proteins very attractive for scientists to test their effect in different diseases, and peptides are undergoing phase 1 trials for indications including cancer, metabolic diseases, inflammation and virology [3]. Compared to traditional small molecule drugs, peptides are said to be more selective with lower affinity for non-target structures, and less toxic [3, 4]. However, their susceptibility to degradation in the gastrointestinal tract and limited permeation of the intestinal epithelium present huge difficulties to the development of peptides as drugs, and they usually show low oral bioavailability and must be given parenterally [5]. Other disadvantages are revealed once the peptide has made it to the systemic circulation: a short half-life because of fast elimination via the kidneys and exposure to proteases; and potential immunogenicity [4]. Fortunately, much progress has been made in developing techniques that improve the stability of peptides, and renal excretion and degradation by enzymes can be reduced by pegylation [3]. In this process, polymers of ethylene glycol are attached to the peptide and several pegylated peptide drugs are marketed [3]. Another way to enhance the stability is to make a peptidomimetic, where the parts of the peptide susceptible to degradation are

replaced by other chemical groups [6]. Nowadays, desired peptides can be isolated from tissues, produced by biotechnological methods or by direct chemical synthesis [1].

1.2 Solid-Phase Peptide Synthesis (SPPS)

Using traditional methods, the direct chemical synthesis of short peptides took place in solution, which posed significant problems in terms of solubility and purification as the peptide chain increased in length [7, 8]. The purification involved the extraction of the desired reaction product and had to be conducted after each attachment of a new residue, a quite laborious procedure [7, 8]. In contrast, the technique of solid-phase peptide synthesis (SPPS), developed by Robert Bruce Merrifield, takes advantage of using a solid support for the peptide synthesis [7]. This solid support is made of polymer beads, also called resin, and the synthesis takes place directly on the resin because the first amino acid is covalently attached to it [7]. The subsequent residues are coupled to the chain individually by repeating the coupling reaction and deprotection reaction for each added residue until the peptide is complete (**figure 1**) [7]. The order of the amino acids is determined by the peptide sequence and one starts with the amino acid at the C-terminus of the peptide, which means that the carboxylic acid group of the first amino acid reacts with the resin and the, still protected, amino group will condense with the carboxylic acid group of the next amino acid to form a peptide bond. The amino group on the α-carbon, as well as the side chains with functional groups, need to be protected so that only the carboxylic acid group of the introduced amino acid is able to take part in the formation of a new peptide bond with the amino group of the residue attached to the resin [8]. Thereafter, the protecting group on the amino group of the residue just coupled to the peptide chain is removed, so that a new peptide bond can be made with the next residue introduced, but it is important not to deprotect the side chains during this process [8]. Elimination of unreacted reagents, liberated protecting groups and by-products is easy with SPPS, because these compounds are dissolved in the reaction solvent, and can be filtered readily without affecting the peptide, which remains attached to the solid support [8]. The final step of the synthesis is the removal of all the remaining protecting groups and the cleavage of the covalent bond between peptide and resin. Boc (*tert*-butoxycarbonyl) and Fmoc (9-fluorenylmethyloxycarbonyl) are the protecting groups mainly used for derivatization of the amino group and are characterized by the requirement of different reagents for deprotection: Boc chemistry

typically uses trifluoroacetic acid (TFA), whereas the base labile Fmoc groups are liberated by piperidine. For detaching the peptide from the resin hydrofluroric acid and TFA are used for Boc and Fmoc chemistry, respectively.

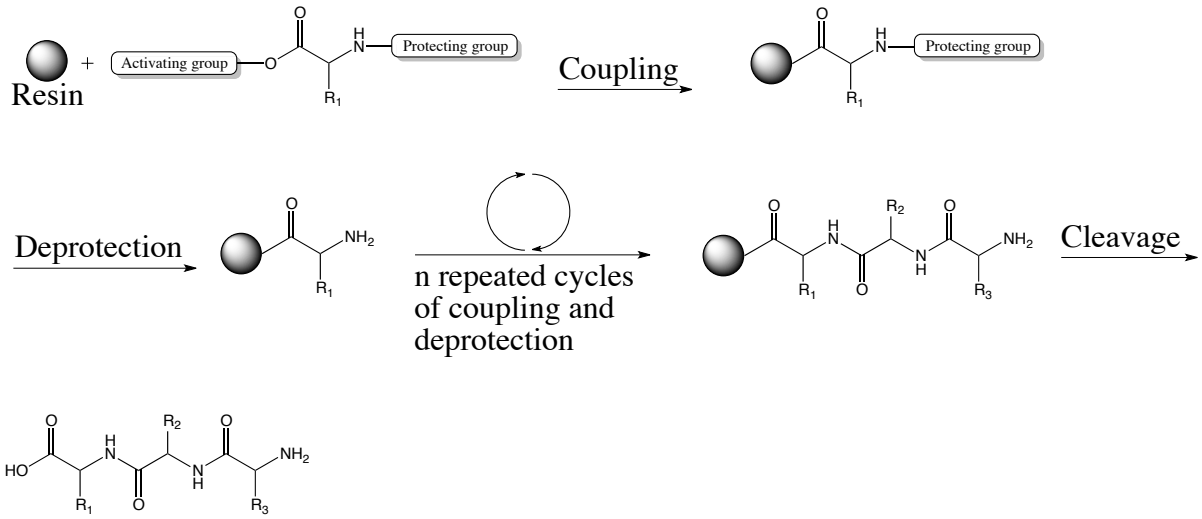

Figure 1: Principles of standard Fmoc-SPPS: The first amino acid is coupled to the resin and deprotected before the next amino acid is coupled. Repetition of this procedure elongates the peptide, which is cleaved from the resin when elongation is complete.

1.3 Autoimmune diseases

The human body fights infectious organisms by sending a great number of different cells and molecules into the battle, and responses can be described as innate, which means that every healthy person possesses them, or adaptive when the host defence adapts to the presence of certain microbes. The innate immune system includes cells that can ingest and kill microorganisms (macrophages and neutrophils), cells that can kill host cells infected by viruses (natural killer cells), protein mediators that regulate and coordinate immunologic activities (cytokines) and protein systems that, when activated, can lead to recognition and destruction of foreign organisms (complement system). These mechanisms elicit very fast responses but they are not pathogen-specific. In contrast, the adaptive immune response, constituted of T cells and B cells (both are lymphocytes), elicits powerful and specific responses to any pathogens encountered because of highly specialized antigen receptors. T cells are further divided into $CD4^+$ helper T cells, which interact with macrophages and B cells; and $CD8^+$ cytotoxic T cells, which destroy infected host cells. B cells produce and secrete antibodies, proteins that

bind to antigens, activate the complement system or promote phagocytosis by macrophages. T cells and B cells can also form memory cells that can mediate rapid and enhanced responses to second and subsequent exposures to antigens [9, 10].

T and B cells can be activated without the presence of an infection-causing microbe, and when these responses harm the body chronically, one speaks of an autoimmune disease [11, 12]. These diseases contribute a significant portion to morbidity and mortality and considering that autoimmune diseases predominantly affect younger people, it is not surprising that they are associated with major health expenses and loss of productivity for the society [12]. Studies have shown that microorganisms can trigger autoreactivity, because microbial proteins resemble host proteins and the immune cells are not able to distinguish between them. Environmental and so-called non-infectious triggers (e.g. penicillin) can also initiate autoreactivity [11]. The pathogenesis of the different autoimmune diseases is very diverse, and a simple classification divides the pathogenic mechanisms into two groups: (1) there is an error in the process that decides which B and T cells are allowed to mature or how long these cells should live; or, (2) a specific antigen (foreign or self) is responsible for an inappropriate immune response that results in an autoimmune disease [11]. An example of an autoimmune disease is systemic lupus erythemasus (SLE) where both of these elements come into play, because self-reactive B lymphocytes escape the mechanisms that should prevent their formation, and they produce antibodies that form complexes with nuclear self-antigens that are exposed on dead and dying cells [13-15]. Chronic inflammation and damage to organs characteristic of SLE is a consequence of the body's inability to eliminate these complexes [16]. Other autoimmune diseases exhibit other pathogenic mechanisms. One purpose of the epithelial barrier in the intestines is to keep the bacterial flora in the intestinal lumen, but when bacteria are able to cross that barrier they come in contact with the mucosal immune system [17]. In Crohn's disease, abnormalities in certain subsets of $CD4^+$ helper T cells, namely T_H1 cells and T_H17 cells, are suspected to cause vigorous inflammation of the mucosa and submucosa of the intestine, but the entire alimentary tract can be affected [9, 17]. Other examples of autoimmune diseases are ulcerative colitis, rheumatoid arthritis, multiple sclerosis and type 1 diabetes mellitus [11].

1.4 Hookworms

1.4.1 Hookworm infection

Hookworms are parasitic nematodes that reside in the intestines of humans and other mammals like cats and dogs. Hookworm infection is considered one of the most important tropical diseases and estimates speak of more than 700 million affected individuals, most of them in Asia, sub-Saharan Africa and South America [18-20]. Complications associated with hookworm infections include iron-defiency anaemia, growth retardation in children and a low birth weight of infants; the mortality, however, is rather low [19, 20]. The soil-living hookworms *Necator americanus* and *Ancylostoma duodenale* are responsible for the majority of human cases and both are able to burrow through the skin when a person is in contact with contaminated soil [20]. Penetration of the skin results in an itching rash accompanied by erythema and papules ("ground itch") [20]. Infectious larvae of the zoonotic hookworm *A. braziliense* cause a particular skin condition known as "larvae migrans", where the larvae move around in the epidermis [20]. *A. duodenale* can also gain access via the oral route [20]. Other hookworms primarily infect animals, but can cause zoonosis in humans; examples are *A. ceylanicum*, which infects dogs and cats, and the canine hookworm *A. caninum* [20].

Overcoming the skin barrier gives the larvae access to the systemic circulation, which transports them to the cardiac and pulmonary system [20]. Arrival in the latter, results in migration to parenchymal tissue and ascent to the trachea, causing a sore throat and cough [20]. Next, swallowing enables the larvae to descend the alimentary tract to the intestine, where they mature to the adult worm stage and attach to the gut wall [20]. In the intestine the worm feeds on blood by biting into mucosa and submucosa, and releases compounds with anticoagulant activity so that the blood flows sufficiently from the damaged vasculature [20]. Finally, the hookworm life cycle is completed when the females start to produce eggs, which are excreted from the host [20]. Persistent blood loss accompanied by low iron intake or high physiological demands can result in iron-deficiency anaemia [20]. Anaemia during pregnancy is particularly problematic because it affects the mother as well as the child thereby increasing the risk for low birth weight and growth retardation [20, 21]. Among non-anaemic manifestations are hypothermia, epigastric pain, nausea, impotence and anasarca, a condition caused by extreme

hypoproteinaemia and characterized by oedema of the face and lower limbs and potbelly [20].

1.4.2 Immunologic aspects to hookworm infections

Antibodies of all five immunoglobulin classes have been reported to recognize hookworm antigens, and a successful skin penetration by infectious larvae results in the earliest immune responses because antibodies are able to target antigens on the surface of the sheath that covers the larvae [19, 22]. Burrowing through the skin causes the majority of the larvae to loose the sheath, and because most of the immunogenicity relies on the sheath, this may serve as a distraction manoeuvre to lead the attention away from the larvae, which would render the antibody response rather ineffective at this infection stage [22]. The larvae are too large to be ingested by macrophages and neutrophils, therefore cellular immune responses against larvae predominantly involve eosinophils, which attach to parasitic organisms and, on activation, release substances toxic to the larvae [22]. However, it is not clear how efficient eosinophilic responses are at killing the larvae and adult worms [22].

In order to combat the adult worm stages in the small intestine, T_H2 cells, a subset of $CD4^+$ helper cells, are activated and start to secrete the cytokines Interleukin (IL)-4, IL-5 and IL-13 [9, 19]. IL-4 stimulates B-lymphocytes to proliferate and mature into antibody secreting plasma cells [9]. Immunoglobulin G1 (IgG1), IgG4 and IgE are the antibodies that make up the most important parts of the humoral response against intestinal hookworm infection, but in what degree they contribute to fight and protection against hookworms requires more research [19, 22]. Particularly, IgE may be attributed beneficial properties, whereas it seems that an ongoing infection correlates best with hookworm-specific IgG4 levels [19]. IgD, IgE and IgG are able to bind to basophils, which are a member of the innate immune system. The binding leads to the liberation of inflammatory mediators and IL-4, which, together with IL-5 and IL-13, are crucial for the immune response driven mainly by T_H2 cells [19]. It is proposed that the hookworm can somehow down regulate the IgD level and thereby manipulate the immune response [19].

1.4.3 Excretory/secretory products (ES)

Suspected to be responsible for the immunomodulatory effects, and thereby enabling an infection, are the so-called excretory/secretory products (ES), which are macromolecules that are excreted or secreted by hookworms [23]. It has been shown that ES products from different parasitic worms are able to affect the production of cytokines, chemokines, and the expression of important co-stimulatory molecules for signal transduction [24]; inactivate chemokines [25]; and modulation of dendritic cells [26]. The neutrophil inhibitory factor (NIF) is a glycoprotein found in the ES of *A. caninum* that exhibits immunomodulatory effects by binding to the integrin CD11b/CD18 located on activated neutrophils [27, 28]. Normally, neutrophils arrive at the location of inflammation via the blood stream, and to gain access to the inflamed tissue, they have to migrate through the endothelium [9]. Before the migration can happen, the neutrophils have to adhere to intercellular adhesion molecules (ICAMs) via integrins [9]. NIF inhibits this binding, as well as the release of hydrogen peroxide (H_2O_2), which is important in the killing of microorganisms [27, 28]. Therefore, the ES products could serve as a starting point for the development of drugs against allergies, autoimmune disease or other immunity-related disorders.

1.5 Prelimenary data

Investigation of the ES products of the dog hookworm *A. caninum* exposed a mixture of over 100 different proteins [29]. Among the proteins were ion channel blockers, carbohydrate-binding proteins (so-called lectins), metallo-proteases, hyaluronidases, lysozyme-like proteins, and transthyretin-like proteins (transthyretin is a protein that transports thyroxine and retinol in the blood and cerebrospinal fluid) [29]. But all preceding studies of the ES products of hookworms have characterized protein components of higher molecular masses (> 5 kDa), and little focus has been on the low molecular weight ES products (1 – 5 kDa). Therefore, the hypothesis of this project is that there are peptide components within the low molecular weight ES products of the canine hookworm *A. caninum* that possess activity as immunomodulators.

1.6 ShK-like peptide sequences

ShK is a 35-residue toxin isolated from the sea anemone *Stichodactyla helianthus* that is able to block voltage-gated potassium channels [30]. Of particular interest is the blockage of the Kv1.3 potassium channel because it is involved in T cell proliferation and may therefore be involved in the pathologic mechanisms of autoimmune diseases [31-34]. Dr Jason Mulvenna performed an *in silico* search of hookworm transcriptomes for peptide sequences that possess the same cysteine framework as ShK and discovered a number of sequences. Two of these putative peptides, Name2 and Acan1, were chosen for synthesis in this project (**figure 2**). The hypothesis is that these peptides will have the same tertiary structure as ShK and may also be able to block potassium channels and thus have an effect on the immune response.

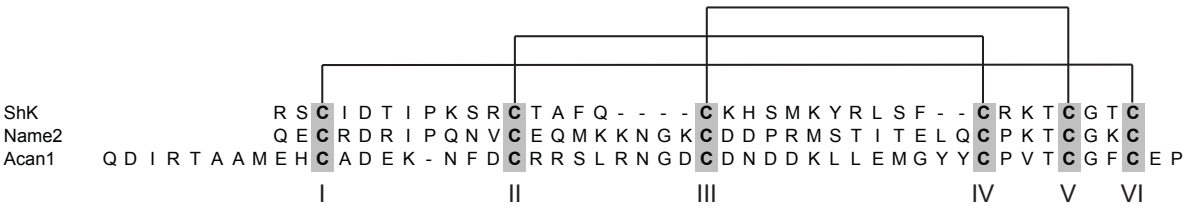

Figure 2: Peptide sequences of ShK, Name2 and Acan1. Name2 was identified in the transcriptome of N. americanus, whereas Acan1 was identified in the transcriptome of *A.* caninum. The conserved cysteine framework is shown by the solid lines as a CysI–VI, CysII–IV and CysIII–V.

1.7 Experimental TNBS colitis in mice

1.7.1 Immunology of TNBS coltitis

TNBS colitis is an experimental model where mice are treated rectally with 2,4,6-trinitrobenzenesulfonic acid (TNBS) as an ethanolic solution in order to cause an intestinal inflammation [35]. The mucous membrane in the colon is damaged by ethanol (EtOH), so that TNBS can react with mouse proteins leaving these macromolecules conjugated with a trinitrobenzene (TNP) group (**figure 3**) [35, 36]. The TNP-proteins are now targeted by the immune system in the form of antigen-presenting cells (APCs), which are able to process these proteins and present the antigens to $CD4^+$ T cells [37]. The activated T cells communicate to the APCs to secrete IL-12, which promotes the differentiation of immature T cells to T_H1 effector cells that produce Interferon (IFN)-γ and tumour necrosis factor (TNF)-α [37]. IFN-γ and TNF-α are then responsible for the secretion of even more IL-12 (by APCs) and TNF-α, as well as the inflammatory

cytokines IL-1β and IL-6 (by macrophages), which cause the inflammation in the colon [37]. Symptoms are the loss of weight, diarrhoea, rectal prolapse and a scruffy fur coat [35].

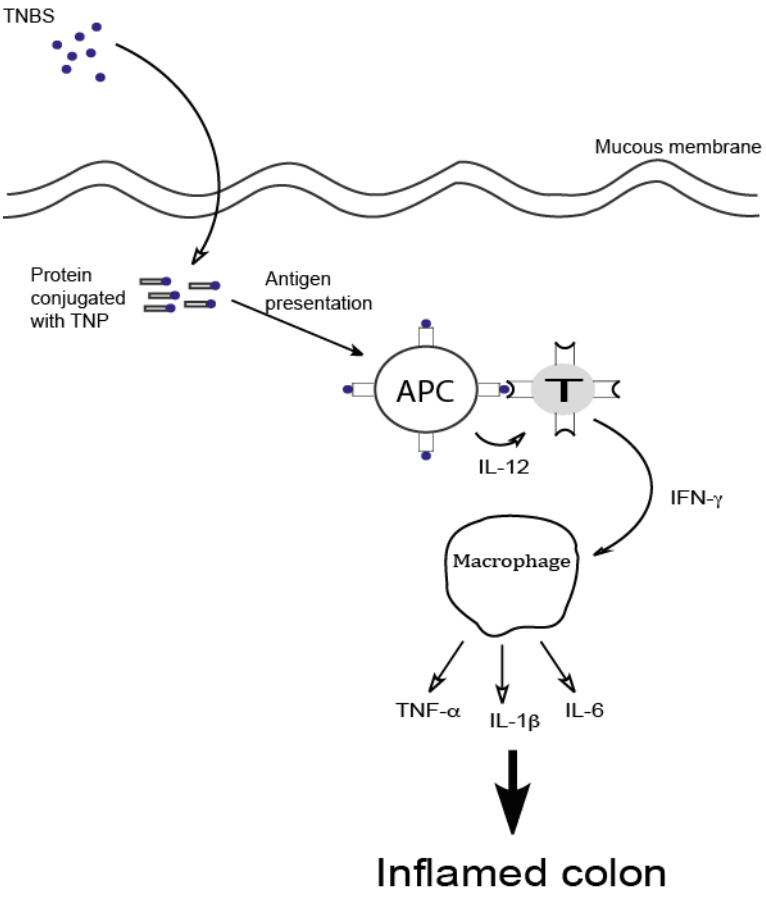

Figure 3: TNBS colitis works by conjugating proteins with a TNP-moiety, which activates T cells via antigen presentation. The T cells secrete IFN-γ that acts on macrophages to produce cytokines that cause the inflammation.

1.7.2 The Relation between the TNBS model and Crohn's disease

Crohn's disease is characterized by inflammation of predominantly gastrointestinal mucous membranes and investigations have revealed that T_H1 and T_H17 cells, as well as the cytokines they produce are involved in the pathogenesis [38]. When macrophages and other APCs come in contact with microorganisms, they secrete IL-12, which activates T_H1 cells, and in the case of Crohn's disease, IL-12 production is increased [38, 39]. Similar to the TNBS mouse model, the T_H1 cells then produce the cytokine IFN-γ, which has pro-inflammatory properties by activating additional macrophages. Also, cytokines (IL-1, IL-6 and IL-23) produced by APCs promote the differentiation and

proliferation of T_H17 cells, but their role in connection with Crohn's disease is still under investigation [38, 40]. To conclude, Crohn's disease and the TNBS colitis model share common immunologic features, inter alia the IL-12 driven T_H1 pathway with increased production of IFN-γ and subsequent secretion of inflammatory mediators (TNF-α, IL-1β and IL-6).

1.8 Aims

As stated earlier, the hypotheses of this project are:

- The low molecular weight ES products of *A. caninum* posses contains peptide components that posses activity as immunomodulators.
- The peptides identified in the hookworm transcriptome have a tertiary structure that resembles ShK.

This will be investigated via three specific aims:

- Fractionation of the low molecular weight ES products of *A. caninum*
- Activity testing of the fractions in the TNBS mouse model
- Synthesis and structure determination of Name2 and Acan1

2. Results

2.1 Fractionation of low molecular weight components of *A. caninum* ES products (LMW AcES)

The low molecular weight components of the hookworm *A. caninum* ES products (LMW AcES) were fractionated by reverse-phase high-pressure liquid chromatography (RP-HPLC) using a preparative column, a 2 % gradient of buffer B and the eluate was collected in intervals of 10 minutes. The RP-HPLC system used in this thesis detects absorbance at 215 nm, where the peptide bond absorbs ultraviolet (UV) light, and at 280 nm, where the aromatic residues Trp and Tyr have an absorbance maximum. In **figures 4** and **5**, the chromatograms of the fractionation of the first batch of LMW AcES are shown with absorbance detection at 215 and 280 nm, respectively. Based on the chromatograms, the fractions containing the largest amounts of peptides are probably fractions B (10 – 20 minutes), C (20 – 30 minutes) and D (30 – 40 minutes). The culture media for the hookworms also contained phenol red, which eluted after approximately 22 minutes, giving fraction C a yellow colour.

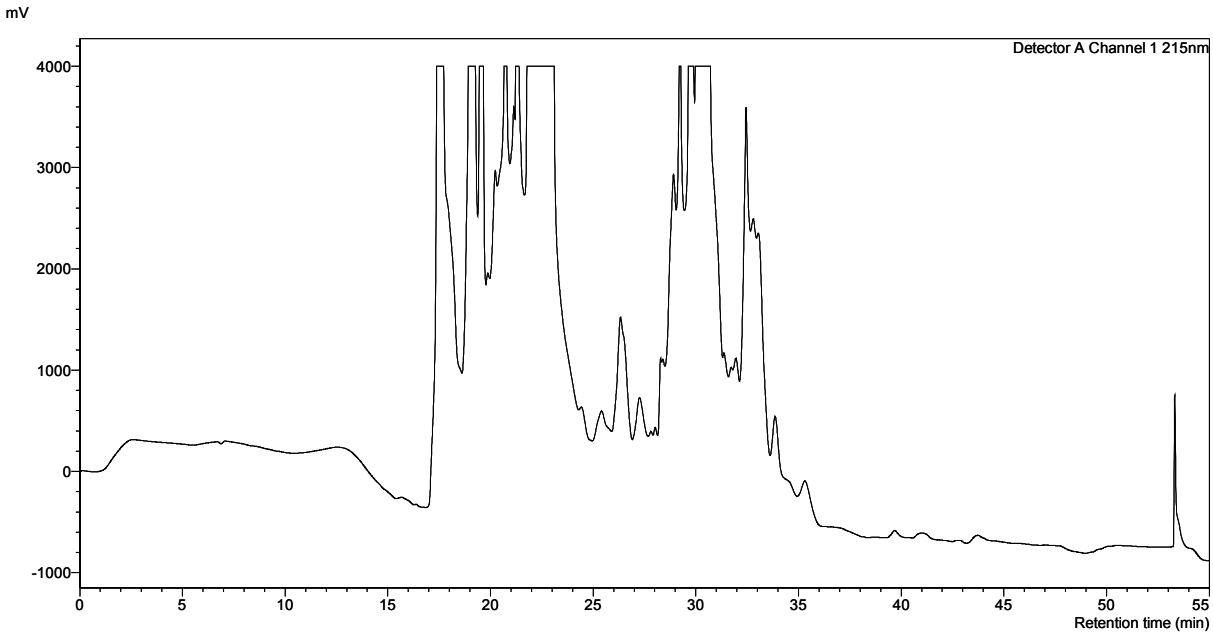

Figure 4: RP-HPLC chromatogram of the first batch of LMW AcES with absorbance detection at 215 nm

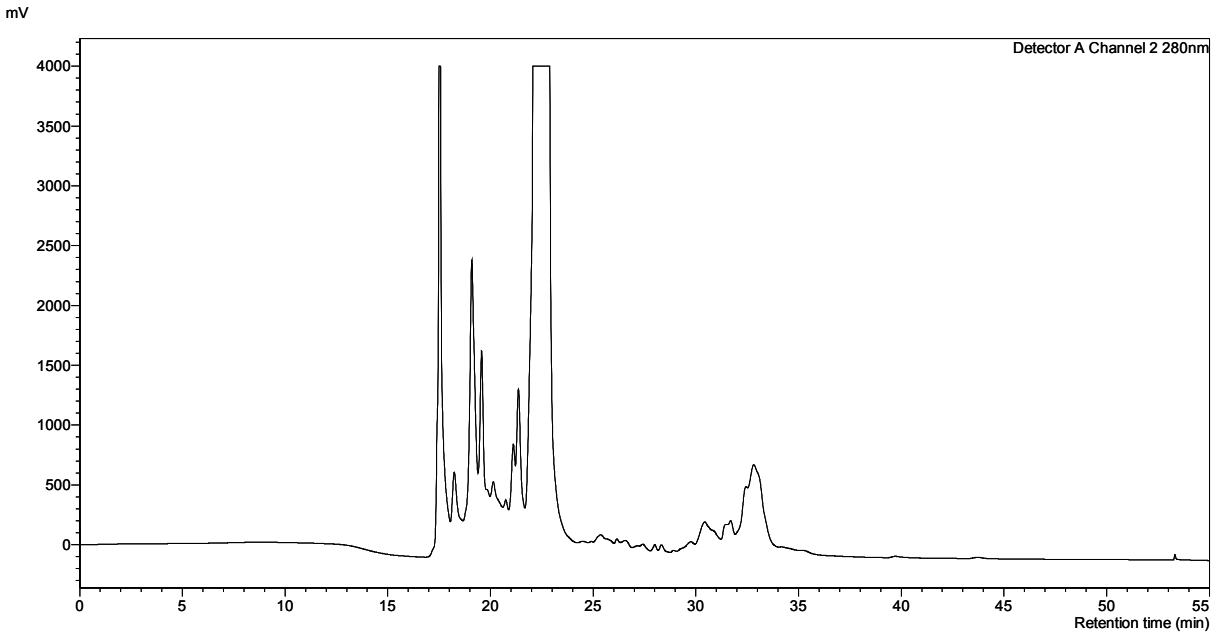

Figure 5: RP-HPLC chromatogram of the first batch of LMW AcES with absorbance detection at 280 nm

Analytical RP-HPLC runs of the individual fractions were conducted (**figures A1 – A5**) and the fractions were tested for bioactivity (section 2.2).

A second, bigger batch of LMW AcES was fractionated exactly in the same way as the first one, giving similar RP-HPLC chromatograms. Fractions from this batch were also tested for bioactivity.

2.2 Bioactivity testing of fractionated LMW AcES in mice with experimental colitis

The animals used in this experiment were mice of the C57Bl/6-strain. In order to investigate the potential of LMW AcES to affect the course of experimental colitis in these animals, fractions obtained by RP-HPLC, as well as unfractionated LMW AcES were injected into different mice prior to colitis induction by TNBS-injection. The mice were organised into groups, where one group served as a positive control (healthy control) that had access to food and water, but did not receive a TNBS-injection, injections of unfractionated or fractionated LMW AcES. Additionally, a negative control group existed (TNBS only) with mice that received only a TNBS-injection. The animals of the other groups received injections of unfractionated LMW AcES or fractions before the induction of colitis. The weight was monitored daily and after three days the mice were sacrificed and dissected to establish the severity of inflammation.

2.2.1 First batch of LMW AcES fractions

Compared to the starting point on day 0, only the animals in the healthy control group gained weight as depicted in **figure 6**. The mice in all the other treatments lost weight during the first three days of the experiment; but the negative controls, the mice that received unfractionated LMW AcES, fraction A, fraction C and fraction E had, on average, gained weight between the measurements on days 2 and 3. Compared to day 0, the animals that were injected with fraction E seemed to have lost less weight than all the other groups, except the healthy control group. Mice that were treated with any of the other fractions (A, B, C or D) or unfractionated LMW AcES seemed to have suffered from greater weight loss than the negative control group. The differences between the treated groups were not statistical significant (one way ANOVA, $F = 1.67$, $p = 0.18$).

This parallel was possibly biased by the different sex of the mice in the different groups. The groups of the healthy control, negative control and fraction E consisted of male animals, whereas the other groups consisted of females.

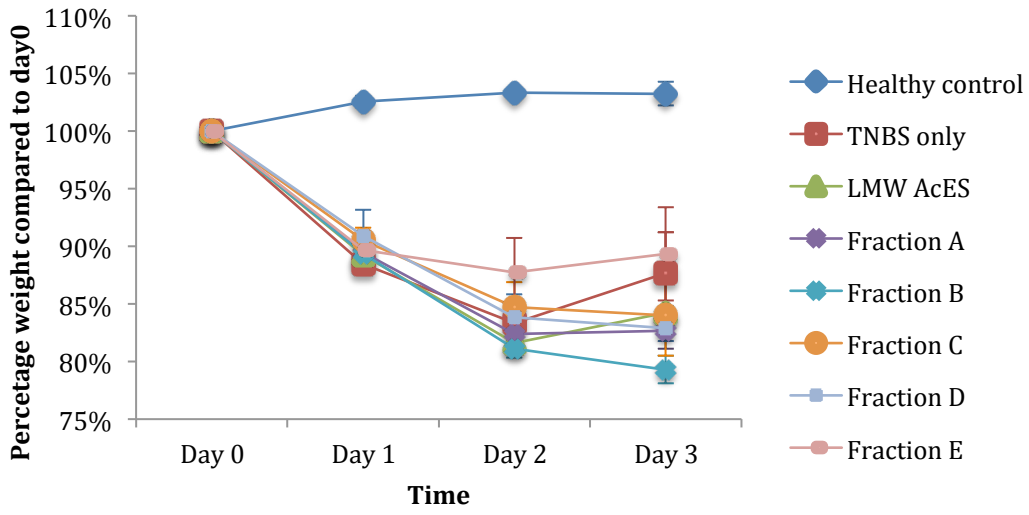

Figure 6: Average percentage weight of each group compared to day 0

Because the mouse colon tends to shrink when it is inflamed, the colon length was measured. The colons of the healthy control animals were not inflamed so they were significantly longer than the colons of the other mice (one way ANOVA, $F = 3.70$, $p < 0.01$), except for the fraction C group, which was not statistically different (two sample t-

test, t = 2.59, p = 0.06) (**figure 7**). But when all the colitis groups were compared, no statistical difference could be found (one way ANOVA, F = 0.32, p =0.92).

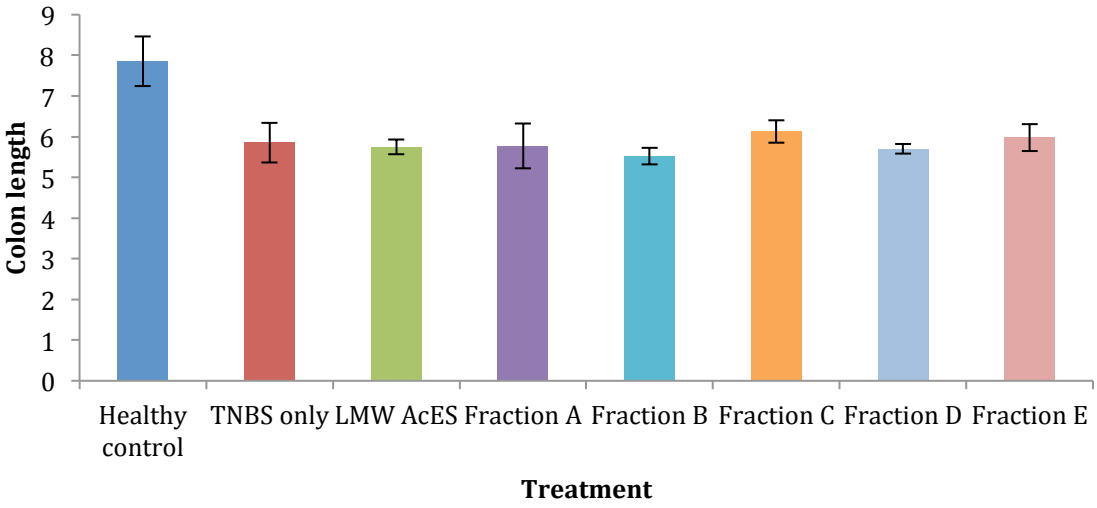

Figure 7: Comparison of the colon length of the different groups

Ulcerations, oedema, thickening of the colon wall, impaired intestinal motility and adhesions are considered signs of colon inflammation. A scoring system was applied to assess the severity of each sign of inflammation (0 = normal to 4 = most severe) [41]. The scores for the individual mouse were summed up and the mean values for each group are shown in **figure 8** (maximum possible score = 20). Not surprisingly, the healthy controls did not show any sign of inflammation, whereas the negative controls ($\bar{x} = 9.5 \pm 2.4$) and the fraction A-group ($\bar{x} = 9.25 \pm 2.6$) had the highest scores. Animals that received fraction E had a score of 1 ± 0.8 and thus the lowest score of all groups, except the healthy controls. The fraction C treated group had only a medium degree of inflammation ($\bar{x} = 2.25 \pm 2.2$). Comparison of the negative controls and the all the other colitis groups did not reveal statistical significant differences (one way ANOVA, F = 1.67, p = 0.18), but a two sample t-test between the negative control and LMW AcES (t = 3.04, p = 0.02), fraction C (t = 4.46, $p < 0.01$) and fraction E (t = 6.76, $p < 0.01$), respectively, revealed significance.

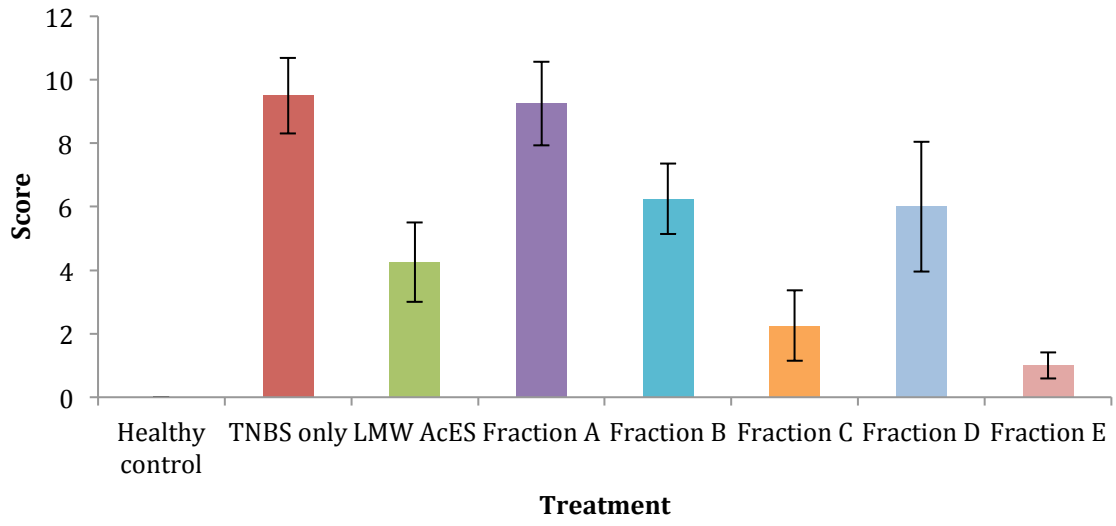

Figure 8: Macroscopic scores of the different groups

2.2.2 Second batch of LMW AcES fractions

The TNBS mouse model was also used to test the second batch of LMW AcES and this time, five animals were in each group. If one disregards the positive control group, then the mice treated with fractions C and E had the highest and second highest mean weight, respectively, compared to the baseline weight on day 0. However, the differences were not significant when compared to the negative control group (one way ANOVA, F = 0.38, p = 0.69) (**figure 9**).

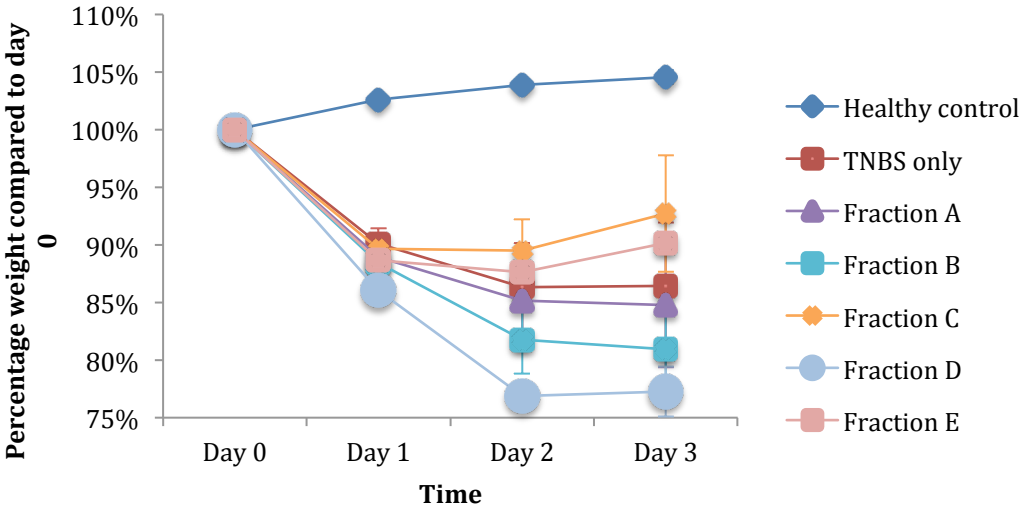

Figure 9: Average percentage weight of each group compared to day 0

The animals that received an injection of fraction C ($\bar{x}$ = 7.04 ± 0.21 cm) had longer colons than those with fraction A ($\bar{x}$ = 5.98 ± 0.86 cm) (two sample t-test, t = 2.68, p = 0.049). And this significance means also that the fraction C group had the longest colons of all the groups treated with TNBS (**figure 10**). The fraction B group seemed to have the shortest colons.

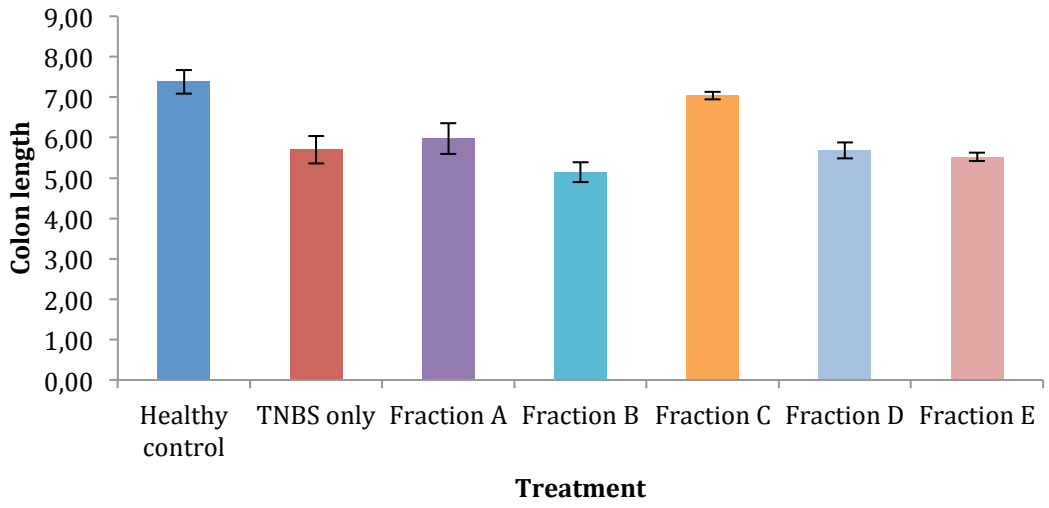

Figure 10: Comparison of the colon length of the different groups

The mice that were injected fraction C were the only colitis group that had a lower macroscopic score than the negative control (two sample t-test, t = 2.41, p = 0.04) (**figure 11**).

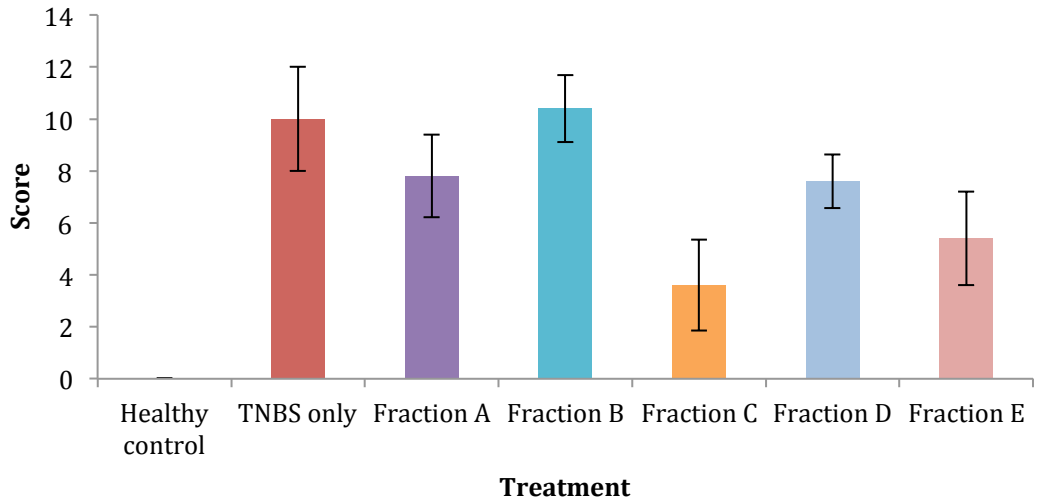

Figure 11: Macroscopic scores of the different groups

2.3 LC/MS analysis of fractions C and E

2.3.1 Fraction C

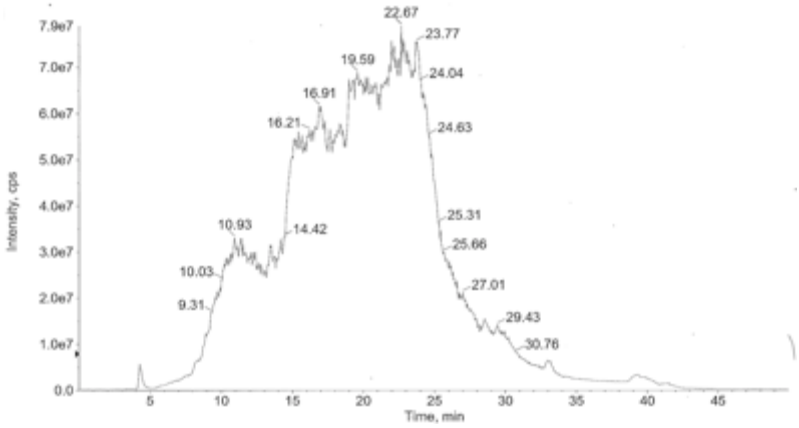

Figure 12: RP-HPLC chromatogram from the LC/MS analysis of fraction C

Fraction C was analysed by LC/MS and the chromatogram is shown in **figure 12**. The software was able to automatically determine the original molecular weight of species bearing several charges by performing a reconstruction. The highest mass that could be reconstructed was 3759.98 and several other masses between this and 2000 Da could be detected. But the most abundant masses all had a molecular weight of below 2000 Da (**figure 13**).

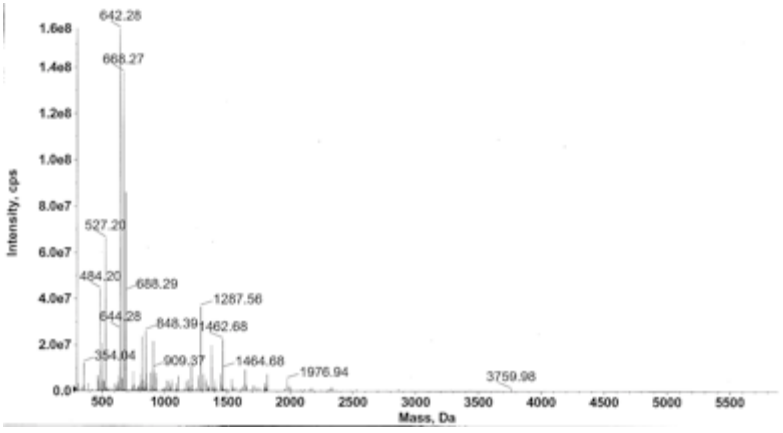

Figure 13: Reconstruction ESI-MS the masses present in fraction C

2.3.2 LC/MS of fraction E

The chromatogram of the LC/MS-analysis of fraction E is shown in **figure A6**. The highest masses reconstructed were 4688.56 and 3306.74. The most abundant mass

found during the reconstruction was 1952.88, which is detected as several different masses 489.23 ($[M+4H]^{4+}$), 651.97 ($[M+3H]^{3+}$) and 977.45 ($[M+2H]^{2+}$). **Figure 14-A** depicts the mass spectrum of the biggest peak in the chromatogram and all three masses can be found. The other peaks in the chromatogram were smaller and the intensity on the mass spectrum was therefore also lower.

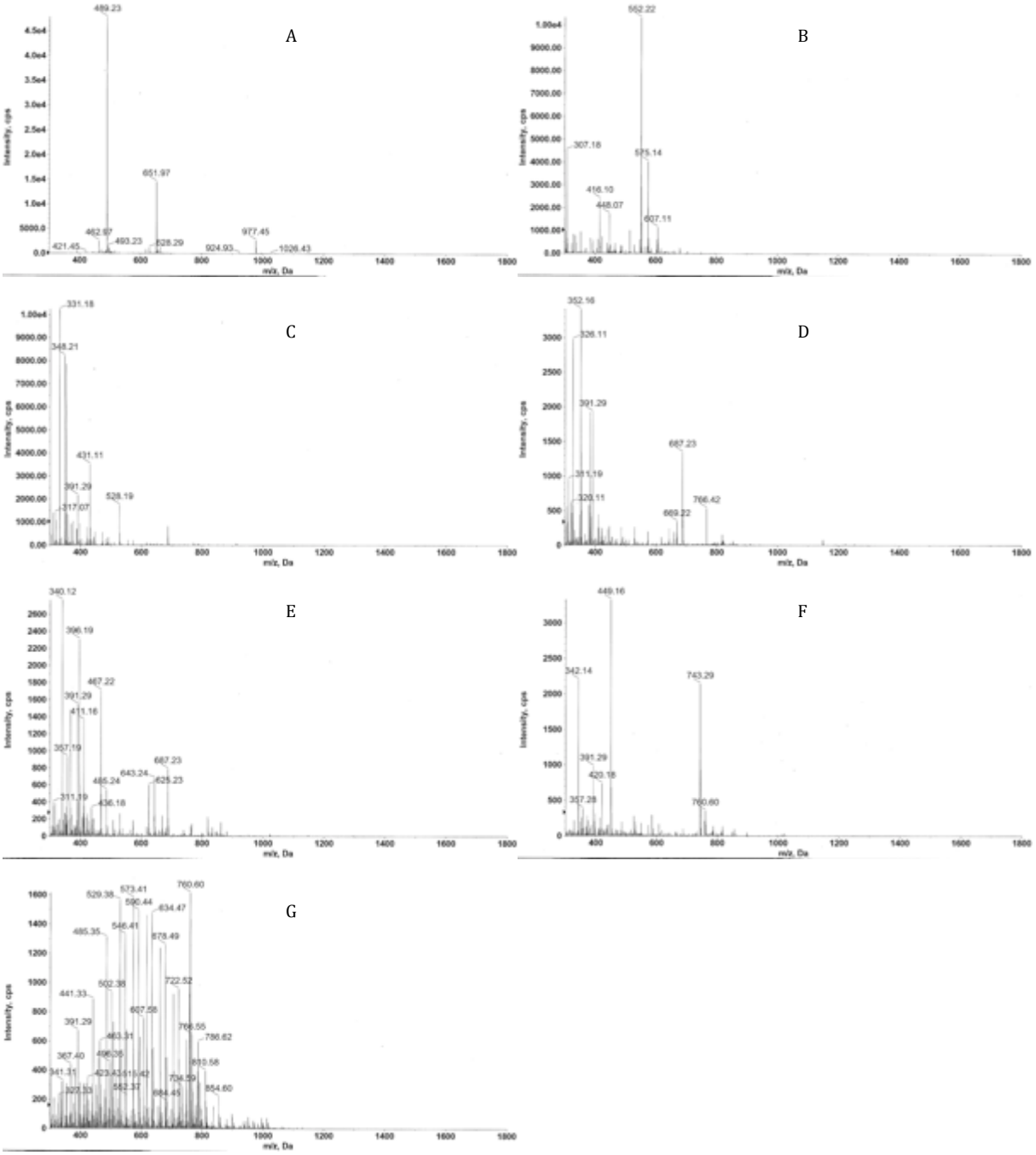

Figure 14 A - G: ESI-MS of the major peaks in the RP-HPLC chromatogram (**figure A7**)

2.4 1D ^{1}H NMR spectroscopy of fraction C

A 1D ^{1}H nuclear magnetic resonance (NMR) spectrum was recorded of fraction C (**figure 15**). The spectrum showed peaks in the amide bond region (7.5 – 9.5 ppm) and therefore it is possible that the constituents of the fraction might be peptides.

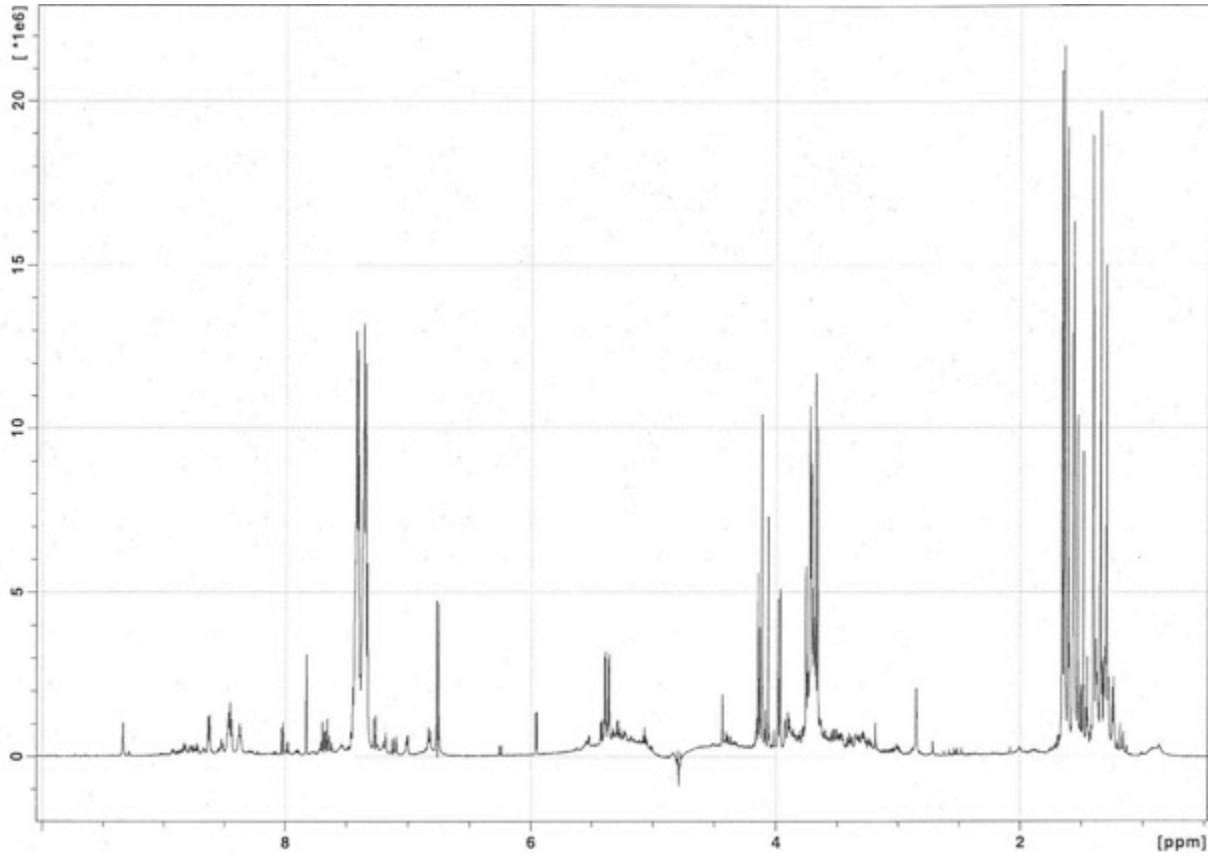

Figure 15: 1D ^{1}H NMR spectrum of fraction C

2.5 Peptide synthesis

2.5.1 Synthesis of Name2

The sequence of Name2 (**figure 16**) was discovered in the transcriptome of the hookworm *N. americanus*. It consists of 41 residues and has a molecular weight of 4716.5 Da. Because of its size it was decided to divide the sequence into approximately equal sized halves and to synthesise them separately. The half with the N-terminus is from now on called Name2 N-terminus, whereas the part with the C-terminus is named Name2 C-terminus. After the successful synthesis of both halves they have to be ligated together by native chemical ligation (NCL). NCL requires that the Name2 C-terminus fragment has a N-terminal Cys-residue, because the thiol group is crucial for the reaction with a thioester formed at the C-terminal of Name2 N-terminus [42].

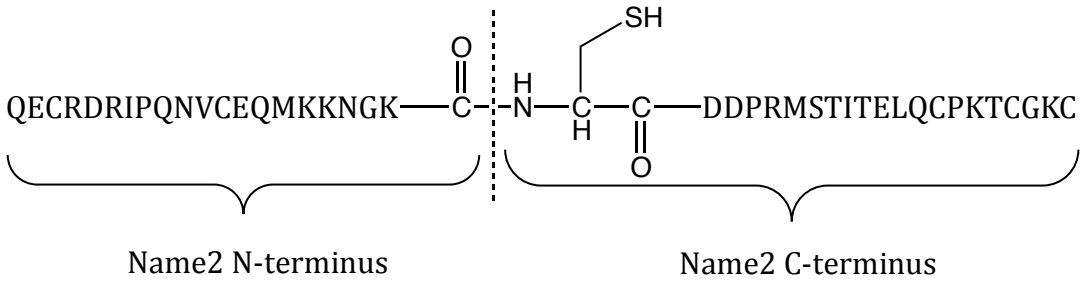

Figure 16: Amino acid sequence of Name2

Figure 17 summarizes the synthetic scheme used for the production of the two fragments. Name2 N-terminus was synthesised with a diaminobenzoic acid (Dbz) group attached to the C-terminal residue. When the chain elongation was complete, this Dbz-group was then converted to a *N*-acylurea moiety, a *N*-acyl-benzimidazolinone (Nbz), which is readily exchanged with an arylthiol to form a thioester [42]. The N-terminal Gln-residue was protected by a base-stable Boc-group, which was removed together with the other protecting groups in the cleaving process. The synthesis of Name2 C-terminus was straightforward. The two peptides were then ligated to yield Name2.

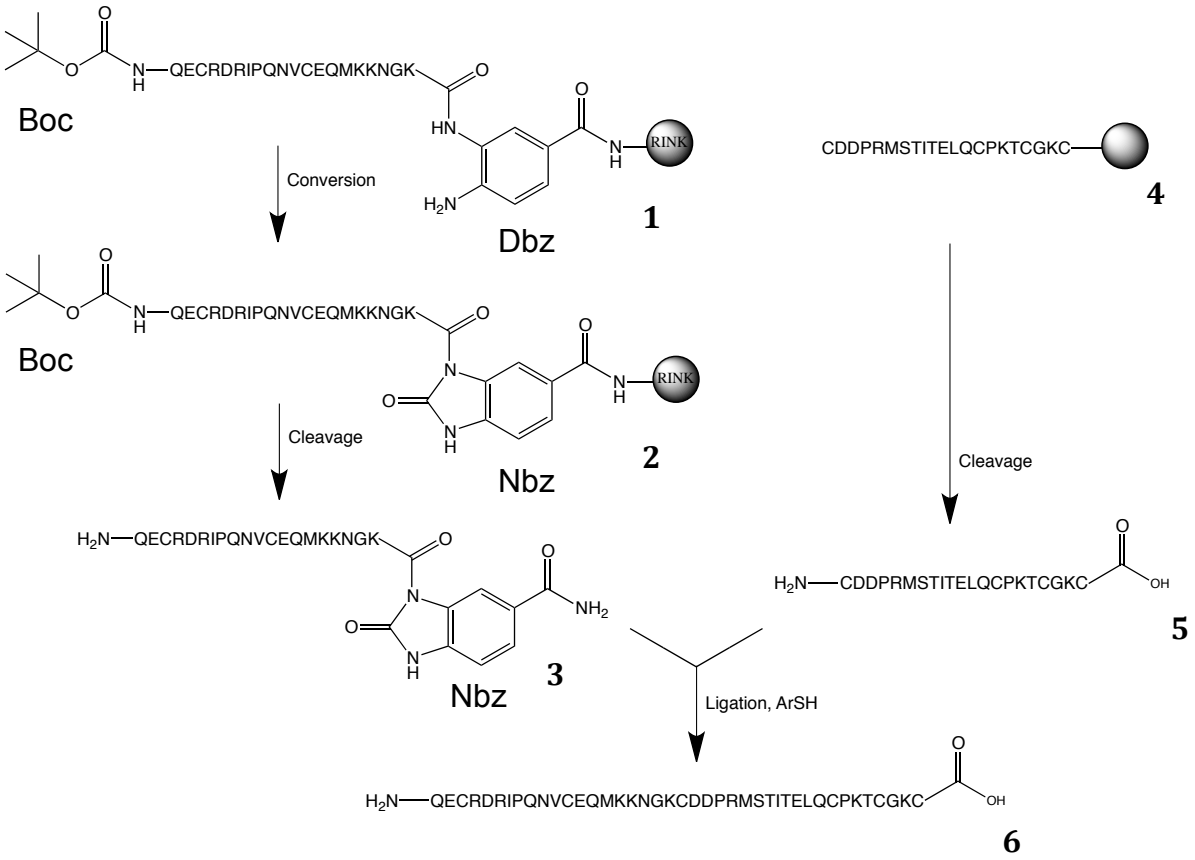

Figure 17: Name2 N-terminus with a Dbz-group attached to the C-terminal residue (**1**) was converted to yield the peptide-Nbz (**2**). The subsequent cleavage liberated the unprotected peptide-Nbz (**3**). Name2 C-terminus was synthesised by standard Fmoc-SPPS and then cleaved (**4**, **5**). **3** and **5** were ligated to Name2 (**6**). Only the Boc-group protecting the N-terminal Gln-residue of **1** and **2** is shown, the other protecting groups are omitted.

2.5.1.1 Synthesis of Name2 N-terminus

Name2 N-terminus was synthesised manually on a 0.25 mmol scale using Fmoc-SPPS. Because the synthesis proceeds from the C- to the N-terminal end of the peptide, the Rink Amide 4-methylbenzhydrylamine (MBHA) resin was initially loaded with 3-Fmoc-4-diaminobenzoic acid (Fmoc-Dbz). The loading had to be repeated twice over the course of three days and the coupling yield was checked by ninhydrin test. After the successful loading, the peptide chain was elongated as determined by the sequence, but every residue had to be coupled several times in order to achieve satisfactory yields, with Arg15 and Arg17 being the residues hardest to couple. After chain assembly was complete, Name2 N-terminus was activated by 4-nitrophenyl chloroformate and *N*,*N*-diisopropylethylamine (DIPEA). A total amount of 1.924 g of activated peptidyl resin

was obtained of which 400 mg was taken out for cleaving using a mixture of TFA, triisopropylsilane (TIPS), 3,6-dioxa-1,8-octanedithiol (DODT) and water, yielding 114 mg of peptide crude. An electrospray ionization mass spectrum (ESI-MS) was recorded of the peptide crude that showed two major products: the activated peptide-Nbz and a by-product with masses of 1193.4 ($[M+2]^{2+}$) and 796.1 ($[M+3]^{3+}$) (**figure A7**). The calculated and observed ions of the correct peptide-Nbz in the crude are depicted in **table 1**. The analytical RP-HPLC carried out to investigate the composition of the peptide crude is shown in **figure 18** and the peaks at 20.4 and 21.9 minutes belong to the by-product and Name2 N-terminus peptide-Nbz, respectively.

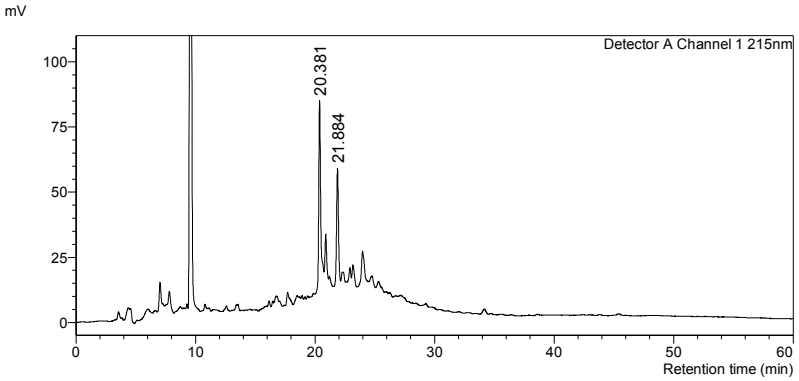

Figure 18: Analytical RP-HPLC of Name2 N-terminus peptide crude

74 mg of the peptide crude was purified by RP-HPLC where the peptide eluted after approximately 29.5 minutes and three fractions could be obtained that contained the activated peptide-Nbz, which was confirmed by ESI-MS (**Figure A8** and **table 1**). Unfortunately, the same major by-product present in the crude eluted together with the correct peptide-Nbz during the purification.

Table 1: Calculated and observed masses of Name2 N-terminus peptide crude and purified fraction

		$[M+2]^{2+}$	$[M+3]^{3+}$
Calculated:		1282.9	855.6
Observed:	Crude	1282.6	–
	Purified	1282.5	855.2

The fractions were analysed by RP-HPLC and **figure 19** shows the RP-HPLC chromatogram of the fraction that generated the highest peaks at retention times similar to the peptide crude, as well as the highest intensity on the mass spectrum. That fraction contained probably the highest amount of correct peptide-Nbz but also considerable amounts of the by-product. The fractions were then lyophilized overnight and 19.67 mg of fractions containing the correct peptide-Nbz were saved for the ligation.

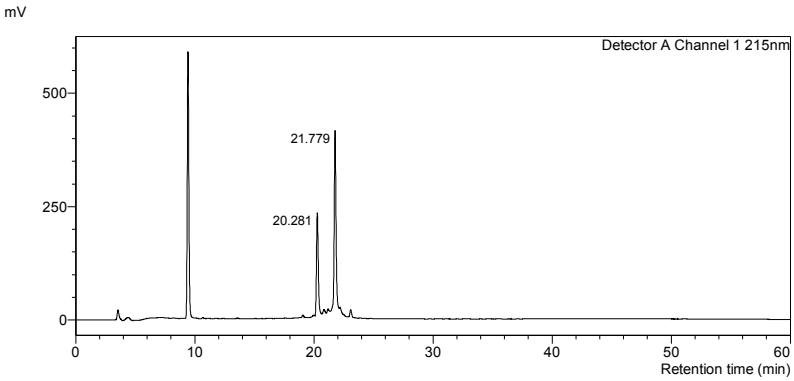

Figure 19: Analytical RP-HPLC of purified Name2 N-terminus

2.5.1.2 Synthesis of Name2 C-terminus

2-Chlorotrityl chloride resin was used for the manual synthesis of Name2 C-terminus on a 0.25 mmol scale. Every residue had to be coupled several times in order to achieve satisfactory coupling yields, which were determined by ninhydrin test. Again, arginine was the residue hardest to couple, with Arg 17 giving a coupling yield below 92 % after the fourth coupling. 521 mg of peptidyl resin was obtained during the synthesis of which half was taken out for cleavage using a mixture of TFA/TIPS/DODT/H_2O. ESI-MS of the peptide crude confirmed the presence of the correct Name2 C-terminus (**figure A9** and **table 2**). The mass of the dry peptide crude was 78 mg and purification by RP-HPLC, where the peptide eluted after approximately 34 minutes resulted in several fractions containing the correct peptide as determined by ESI-MS (**figure A10**).

Table 2: Calculated and observed masses of Name2 C-terminus peptide crude and purified fraction

		$[M+2]^{2+}$	$[M+3]^{3+}$
Calculated:		1165.9	777.6
Observed:	Crude	1165.2	776.8
	Purified	1165.4	777.4

Analytical RP-HPLC chromatograms of the peptide crude and the most pure fraction are depicted in **figures 20** and **21**, respectively. Name2 C-terminus has a retention time of approximately 29 minutes. The fractions were lyophilized.

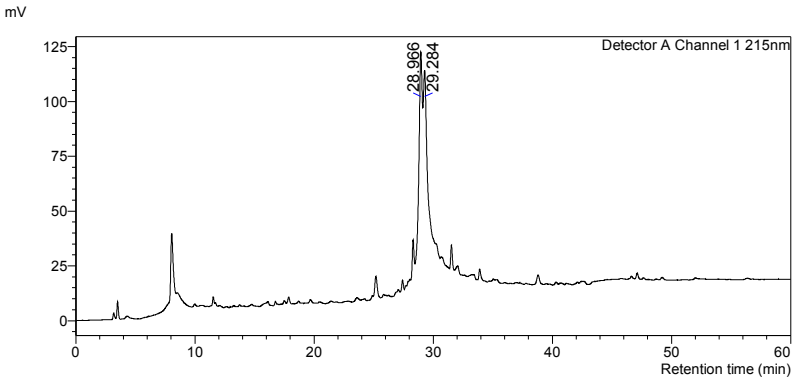

Figure 20: Analytical RP-HPLC chromatogram of Name 2 C-terminus peptide crude

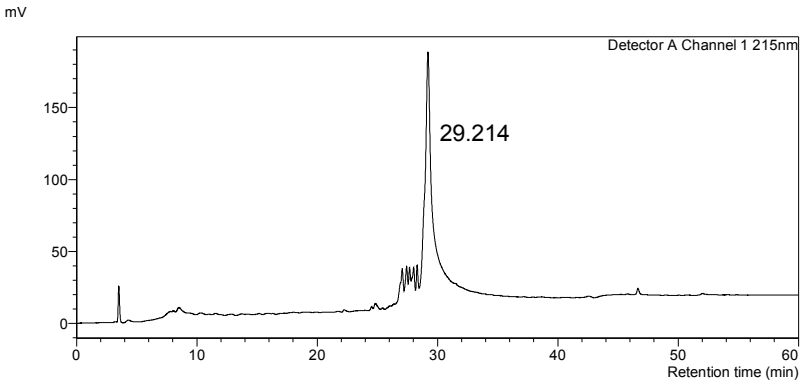

Figure 21: Analytical RP-HPLC of purified Name 2 C-terminus

The rest of the peptidyl resin was also cleaved and all peptide crude obtained was purified, which resulted in 14.66 mg of fractions containing Name2 C-terminus saved for ligation.

2.5.1.3 Native chemical ligation of Name2 N-terminus and C-terminus

1. Ligation attempt:

Because a by-product eluted together with Name2 N-terminus during purification, this starting material for the ligation was not pure and the decision was made to use twice the amount of Name2 N-terminus compared to the C-terminus, which was relatively pure for this reaction. Name2 N-terminus (3.98 mg) and C-terminus (1.98 mg) were ligated using a ligation buffer made of guanidine hydrochloride (Gn · HCl) and disodium hydrogen phosphate (Na_2HPO_4) at pH 7.91. Mercaptophenylacetic acid (MPAA) in a concentration of 0.202 M accounted for the formation of the thioester that reacts with the Cys-residue of Name2 C-terminus and 0.0206 M of Tris(2-carboxyethyl)phosphine hydrochloride (TCEP · HCl) kept the Cys-residues reduced. Success of the ligation was examined by LC/MS and the ESI-MS is shown in **figure A11**. The calculated and observed ion masses of the correct ligation product are depicted in **table 3**.

Table 3: Calculated and observed masses of Name2 after the first ligation attempt

	$[M+3]^{3+}$	$[M+4]^{4+}$	$[M+5]^{5+}$	$[M+6]^{6+}$	$[M+7]^{7+}$
Calculated:	1573.2	1180.1	944.3	787.1	674.8
Observed:	1572.9	1179.9	943.1	787.1	674.8

Subsequent to the LC/MS, purification by RP-HPLC was carried out and the fractions were analysed by ESI-MS. Unfortunately no masses belonging to the correct ligation product could be identified.

2. Ligation attempt

MPAA, TCEP · HCl and a buffer made of Gn · HCl and Na_2HPO_4 were also used for this ligation attempt, but the reaction was carried out at a pH of 6.98 and larger amounts of starting material were used (15.33 mg N-terminus and 9.30 mg C-terminus). Additionally, the reaction mixture was degassed under nitrogen. After 24 hours, the mixture was loaded onto a preparative column and purified by RP-HPLC, where the correct ligation product eluted after approximately 34 minutes (**figure 22**).

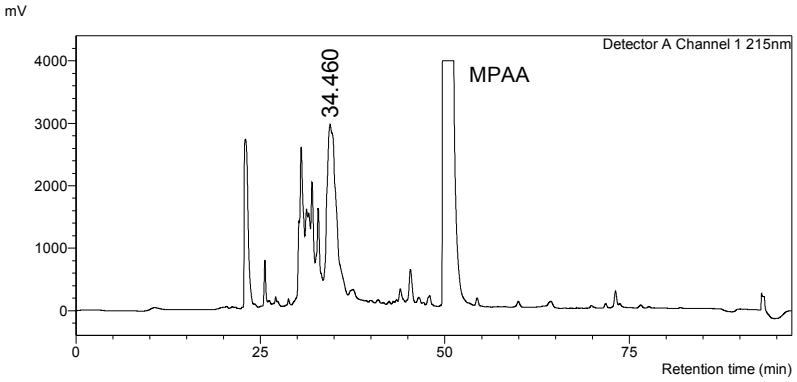

Figure 22: RP-HPLC chromatogram of the purification of the Name2 ligation mixture

The presence of the ligation product was determined by ESI-MS and the calculated and observed masses are depicted in **table 4**. Because the ESI-MS (**figure A12**) also showed peaks of unrelated masses, an analytical RP-HPLC (**figure 23**) was performed to check the purity, which showed several other peaks, but the dominant peak belonged to the correct ligation product. The mass of dry product obtained during the ligation was 4.55 mg.

Table 4: Calculated and observed masses of Name2 after the second attempt of ligation

	$[M+3]^{3+}$	$[M+4]^{4+}$	$[M+5]^{5+}$	$[M+6]^{6+}$	$[M+8]^{8+}$	$[M+11]^{11+}$
Calculated:	1573.2	1180.1	944.3	787.1	590.6	429.8
Observed:	1572.6	1179.6	943.8	786.9	590.1	430.0

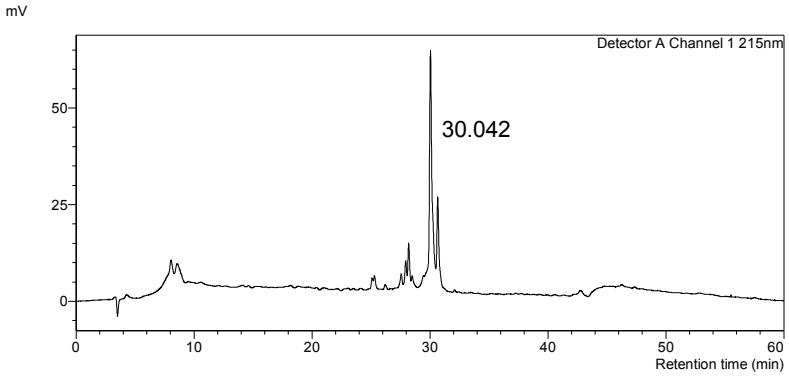

Figure 23: Analytical RP-HPLC chromatogram of Name2 obtained during the ligation

2.5.1.4 Folding of Name2

In the folding process, the thiol groups of two Cys-residues are oxidised to a disulfide bond. Name2 has six Cys-residues, so three disulfide bonds are established and because one Cys-residue can form a bond with any of the other ones, 15 isomers are possible. A trial oxidation is therefore performed to find the optimal buffer conditions that favour the correctly folded peptide. The analytical RP-HPLC chromatograms of oxidations under eight different conditions are shown in **figure 24**.

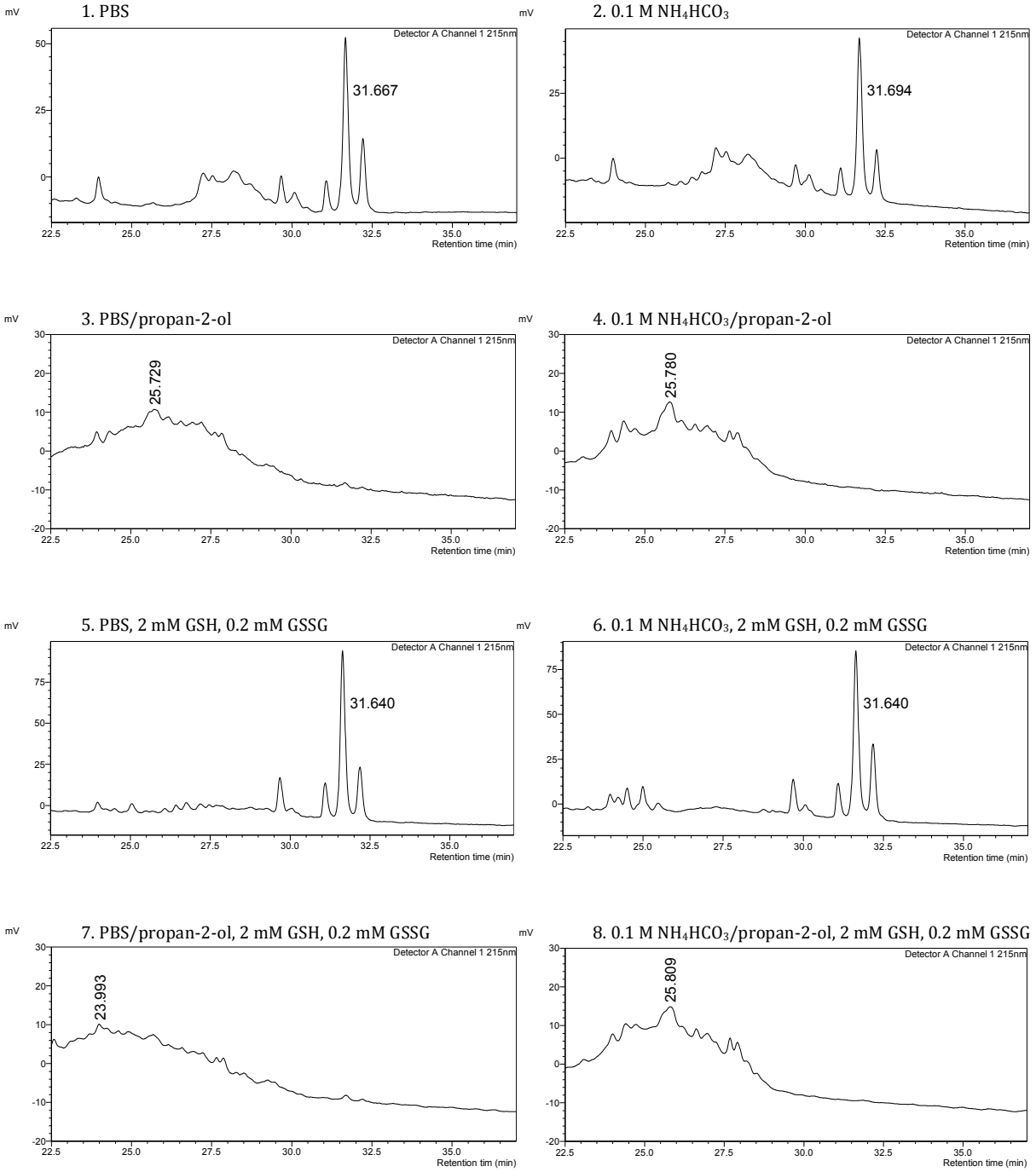

Figure 24: Analytical RP-HPLC chromatograms of the Name2 trial oxidation under different conditions

Condition 5 was found not only to result in the highest peak, but also in the best peak height ratio between the major product and other constituents of the mixture. Oxidation conditions that included the use of propan-2-ol resulted in no clear peak. 1.91 mg of reduced Name2 was then oxidised in phosphate buffered saline (PBS), 2 mM reduced glutathione (GSH) and 0.2 mM oxidised glutathione (GSSG) overnight at 23 °C, before the oxidation mixture was purified by RP-HPLC (**figure 25**).

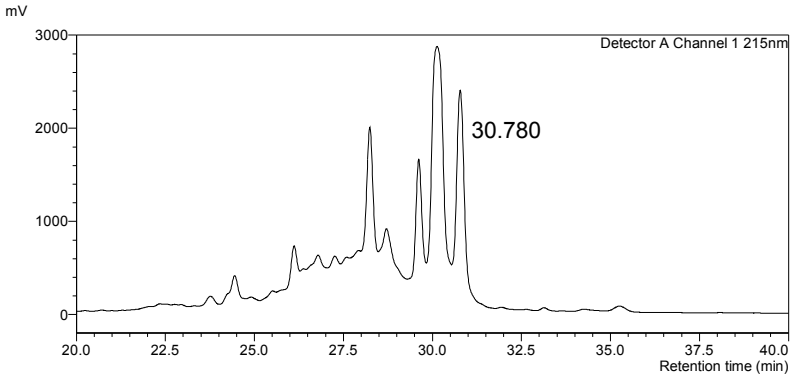

Figure 25: RP-HPLC chromatogram of the Name2 oxidation mixture; oxidised Name2 eluted after 30.8 minutes

ESI-MS was used to analyse the eluate the ESI-MS of oxidised Name2 is shown in **figure A13**, whereas the calculated and observed masses of oxidised Name2 are summarized in **table 5**. The oxidation of the Cys-residues formed three disulfide bonds and caused the peptide to loose six masses. 1.27 mg of oxidised Name2 was obtained and the chromatogram of the analytical RP-HPLC performed to check the purity of the product is shown in **figure 26**.

Table 5: Calculated and observed masses of oxidised Name2

	$[M+3]^{3+}$	$[M+4]^{4+}$	$[M+5]^{5+}$	$[M+6]^{6+}$	$[M+11]^{11+}$
Calculated:	1571.2	1178.6	943.1	786.1	429.2
Observed:	1570.5	1178.0	942.7	786.1	430.3

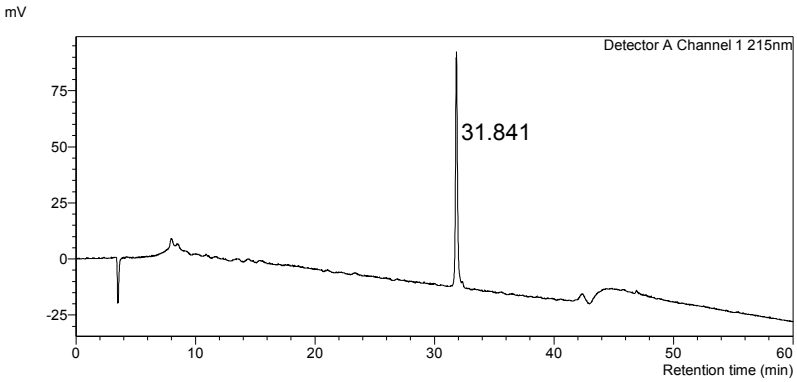

Figure 26: Analytical RP-HPLC of oxidised Name2

2.5.1.5 NMR of Name2

A 1D ^{1}H NMR spectrum of oxidised Name2 was recorded and it showed well dispersed peaks, which indicates that the peptide is folded properly and adopts an ordered structure in solution. Next, 2D NMR spectroscopy was used to determine the structure. The ^{1}H chemical shifts were assigned as described before [43]. Briefly, total correlation spectroscopy (TOCSY) spectra were recorded and used to identify the ^{1}H spin system of each residue and the connectivities between the amino acids, determined by assigning the peaks for NH-NH_{i+1}, Hα-NH_{i+1} and Hβ-NH_{i+1} in the nuclear Overhauser enhancement spectroscopy (NOESY) spectrum, were used to assign each residue to a specific position in the sequence (**figure 27**). Proline, which Name2 has three of in its sequence, does not have a proton attached to the nitrogen when it is part of a peptide bond, therefore no Hα-NH_{i+1} connectivities could be assigned for these residues. Instead, sequential connections to the proline Hδ protons were used to confirm assignments and to confirm that all three Pro-residues are in a trans conformation.

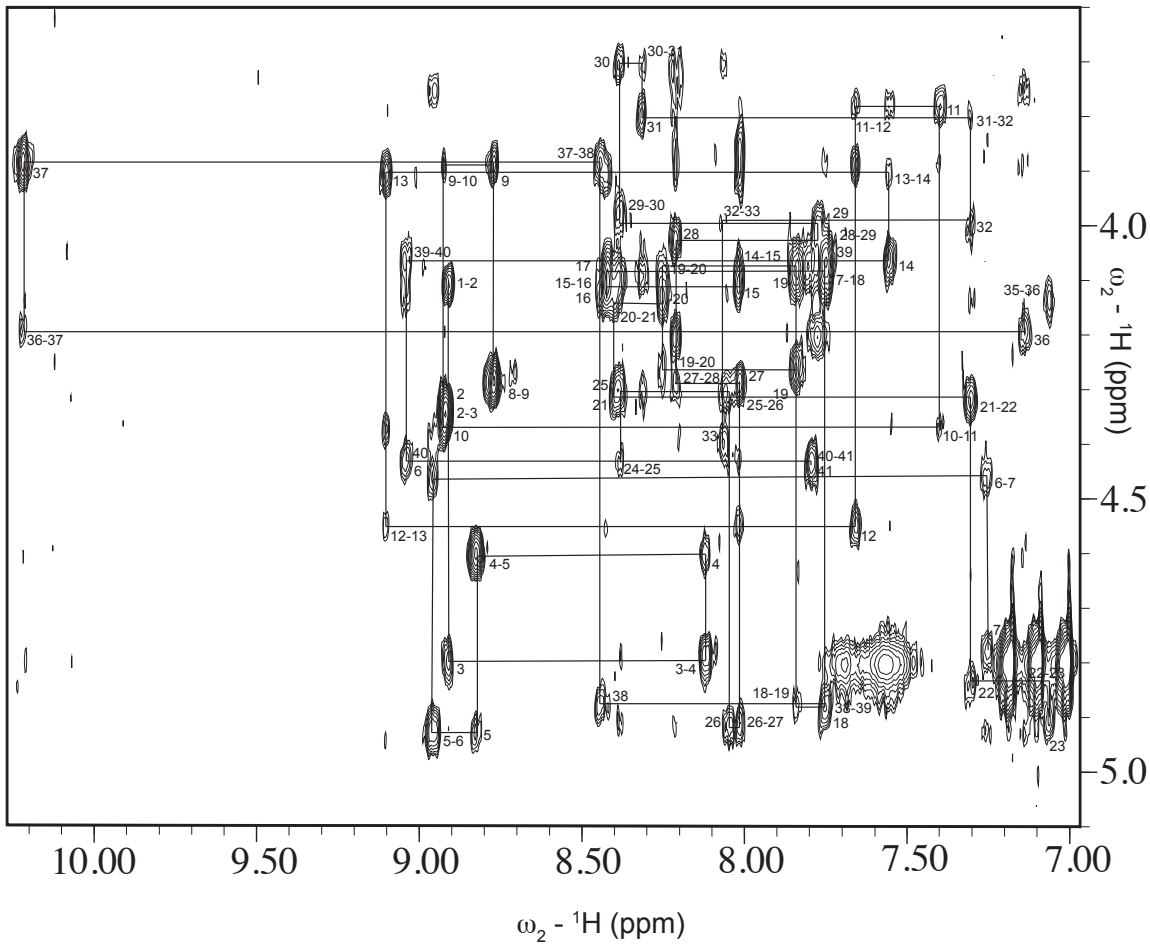

Figure 27: ^{1}H NOESY spectrum showing the sequential assignment of Name2 by connecting the Hα-NH_{i+1} cross peaks. The cross peak of $H\alpha_{33}$-NH_{34} was not observed in this spectrum.

Figure 28 shows the Hα secondary chemical shifts for Name2, which were calculated by taking the difference of the observed Hα chemical shifts and Hα random coil chemical shifts of the same residue [44]. Cα and Cβ secondary chemical shifts are shown in **figure 29**. The secondary chemical shifts can provide important data about the secondary structure of the peptide. Hα secondary chemical shifts below –0.1 ppm of four or more residues is indicative of a helix, whereas β-strand like structures have Hα secondary chemical shifts greater than +0.1 ppm of at least three residues [45]. Between Pro8 and Lys17, as well as between Ser27 and Leu32 Hα secondary chemical shift values are all more negative than –0.1 ppm, which suggests that Name2 has two regions of helical secondary structures but no β-strand.

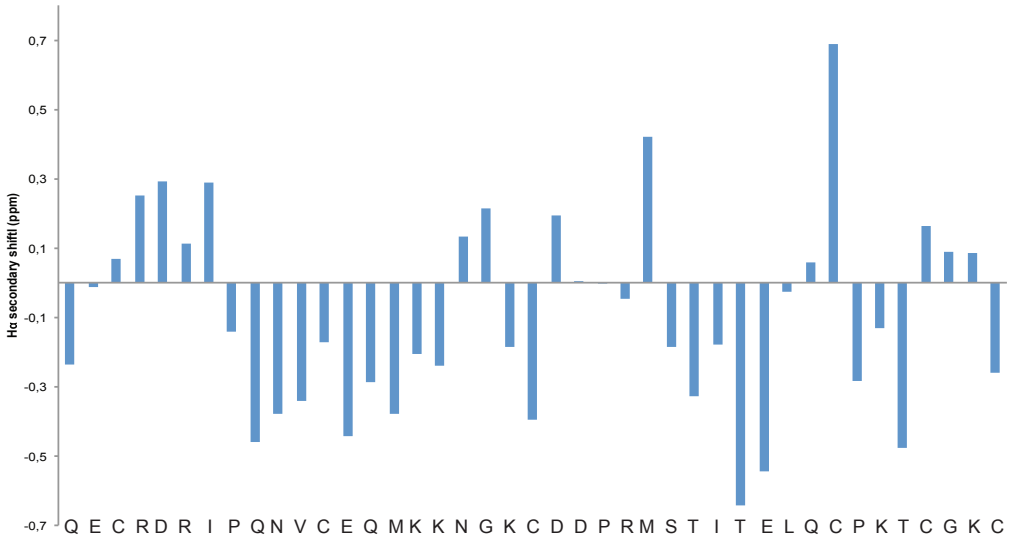

Figure 28: Hα secondary chemical shifts of Name2

Similarly, secondary structure can be inferred by using the secondary chemical shift of the carbon atoms [46]. For this purpose a 2D ^{1}H – ^{13}C heteronuclear single quantum coherence (HSQC) spectrum was recorded at natural abundance and analysed. The Cα secondary chemical shifts of Pro8 to Lys17 and Ser27 to Gln33 exceed +0.7 ppm, which is also indicative of a helical structure. The secondary chemical shift of the β-carbons can only be used for the identification of β-strands, and the Cβ of at least three consecutive residues should have secondary chemical shifts that exceed +0.7 ppm (4.0 ppm for Pro) to indicate a β-strand, which is not the case for Name2.

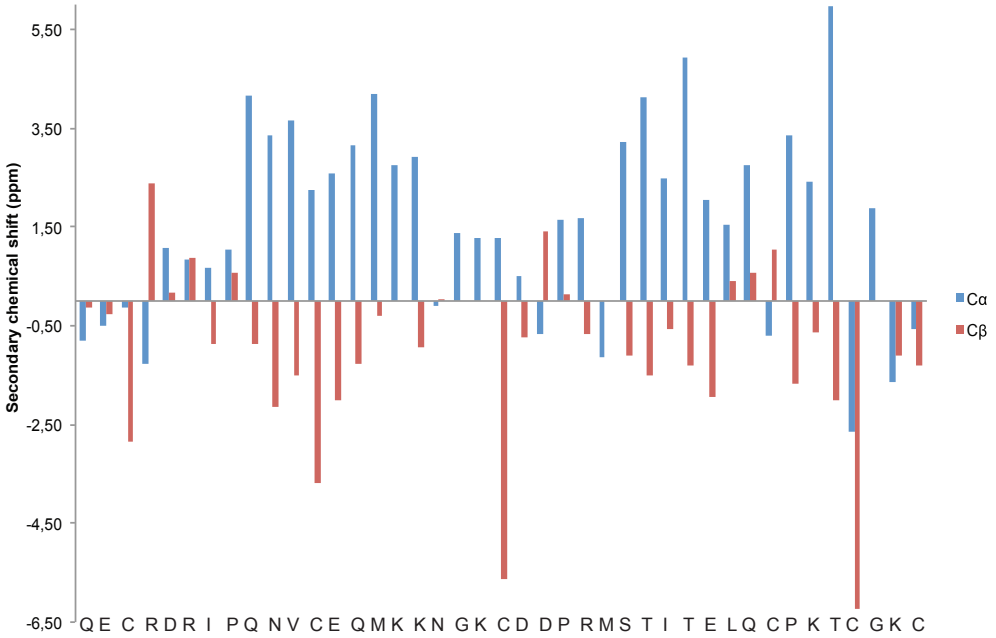

Figure 29: Cα and Cβ secondary chemical shifts of Name2

Determination of the three dimensional structure of Name2 was based on distance restraints from NOESY cross peaks, dihedral angle restraints derived from coupling constants and on patterns of chemical shifts. **Table 6** lists the statistics for the ensemble of the 15 lowest energy structures of Name2. 409 distance restraints and 73 dihedral angle restraints were included in structure calculations performed with the program CYANA and the ensemble of the 15 lowest energy structures chosen to represent the solution structure of Name2 is shown in **figure 30.** The structures did not have nuclear Overhauser effect (NOE) violations exceeding 0.2 Å or dihedral violations exceeding 2.0 Å and have good covalent geometry as evident from low target functions and good Ramachandran statistics.

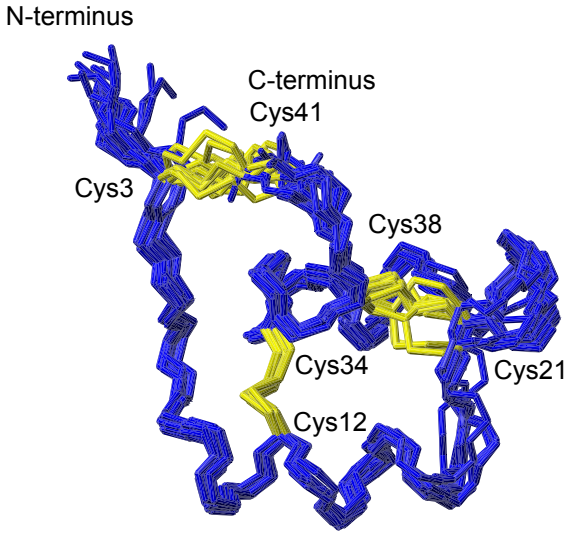

Figure 30: Ensemble of the 15 lowest energy structures of Name2. The backbone of the peptide is shown in blue and the cystines are shown in yellow.

Table 6: Statistics for the ensemble of the 15 lowest energy structures of Name2

Distance restraints	
Intraresidue (i-j = 0)	197
Sequential (/i-j/ = 1)	140
Medium range (/i-j/ <5)	51
Long range (/i-j/ ≥5)	21
Hydrogen bonds	28 (for 14 hydrogen bonds)
Total	409
Dihedral angle restraints	
Φ	29
X^1	12
Ψ	32
Total	73
CYANA score (kcal/mol)	
Target function	$7.49 \bullet 10^{-2} \pm 2.19 \bullet 10^{-2}$
Violations from experimental restraints	
NOE violations exceeding 0.2 Å	0
Dihedral violations exceeding 2.0 °	0
Ramachandran statistics	
Most favoured	84.5 %
Additionally allowed	12.3 %
Generously allowed	0 %
Disallowed	0 %
Atomic RMSD (Å)	
Backbone atoms	0.95 ± 0.28
Heavy atoms	1.79 ± 0.43

The calculated structure has a root mean square deviation (RMSD) of 0.95 ± 0.28 Å for the backbone atoms and 1.79±0.49 Å for the heavy atoms. The ribbon depictions of the mean structure of Name2 and ShK are shown in **figure 31**. Name2 has two α-helices, one between Pro8 – Lys17 and the other between Ser27 – Leu32. The fold resembles ShK, which has two helical structures between Ala14 – His19 and Met21 – Arg24, but the length and positioning of the helices differ, presumably due to differences in the number

of residues between CysII – CysIII (9 residues in Name2 and 5 residues in ShK) and CysIII – CysIV (13 residues in Name2 and 11 residues in ShK) [47]. The disulfide connectivity in Name2 has been assumed to be similar as proposed for ShK, which is consistent with our data [47].

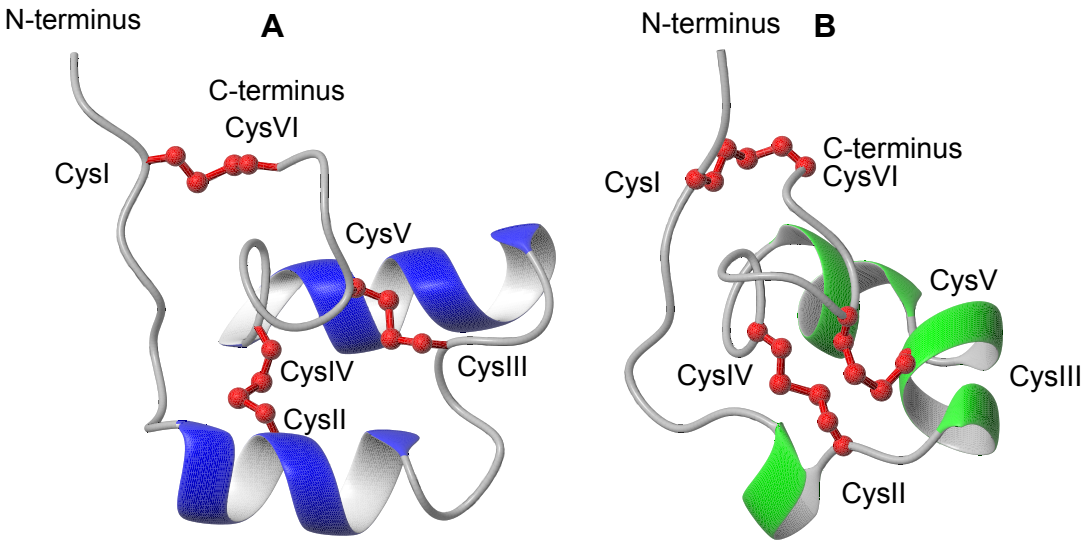

Figure 31: Ribbon depiction of the mean structures of Name2 (**A**) and ShK (**B**).

2.5.2 Synthesis of Acan1

Acan1 is a 51 residue long peptide with a molecular weight of 5865.5 Da. It was discovered in the transcriptome of the dog hookworm *A. caninum* and its synthesis was attempted as a part of this project. Similar to the synthesis of Name2, the sequence was divided into two halves; a requirement is that Acan1 C-terminus must have a Cys-residue at its N-terminal end (**figure 32**).

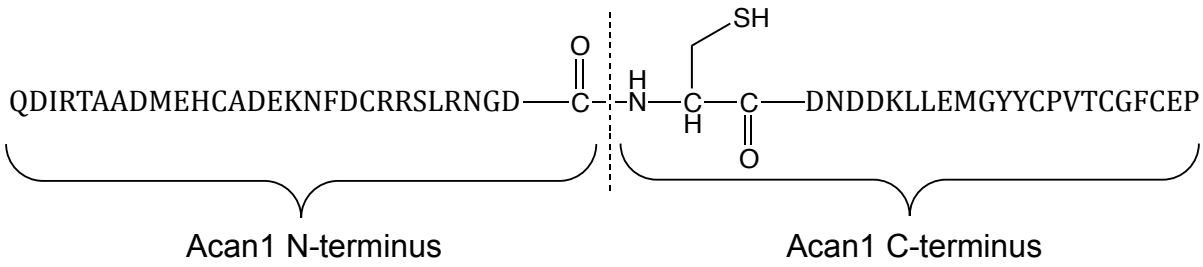

Figure 32: Amino acid sequence of Acan1

Two different strategies for the synthesis of the precursor for the Acan1 N-terminus thioester peptide were applied (**figure 33**):

1) Acan1 N-terminus was synthesised as a peptide hydrazide, which was then oxidised to the peptide azide after cleavage from the resin. The azide group is displaced by the arylthiol that forms the peptide thioester required for the ligation.

2) Because the first strategy was not successful, Acan1 N-terminus was synthesised with a Dbz group attached to the C-terminal residue, which is then converted to a peptide-Nbz before exchanged with an arylthiol. The thioester is then supposed to take part in the ligation with Acan1 C-terminus. The N-terminal Gln-residue had again to be Boc-protected.

The synthesis of Acan1 C-terminus should have been straightforward and 2-chlorotrityl chloride resin was used in the first synthesis attempt. But, ESI-MS of a test cleavage carried out after attachment of ten residues showed no masses belonging to the correct peptide. This might have been due to peptide aggregation caused by the high loading of the resin (1.3 mmol/g). Then, Wang resin was used as a solid support for the synthesis, but this also failed because, proline, which is the C-terminal residue, may have formed a diketopiperazine [48]. Finally, Rink Amide MBHA resin was tried for the synthesis of Acan1 C-terminus using an automated peptide synthesiser, although it would result in the amidation of the C-terminal residue.

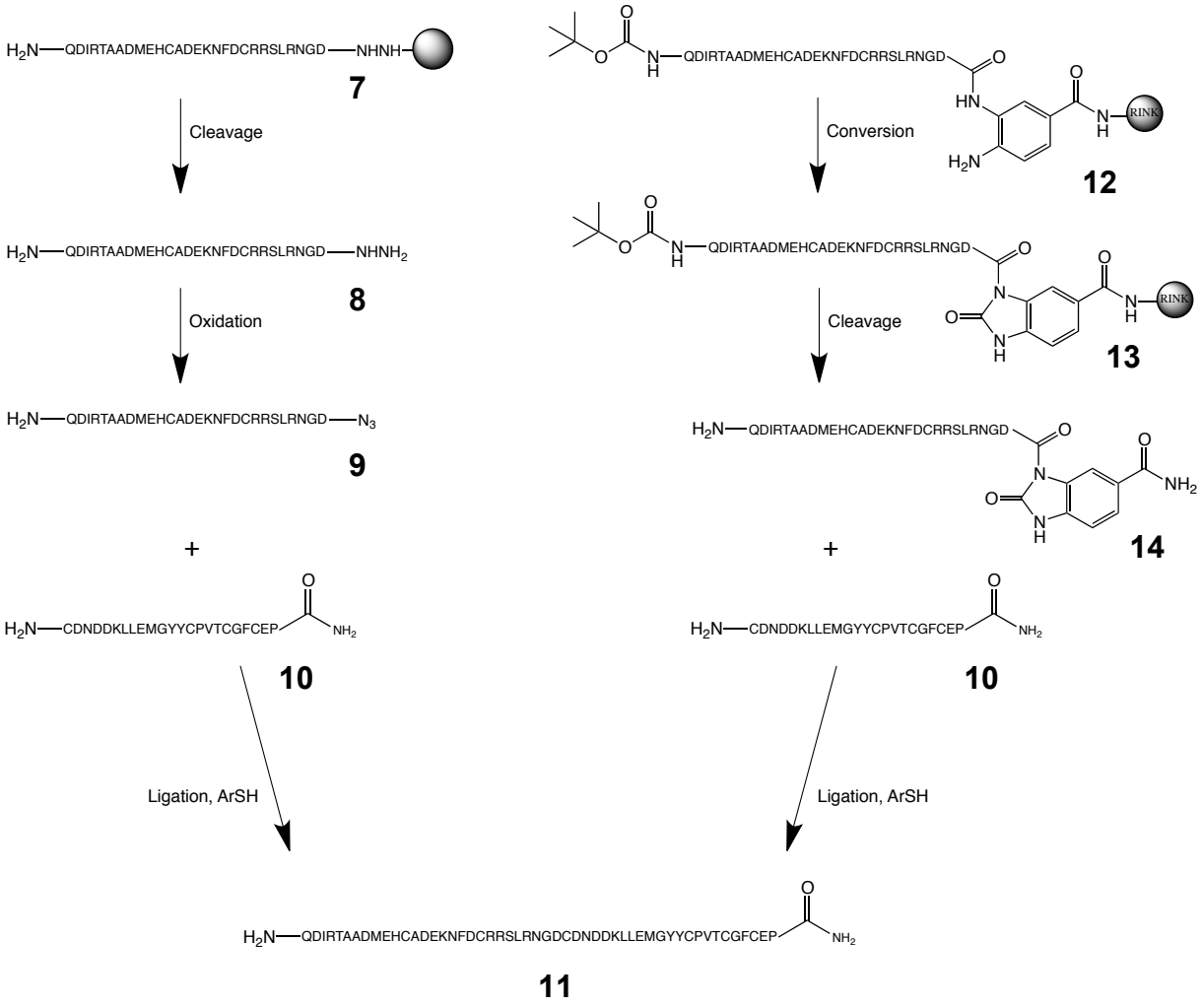

Figure 33: In the first synthesis strategy applied, Acan1 N-terminus peptide hydrazide bound to the resin (**7**) is liberated by TFA-cleavage to yield the unprotected peptide hyrazide (**8**), which is subsequently oxidised to the peptide azide (**9**). Acan1 C-terminus (**10**) and **9** were then thought to ligate, giving Acan1 (**11**). Second strategy: Acan1 N-terminus with a Dbz-group attached to the C-terminal residue (**12**) was converted to yield the peptide-Nbz (**13**). A cleavage liberated the unprotected peptide-Nbz (**14**). **10** and **14** were supposed to yield Acan1 by ligation. Only the Boc-group protecting the N-terminal Gln-residue of **12** and **13** is shown, the other protecting groups are omitted.

2.5.2.1 Synthesis of the Acan1 N-terminus as a peptide hydrazide

The Acan1 N-terminus was synthesised manually as a peptide hydrazide on a 0.25 mmol scale using the 2-chlorotrityl chloride resin. Loading of hydrazine hydrate onto the resin and standard Fmoc-SPPS were applied to assemble the peptide hydrazide. Repetitive couplings of almost every residue were necessary to achieve satisfactory coupling yields.

Cleavage of 336 mg peptidyl resin using a mixture of TFA/TIPS/DODT/H_2O resulted in 159 mg of peptide crude, which was analysed by ESI-MS. The $[M+3]^{3+}$ and $[M+4]^{4+}$ of the peptide could be identified (**figure A14** and **table 7**). The peptide crude was purified by RP-HPLC where the peptide hydrazide eluted after approximately 31 minutes (**figure 34**).

Table 7: Calculated and observed masses of Acan1 N-terminus peptide hydrazide crude and purified fraction

		$[M+3]^{3+}$	$[M+4]^{4+}$
Calculated:		1094.8	821.4
Observed:	Crude	1094.6	820.8
	Purified	1094.4	821.1

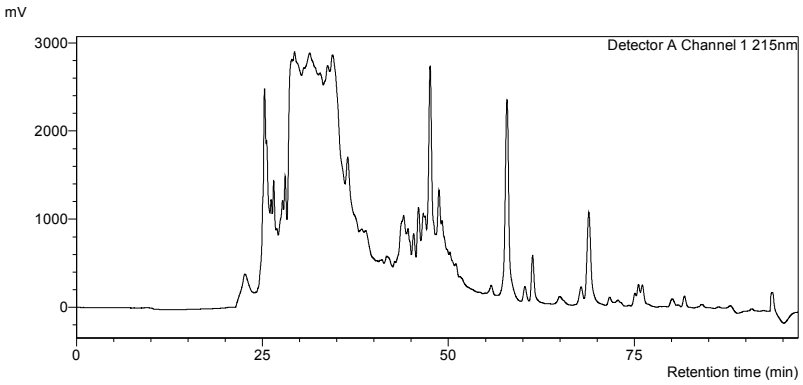

Figure 34: RP-HPLC chromatogram of the purification of Acan1 N-terminus peptide hydrazide

Fractions containing the correct product were identified by ESI-MS, and analytical RP-HPLC was used to determine the purity of the fractions. The ESI-MS and analytical RP-HPLC chromatogram for the most pure fraction that will be used for the ligation is shown in **figures A15** and **35**, respectively. The observed masses are depicted in **table 7**. The mass of dry product at the end was 17.4 mg.

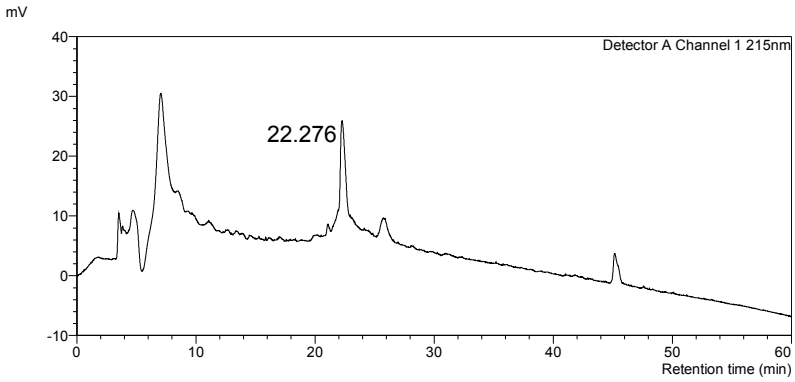

Figure 35: Analytical RP-HPLC chromatogram of purified Acan1 N-terminus peptide hydrazide

2.5.2.2 Synthesis of Acan1 C-terminus

The Acan1 C-terminus was synthesised on a 0.25 mmol scale using Rink Amide MBHA resin and an automated synthesiser. 1.661 g of peptidyl resin was obtained, of which 379 mg was cleaved using TFA/TIPS/DODT/H_2O, resulting in 159 mg of dry peptide crude. In order to confirm the presence of the correct peptide in the crude, an ESI-MS (**figure A16**) was recorded and the calculated and observed masses are summarized in **table 8**. The chromatogram of the analytical RP-HPLC of the peptide crude is shown in **figure 36**.

Table 8: Calculated and observed masses of Acan1 C-terminus peptide crude and purified fraction

		$[M+2]^{2+}$
Calculated:		1308.5
Observed:	Crude	1307.9
	Purified	1307.9

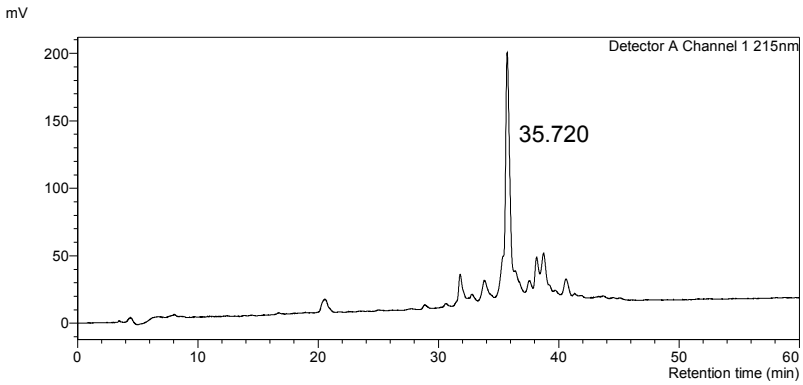

Figure 36: Analytical RP-HPLC chromatogram of Acan1 C-terminus peptide crude

In the next step, 73 mg of peptide crude was purified by RP-HPLC, where the peptide eluted after approximately 48.5 minutes. A total of six fractions containing the correct peptide were identified by ESI-MS and analytical RP-HPLC was used to evaluate the purity of each fraction. The observed mass of the $[M+2]^{2+}$ is shown in **table 8** and the ESI-MS and analytical RP-HPLC chromatogram of the most pure fraction is depicted in **figures A17** and **37**, respectively. 20.71 mg of dry product was saved for the ligation.

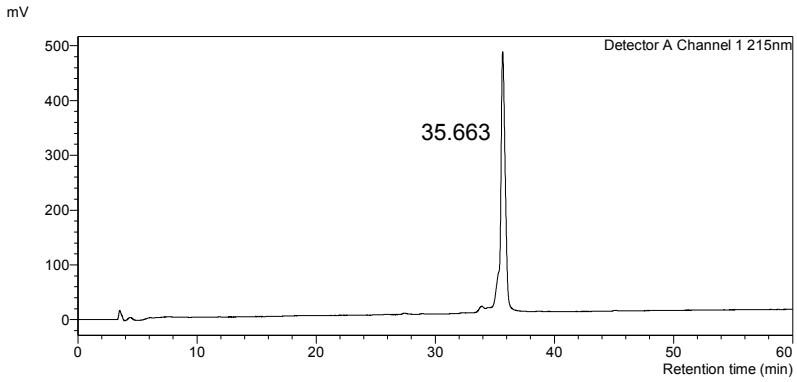

Figure 37: Analytical RP-HPLC chromatogram of purified Acan1 C-terminus

2.5.2.3 Native chemical ligation of Acan1 using a peptide hydrazide

Acan1 N-terminus peptide hydrazide and Acan1 C-terminus were dissolved in ligation buffer at a low pH and sodium nitrite ($NaNO_2$) was then added for the oxidation step. MPAA was introduced for the thioester formation followed by a pH adjustment to 7.6 and the reaction mixture was then allowed to react overnight at 23 °C. The mixture was loaded onto an analytical column and purified by RP-HPLC. The chromatogram is shown in **figure 38**.

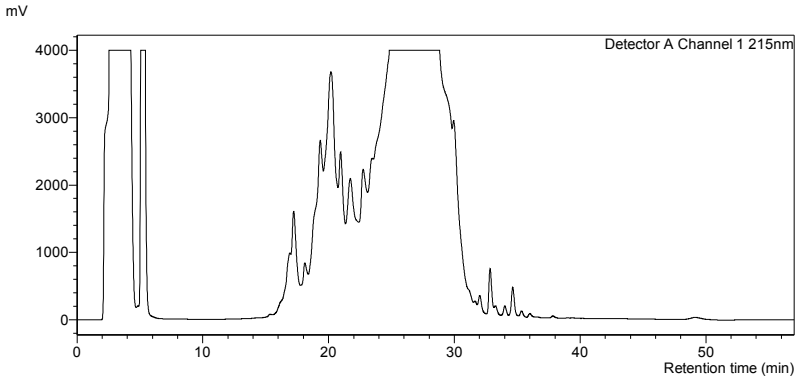

Figure 38: RP-HPLC chromatogram of the purification of the Acan1 ligation mixture

The eluate was analysed by ESI-MS, but no correct ligation product could be detected. The ESI-MS of the fraction collected at 17.5 minutes is depicted in **figure 39** and shows masses of 817.3 ($[M+4]^{4+}$) and 1089.1 ($[M+3]^{3+}$) that could correspond to a molecule with a molecular weight of 3265 Da. A possible explanation for this is that the side chain of the C-terminal Asp-residue reacted with the hydrazide group and formed a cyclization product (**figure 40**) which is unable to take part in the ligation process [49].

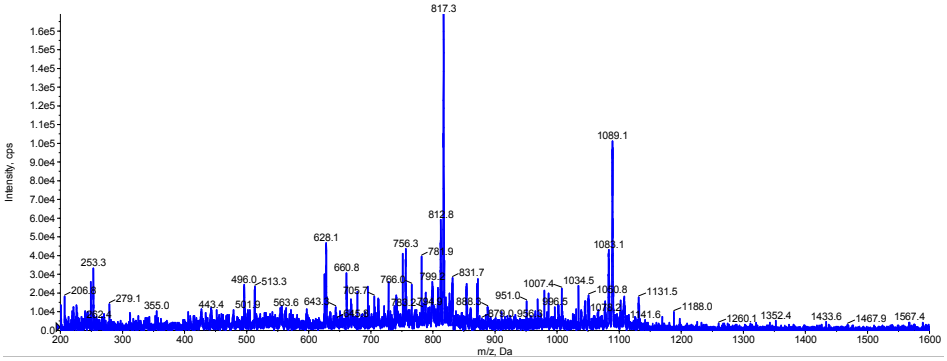

Figure 39: ESI-MS of the fraction that presumably contains the cyclization product of Acan1 N-terminus peptide hydrazide

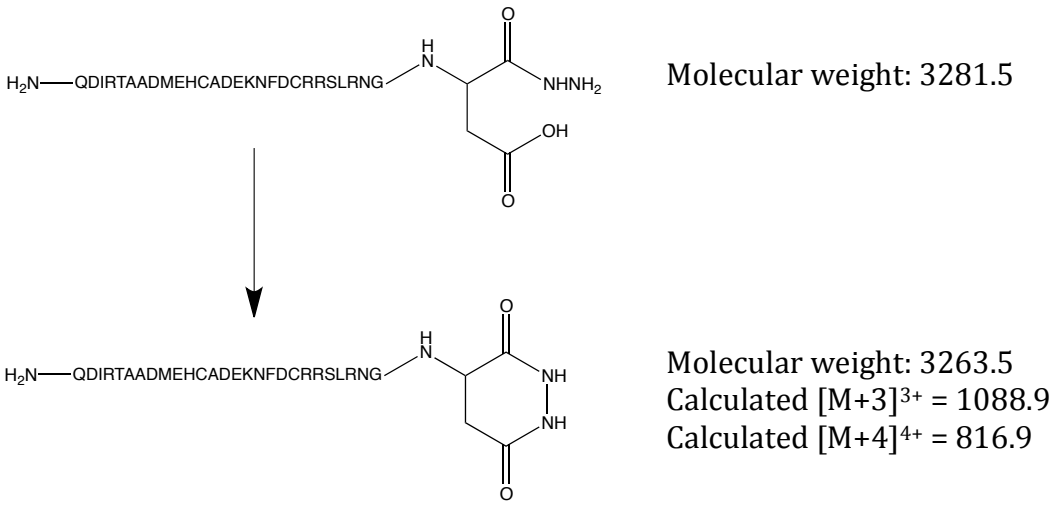

Figure 40: Aspartic acid reacts with the hydrazide group and forms an intra-molecular cyclization product

2.5.2.4 Synthesis of Acan1 N-terminus with a Dbz-group

For this synthesis, Dbz was manually loaded onto the Rink Amide MBHA resin using Fmoc-Dbz. The loaded resin was transferred to an automated synthesiser, which carried out the chain elongation of the peptide. A test cleavage was carried out right after the

synthesis and the ESI-MS (**figure A18**) showed the presence of the desired product and a by-product having a calculated molecular weight of approximately 116.5 Da less than the correct product (**table 9**).

Table 9: Overview of the calculated and observed masses of correct Acan1 N-terminus with the Dbz group and the by-product

		Molecular weight	$[M+3]^{3+}$	$[M+4]^{4+}$
Calculated for Acan1 N-terminus with Dbz:		3400.8	1134.6	851.2
Observed:	Acan1 N-terminus peptide with Dbz	–	1134.2	851.0
	By-product	3283.8 –3284.4 (calculated)	1095.6	822.1

For the formation of the peptide-Nbz, 397 mg of peptidyl resin was treated with 4-nitrophenyl chloroformate and DIPEA. The subsequent cleavage, using a mixture of TFA/TIPS/DODT/H_2O, resulted in the peptide crude, which was analysed by ESI-MS and showed only a minor peak for the $[M+3]^{3+}$ of the correct peptide-Nbz (**figure A19** and **table 10**). The peaks indicating masses of 1104.8 and 828.5 correspond to the by-product activated to a peptide-Nbz.

Table 10: Calculated and observed masses of Acan1 N-terminus peptide-Nbz and the observed masses of the by-product as a peptide-Nbz

		$[M+3]^{3+}$	$[M+4]^{4+}$
Calculated for Acan1 N-terminus peptide-Nbz:		1143.2	857.7
Observed:	Acan1 N-terminus peptide-Nbz	1143.8	–
	By-product peptide Nbz	1104.8	828.5

65 mg of peptide crude was then purified by RP-HPLC using a preparative column (**figure 41**). The fractions were analysed by ESI-MS and several fractions contained the peptide-Nbz of the by-product (**figure A20**), which eluted after approximately 33 minutes, but only one fraction contained the correct Acan1 N-terminus peptide-Nbz, which eluted after 43.5 minutes (**figure A21**). Analytical RP-HPLC chromatograms of the

most pure by-product peptide-Nbz and fraction containing the correct Acan1 N-terminus peptide-Nbz are shown in **figures 42** and **43**, respectively.

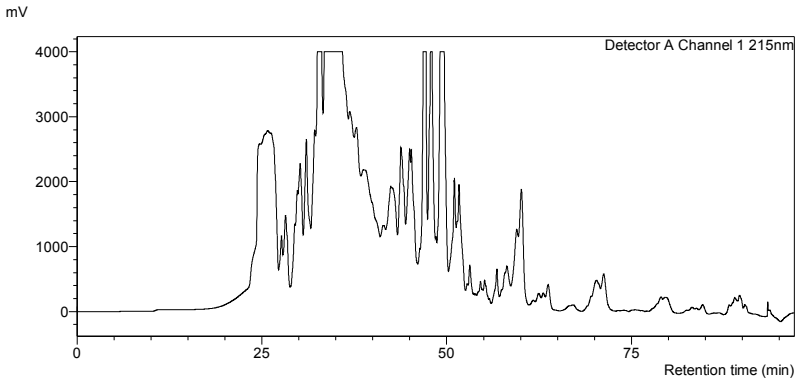

Figure 41: RP-HPLC chromatogram of the purification of the first batch of Acan1 N-terminus peptide crude

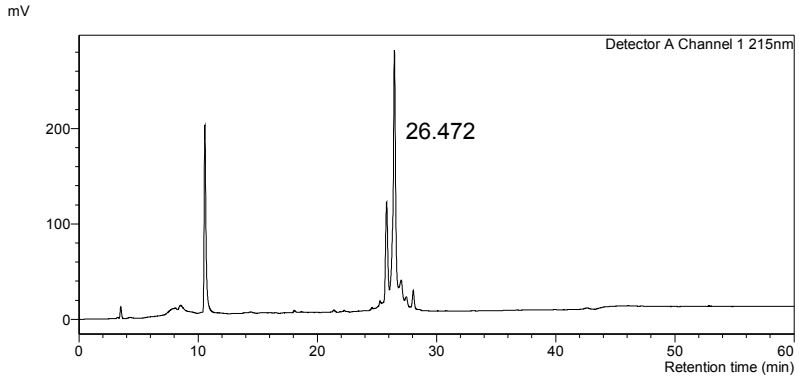

Figure 42: Analytical RP-HPLC chromatogram of purified by-product peptide-Nbz

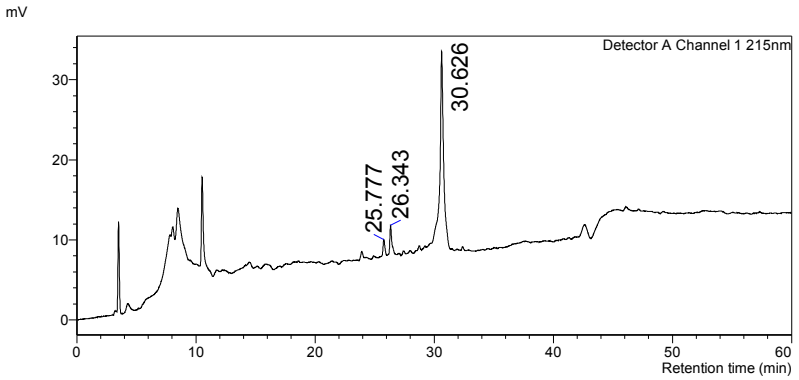

Figure 43: Analytical RP-HPLC chromatogram of the fraction containing the correct Acan1 N-terminus peptide-Nbz

Another batch of peptidyl resin (407 mg) was activated using 4-nitrophenyl chloroformate and DIPEA. After the cleavage with TFA/TIPS/DODT/H_2O, ESI-MS was

used to analyse the peptide crude, and this time no ions of the Acan1 N-terminus peptide-Nbz could be detected. The $[M+3]^{3+}$ (1104.5) and $[M+4]^{4+}$ (828.6) of the by-product peptide-Nbz can be seen on the spectrum (**figure A22**). 60 mg of peptide crude was then purified by RP-HPLC and ESI-mass spectra of the fractions were recorded (**figure A23**). The by-product peptide-Nbz eluted after approximately 31.5 minutes (**figure 44**). To determine the purity of the fraction an analytical RP-HPLC was carried out, which is shown in **figure 45**.

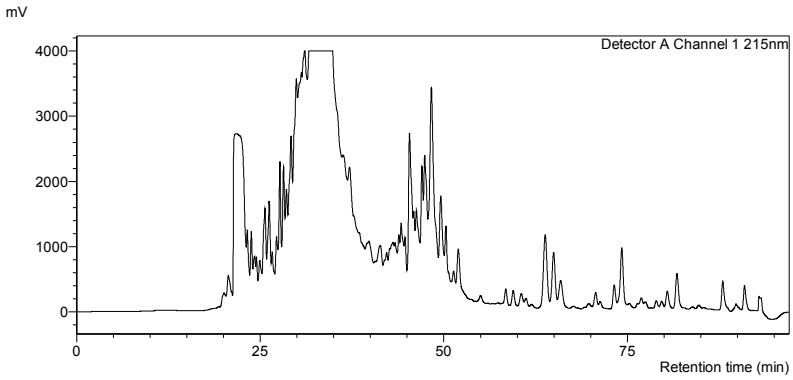

Figure 44: RP-HPLC chromatogram of the purification of the second batch of Acan1 N-terminus peptide crude

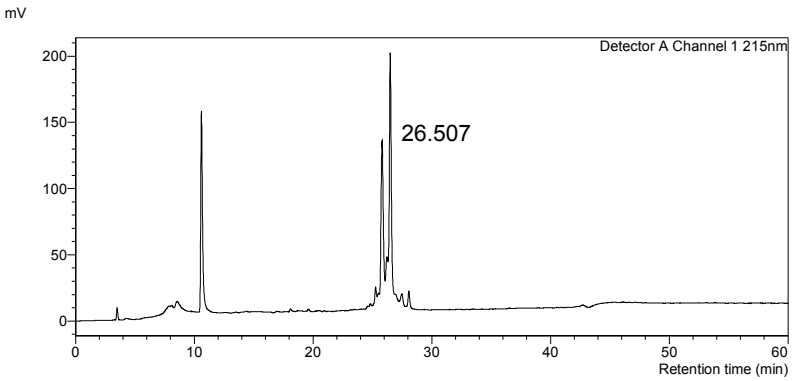

Figure 45: Analytical RP-HPLC chromatogram of purified by-product peptide-Nb

*2.5.2.5 Native chemical ligation of of Acan1**

It was decided to use the by-product peptide-Nbz obtained during the synthesis of Acan1 N-terminus, from now on called Acan1* N-terminus, for a ligation with Acan1 C-terminus. The starting material, 11.37 mg Acan1* N-terminus and 9.40 mg Acan1 C-terminus, was dissolved in pH-adjusted ligation buffer. After 24 hours, the ligation mixture was purified by RP-HPLC, where Acan1* eluted after approximately 49 minutes

partially overlapping with the elution of MPAA. The chromatogram is shown in **figure 46**.

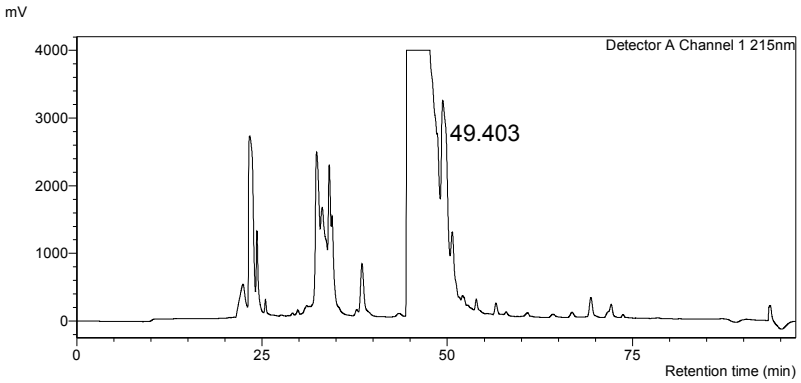

Figure 46: RP-HPLC chromatogram of the purification of the Acan1* ligation mixture

Three fractions containing Acan1* could be obtained and mass spectra of the fractions are shown in **figures A24 – A26**. The observed masses are summarized in **table 11**.

Table 11: Overview of the masses observed on the ESI-MS of the three fractions containing Acan1*

		$[M+4]^{4+}$	$[M+5]^{5+}$
Observed:	Fraction 37	1438.0	1150.6
	Fraction 38	1438.0	1150.5
	Fraction 39	1437.8	1150.8

Because the ESI-MS of the fractions also showed other major peaks, they were further analysed by RP-HPLC (**figure 47**) and the chromatograms showed a peak at a retention time of approximately 29 minutes, which is probably caused by MPAA. Acan1* has a retention time of 37.4 minutes and its peak can be seen in all three chromatograms. But, none of its peaks are perfect. In the chromatogram of fraction 37 the peak forms a shoulder, whereas it is possible to see the top of a second peak immediately to the right of the Acan1* peak in the chromatogram of fraction 38. The chromatogram of fraction 39 shows only a minor peak at a retention time of 37.4 minutes and a major peak around 37.9 minutes, meaning that this fraction is highly impure and only contains a little amount of Acan1*. The best candidates for an oxidation were therefore fractions 37 and 38, although they were not pure as well.

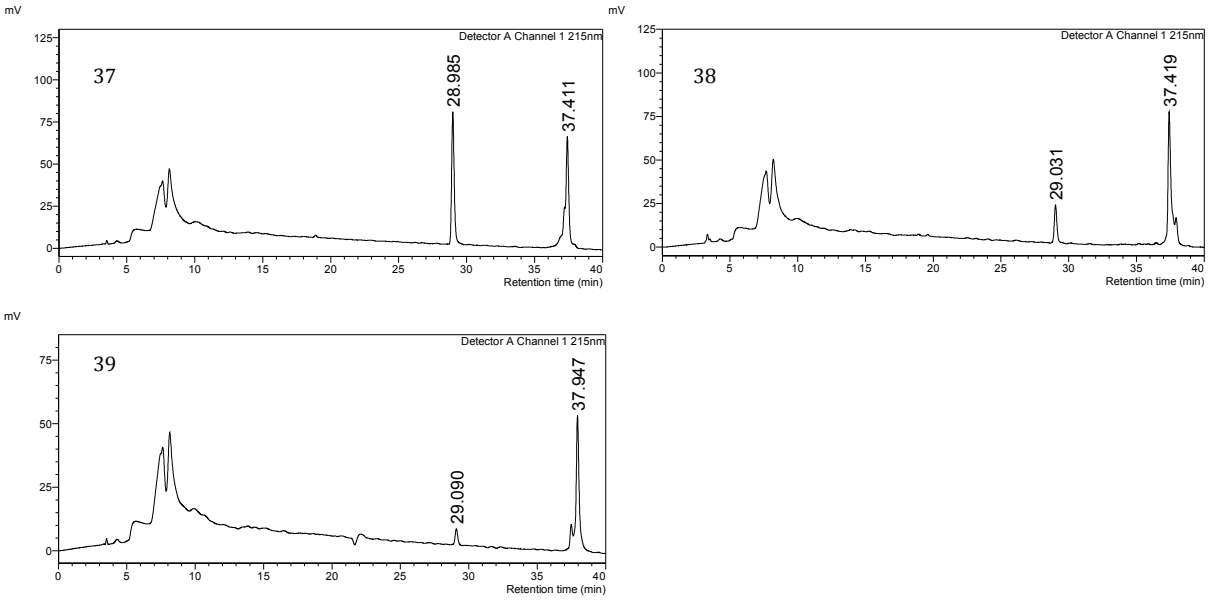

Figure 47: Analytical RP-HPLC of the fractions containing Acan1*

*2.5.2.6 Folding of Acan1**

The analytical RP-HPLC chromatograms of the trial oxidation under eight different conditions are shown in **figure 48**.

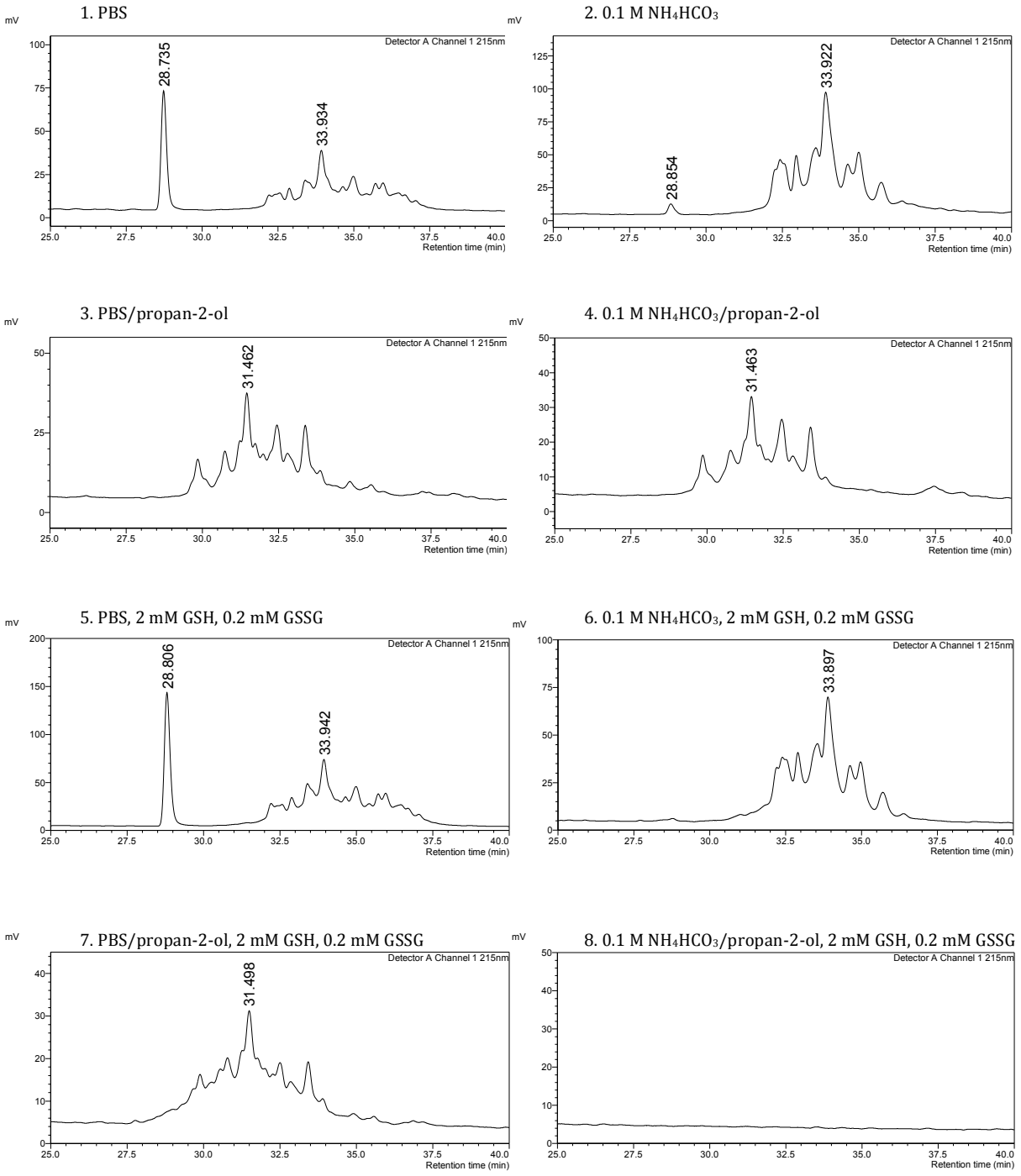

Figure 48: Analytical RP-HPLC chromatograms of the Name2 trial oxidation under different conditions

Comparison of the chromatograms shows that treatment with condition 2 leads to the highest peak at a retention time of 33.9 minutes. Three chromatograms show a peak for

MPAA around 28.8 minutes, which is the same retention time as can be seen in the chromatograms of the fractions with reduced Acan1*, whereas the peaks presumably belonging to oxidised Acan1* all have a shorter retention time compared to reduced Acan1*. Condition 8 resulted in no visible peak. 2.00 mg of reduced Acan1* was then oxidised in 0.1 M ammonium bicarbonate (NH_4HCO_3) and the oxidation mixture was purified by RP-HPLC (**figure 49**).

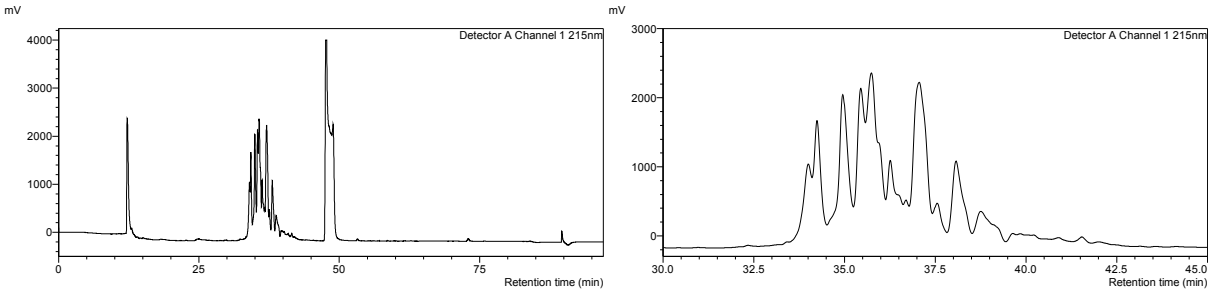

Figure 49: RP-HPLC chromatogram of the Acan1* oxidation mixture

ESI-MS was used to analyse the eluate and most of the fractions collected from 34 to 40 minutes contained oxidised Acan1*. The ESI-MS of the three fractions that generated the highest intensity on the mass spectrometer are shown in **figures A27 – A29**, whereas the observed masses of oxidised Acan1* are summarized in **table 12**.

Table 12: Overview of the masses observed on the ESI-MS of the three fractions containing oxidised Acan1*

		$[M+4]^{4+}$	$[M+5]^{5+}$
Observed:	Fraction 9	1436.7	1149.5
	Fraction 10	1436.3	1149.4
	Fraction 11	1436.4	1149.5

1.84 mg of oxidised Acan1* was obtained and the chromatograms of the analytical RP-HPLC performed to check the purity of the fractions containing oxidised Acan1* are shown in **figure 50**.

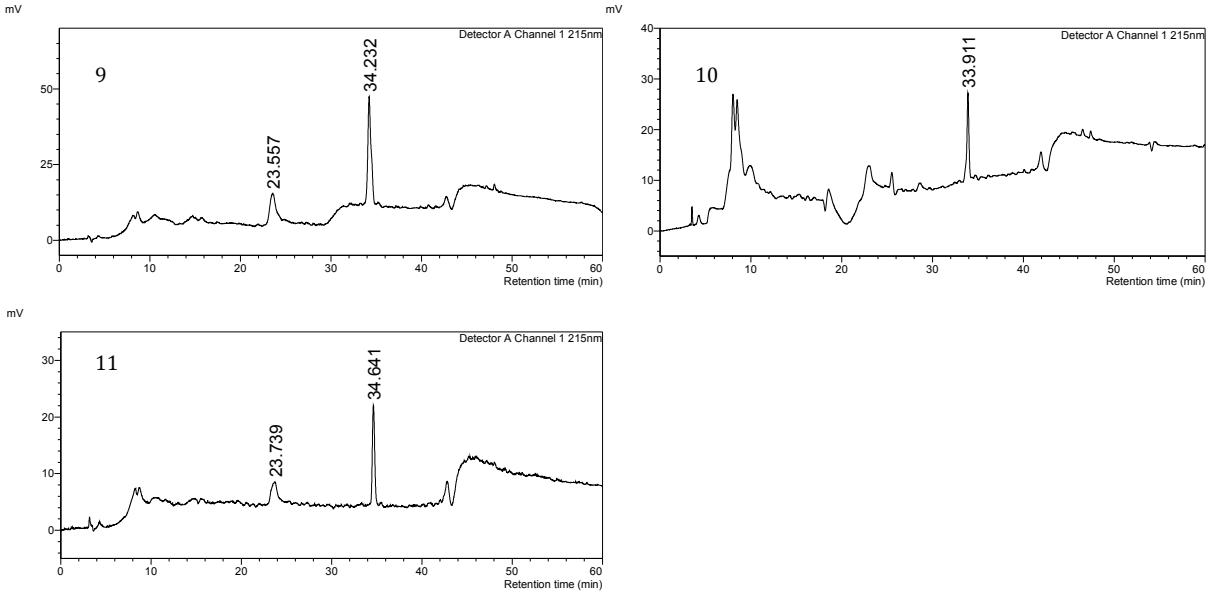

Figure 50: Analytical RP-HPLC chromatograms of the fractions that contained oxidised Acan1*

*2.5.2.7 NMR of Acan1**

A 1D ^{1}H NMR spectrum of Acan1* (**figure 51**) was recorded and the peaks in the amide bond region (7.8 – 8.5 ppm) are not well dispersed, which indicates that the peptide does not possess a well defined three dimensional structure.

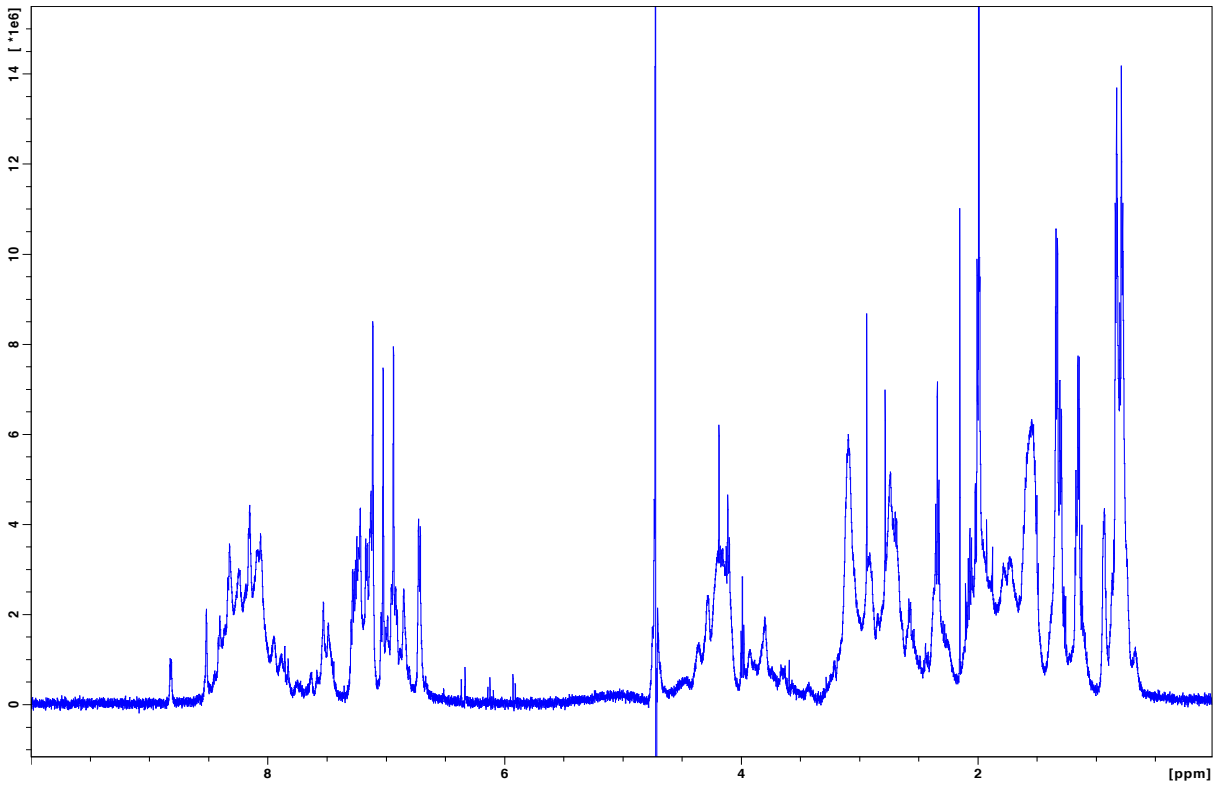

Figure 51: 1D ^{1}H NMR spectrum of Acan1*

2.5.2.8 Ligation of Acan1

The one fraction that contained the correct Acan1 N-terminus peptide-Nbz was used to try a ligation with Acan1 C-terminus to yield Acan1. After 24 hours, the ligation mixture was purified by RP-HPLC and the eluate was analysed by ESI-MS, but no correct ligation product could be detected.

3. Discussion

3.1 Bioactivity testing of fractionated LMW AcES

Autoimmune diseases are a major health burden and associated with an increasing number of cases in the developed world [50]. Therefore it is pivotal to have effective therapy options available, and for the inflammatory bowel diseases like ulcerative colitis and Crohn's disease a long list of selectable drugs exists, ranging from aminosalicylates over corticosteroids and immunosuppressants, to the novel biological TNF-α blockers [50]. But however effective these drugs are, they do not come without serious adverse effects like metabolic disturbances or a susceptibility to infections [50]. When the diseases progresses in spite of drug treatment or when patients are not able to take the drugs because the adverse effects are too severe, even invasive actions like surgery have to be considered [51, 52]. Therefore, new options for the treatment of autoimmune diseases are needed and they have to be effective, payable, convenient and safe.

The ability to infect a great number of individuals and to survive inside the host for several years has drawn the attention of researchers towards hookworms [18, 26]. The ES products of the hookworms are suspected to contribute an important part to the modulation of the host immune system and one aim of this project was therefore to fractionate crude LMW AcES and investigate the potential of the fractions to affect the course of experimental colitis in mice, which has similarities with Crohn's disease in humans [35].

Unfractionated LMW AcES is able to reduce the inflammatory cytokine IFN-γ and increase the level of IL-4, which shifts the immune response to the T_H2 branch (unpublished data). The first LMW AcES batch was fractionated and then tested in the

TNBS mouse model. Normally, the animals rapidly lose weight, but start to recover after 2 or 3 days. If the samples tested have any protective effect against the experimental colitis, the weight of those animals should be higher than the weight of the negative controls. When the first batch was tested, it looked like fraction E was able to achieve this, but this result was not significant. The colons of the healthy controls are significantly longer than the colons of all the other groups, except the fraction C group. In contrast, there was not found any statistical difference between the treated groups, including fraction C. Colon health was also assessed and the animals treated with unfractionated LMW AcES, fractions C and E had lower macroscopic scores than the negative control group. A probable bias for this parallel is the fact that three groups consisted of male animals (positive and negative controls, fration E), whereas the rest consisted of females. A second batch of LMW AcES was fractionated and tested in the TNBS model. Again, the weight monitoring did not show significant improvements on animals treated with hookworm fractions, but the trend was that fractions C and E caused the mice to gain more weight than the negative control group. The mice treated with fraction C had longer colons than all the other colitis groups and also significantly healthier colons than the negative control.

The results of these two test runs are not very meaningful, the weight monitoring, the most important parameter, did not give significant results. But a trend can be seen: mice treated with fraction E from both batches seemed to weigh more than the negative control group. And when the second batch was tested, fraction C gave the best results with longer and healthier colons (compared to the negative control). LC/MS and NMR spectroscopy were also used to examine fraction C and it appears that it might contain peptides with molecular weights above 3000 Da. Fraction E was also analysed by LC/MS and contained masses of higher molecular weight.

For the future, the activity testing should be scaled up with more animals in each group to see if any of the fractions significantly can protect against weight loss. Injecting larger amounts to see if the effect increases, can also be tried. The results of this project suggest that the activity may reside in fractions C and E. These fractions should also be further investigated to characterise what kind of molecules that might be responsible for the protective effects.

3.2 Synthesis of Name2

Name2 was identified from the transcriptome of the hookworm *N. americanus* and possesses the cysteine framework of ShK. Name2 has 41 residues in its sequence, thus it is six amino acids longer than Shk, and therefore it was interesting to see if the three dimensional structure of Name2 resembled the structure of ShK. Because Name2 has a considerable length, its sequence was divided into two halves and ligated via NCL. The synthesis of both fragments was challenging and even after purifying both fragments, they contained by-products. This might also be the reason for why no correct ligation product could be obtained after the first ligation reaction. Due to the impurities, the amounts of product formed were not large enough to be isolated by RP-HPLC and confirmed by ESI-MS. That the ligation method did work was confirmed by the LC/MS run. The second ligation attempt was successful and 4.55 mg of ligated product could be obtained, but over 24 mg of starting material had to be used as input. After assembly of the peptide chain, formation of the disulfide bonds was required. Name2 has six cysteines and therefore there are 15 different isormers that can theoretically be formed. Eight oxidation conditions were trialed for the oxidative folding of Name2. The condition that resulted in one major oxidised product, based on RP-HPLC and MS analysis, was then used for the large-scale oxidation of Name2. Subsequent purification and ESI-MS analysis, revealed a major peptide product with a mass corresponding to oxidised Name2. This peptide was analysed by RP-HPLC and was found to be pure enough for NMR analysis. The NMR spectroscopy revealed that the fold of Name2 resembled ShK, both having two helical structures. However, the number of residues between CysII – CysIII and CysIII – CysIV differs and therefore, the length and positioning of the helices is different in the two peptides.

It should be investigated if Name2 has any bioactivity, for example the ability to block potassium channels like ShK. And if it does, the important residues for the binding to its target should be elaborated by doing alanine scans, where the residues in the sequence are replaced by alanine one by one.

3.3 Synthesis of Acan1

Acan1 was another sequence that has the ShK cysteine framework and was found in the transcriptome of the hookworm *A. caninum*. As a part of this project the synthesis of Acan1 was tried using Fmoc-SPPS, which posed several difficulties. The peptide was divided into two halves because it has a length of 51 residues, which means it is longer than Name2. In order to ligate the halves, two different NCL strategies were tried. First, NCL via the formation of peptide hydrazide was attempted, and when this method did not work, the same NCL strategy, using the Dbz group, as for the synthesis of Name2 was applied. Both ligation strategies function via the formation of peptide thioesters.

NCL via the formation of a peptide hydrazide proved unsuccessful because the C-terminal Asp-residue of Acan1 N-terminus formed a cyclization product with the hydrazide group that is unable to be ligated. Because the cyclization will happen when the C-terminal residue is Asp, Asn or Gln, this NCL strategy cannot be used for the synthesis of Acan1 if the peptide is not divided at a different place in its sequence [49]. Since a Cys-residue is required at the N-terminal residue of one peptide fragment and Acan1 has six Cys-residues, there are six potential places where the peptide can be divided. To divide it between Asp28 and Cys29, which was tried in the synthesis, turned out not to work. The same residue combination appears earlier in the sequence (Asp19/Cys20). Therefore, the only real options with this method are His11/Cys12, Tyr41/Cys42 and Thr45/Cys46. But then will one fragment be very much longer than the other one and one can assume that the synthesis yield of the longer fragment will probably be quite low. Another possibility would be to divide the peptide into three parts. Work on the rate of ligation reactions have shown that His and Tyr at the C-terminus favour fast reactions, whereas Thr is among the slowest reacting residues [53].

Because the NCL using a peptide hydrazide did not work, the Acan1 N-terminus was synthesised as a peptide-Dbz on an automated synthesiser. A 50:50 mixture of correct product and by-product was obtained, but conversion to the peptide-Nbz gave bad results and only one fraction with the correct peptide-Nbz could be obtained. On the other hand, quite a lot peptide-Nbz could be produced of the by-product, which was used to ligate with Acan1 C-terminus to yield Acan1*. It seemed that the conversion step from Dbz to Nbz was the most difficult one in the synthesis. The synthesis of the C-terminus was also challenging in that different resins had to be tried, and at the end the

Rink Amide MBHA resin was used, which resulted in an amide at the C-terminal residue, where the native peptide has a free carboxylic acid. But compared to the N-terminal part, this synthesis was considerable easier and resulted in a crude peptide product with the fewest by-products and pure peptide in large quantities. Oxidative folding of Acan1* was attempted, but the 1D ^{1}H NMR spectrum of the main product revealed that this peptide had a poorly defined 3D structure.

Regarding these ligation methods, the purity of the fragment to be ligated is important. Because it is a low yielding procedure, the ligation might fail if the starting material contains too many impurities.

4. Conclusion

In this project, low molecular weight excretory/secretory products (LMW AcES) of the dog hookworm *A. caninum* was fractionated by RP-HPLC and tested for activity in the TNBS colitis model. The bioactivity tests were inconclusive, but trends could be identified and it seems that the activity resides in two of the fractions. These two fractions have been further investigated by LC/MS to characterise their content and compounds of molecular weights above 3000 Da have been found in both of them, but this needs further elaboration. The fractions should also be retested in larger trials to see if significance in the weight monitoring can be achieved. The weight monitoring gives, in my opinion, the most objective impression of potential protection against the detrimental colitis.

In the second part of this project, the synthesis of two peptides, Name2 and Acan1, that have the characteristic cysteine framework of the ShK toxin was tried. Because of its size (41 residues) the synthesis of Name2 was accomplished by dividing the peptide into two fragments that were synthesised separately using Fmoc-SPPS and then ligated together by native chemical ligation (NCL). The successful folding of Name2 was confirmed by NMR spectroscopy, which was also used to determine the structure of the peptide. Name2 has two helical structures between Pro8 – Lys17 and Ser27 – Leu32. ShK also has two helices, but they are shorter with only two residues between the helices.

The synthesis of Acan1 was more challenging and unfortunately unsuccessful. NCL via the formation of a peptide hydrazide is not applicable for this peptide and NCL with a C-terminal acylurea moiety involves a conversion step that did not result in the intermediate of the N-terminus fragment needed for the ligation. A substantial amount of a converted by-product could be obtained, which was successfully ligated to the correct C-terminus fragment of Acan1 but NMR spectroscopy after oxidative folding revealed that it did not possess a well defined three dimensional structure.

This project is part of the exciting research that happens on the immunomodulatory effects of hookworms. Hopefully, the LMW AcES and ShK-like peptides can in the future contribute to the treatment of autoimmune diseases.

5. Materials and Methods

5.1 Fractionation of low molecular weight components of *A. caninum* ES products (LMW AcES)

5.1.1 Origin of LMW AcES material analysed in this project

Stray dogs were euthanized at The University of Queensland Veterinary School and *A. caninum* was obtained from their small intestines. The worms were washed in PBS and cultured for 3 hours at 37 °C with 5 % CO_2 in RPMI 1640 medium, 100 units/ml penicillin G sodium, 100 µg/ml streptomycin sulfate, and 0.25 µg/ml amphotericin B. A 10 kDa cutoff membrane was used to isolate the low molecular weight fraction of the ES products.

5.1.2 Fractionation of LMW AcES

After thawing the samples slowly at 23 °C, a disposable syringe and a syringe filter (pore size: 0.45 µm) were used to filter the sample. The filtered sample was manually loaded onto a C_{18} protein and peptide column from GRACE VYDAC (250 mm x 22 mm, 300 Å pore size, 10 µm particle size) using a Shimadzu Prominence HPLC system: Shimadzu Prominence DGU-20A5 (degasser), Shimadzu Prominence LC-20AT (solvent delivery unit), Shimadzu Prominence CBM-20A (system controller), Shimadzu Prominence SPD-20A (UV/VIS detector) and Lab solutions software. The mobile phase was constituted of two different buffers, buffer A and buffer B (**table 13**). UV absorbance was monitored at 215 nm and 280 nm.

Table 13: RP-HPLC mobile phase buffers

	Constituents
Buffer A	0.05 % TFA in H_2O
Buffer B	0.045 % TFA in acetonitrile/H_2O (90:10 *v*/*v*)

For the sample elution a gradient program that consisted of a 2 % linear gradient of buffer B (0 – 40 minutes), then ramping to 100 % buffer B over 1 minute, holding at 100 % buffer B for 4 minutes, ramping back to 0 % buffer B over 1 minute and holding at 0 % buffer B for 11 minutes. The flow rate was set to 8 ml/minute. Samples were collected

according to the scheme shown in **table 14**. The fractions were shock frozen in a dry ice/acetone bath and lyophilized.

Table 14: Fraction collection scheme

Time of elution (minutes)	Fraction
0 – 10	A
10 – 20	B
20 – 30	C
30 – 40	D
40 – 50	E

The trifluoroacetate ion forms hydrogen bonds with peptides, thereby potentially disturbing the analysis of the fractions, but also affecting biological assays [54]. The fractions B, C and D were therefore re-dissolved in 10 mM hydrochloric acid (HCl (aq)) and some acetonitrile in order to remove the trifluoroacetate [54]. The fractions were then lyophilized.

5.2 Bioactivity testing of fractionated LMW AcES in mice with experimental colitis

5.2.1 Endotoxin removal with Endo Trap®

Endotoxins are components of the outer cell membrane of Gram-negative bacteria, normally called lipopolysaccharide. As a result of cell lysis, these components are released and can trigger the release of cytokines by phagocytes, which can potentially affect the results of the bioassay [55]. Because the LMW AcES was obtained from hookworms that previously lived in the small intestines of dogs, it was possible that the sample was contaminated by endotoxins. Therefore an Endo Trap® endotoxin removal system was used to clear all samples before biological testing. Because this system is an affinity matrix it selectively binds the toxins. Aliquots from each sample were taken before (40 µl) and after (50 µl) endotoxin removal to determine peptide concentrations. An endotoxin quantification using Limulus Amebocyte Lysate was performed and the amount of endotoxin was below detection levels.

5.2.2 Peptide quantification with Micro BCA™ Protein Assay Kit

At alkaline pH, peptides/proteins can reduce cupric ions (Cu^{2+}) to cuprous ions (Cu^{1+}). The Micro BCA™ Protein Assay Kit utilizes bicinchonic acid (BCA) to detect cuprious ions in solution by chelation because two BCA molecules chelate one Cu^{1+}, and the product of this reaction strongly absorbs light at 562 nm. Absorbance increases linearly with increasing peptide concentration [56]. Peptide concentrations of the samples taken before, and after endotoxin removal were measured according to the assay kit manual. Bovine serum albumin was used as a standard. After incubating for 2 hours the absorbance was measured with a POLARstar Omega (BMG LABTECH) microplate reader with MARS Data Analysis Software. The analysis software also calculated the peptide concentrations (**table 15**).

Table 15: Peptide concentrations before and after endotoxin removal

Fraction:	Peptide concentration before endotoxin removal	Peptide concentration after endotoxin removal
A	865.4 µg/ml	1032.6 µg/ml
B	4213.3 µg/ml	9070.7 µg/ml
C	4728 µg/ml	8040 µg/ml
D	6096 µg/ml	8373.3 µg/ml
E	208 µg/ml	234.5 µg/ml

Because the peptide concentration appears to be higher after the removal of endotoxin than before, the concentration values for the aliquots that did not underwent the removal procedure were used for further experiments.

5.2.3 Mouse experiment

The C57Bl/6 mouse strain was used for the experiment, and the animals were purchased from the Animal Resource Centre (Canning Vale, Western Australia, Australia). The mice had access to food and water *ad libitum*. The experiment lasted 4 days and was performed twice. **Tables 16** and **17** list the animal characteristics for testing of batch 1 and 2, respectively. For batch 1, three groups consisted of only male, and the remaining groups of female animals. Only male animals were used for batch 2.

Table 16: Characteristics of the experimental animals – batch 1

Species	Mouse
Strain	C57Bl/6
Sex	Groups 1, 2 & 8: male Groups 3 – 7: female
Age:	6 weeks
Weight (g)	Males: 23.96 – 26.88 Females: 18.56 – 21.66

Table 17: Characteristics of the experimental animals – batch 2

Species	Mouse
Strain:	C57Bl/6
Sex:	Male
Weight (g)	19.24 – 24.10

5.2.4 Experimental design

The mouse experiment included 8 groups with 4 animals in each group for testing of the fractions from the first LMW AcES batch (**table 18**). Five animals were in each of the seven groups when the second batch was tested (**table 19**). The mice in group 1 served as positive controls and were untreated. The animals in the second group represented the negative control, and underwent only TNBS administration. All animals in the other groups were administered TNBS for colitis induction. In addition, they were injected with 500 µl of unfractionated LMW AcES (group 3 – first LMW AcES batch) or 20 µg of one of the fractions in PBS (200 µl injection volume).

Table 18: Overview of the groups for testing of the first batch of LMW AcES

No.	Group name	TNBS administration	Amount of sample to inject
1	Healthy control	✗	✗
2	TNBS only	✓	✗
3	LMW AcES	✓	500 µl of LMW AcES
4	Fraction A	✓	20 µg of LMW AcES fraction A in PBS
5	Fraction B	✓	20 µg of LMW AcES fraction B in PBS
6	Fraction C	✓	20 µg of LMW AcES fraction C in PBS
7	Fraction D	✓	20 µg of LMW AcES fraction D in PBS
8	Fraction E	✓	20 µg of LMW AcES fraction E in PBS

Table 19: Overview of the groups for testing of the second batch of LMW AcES

No.	Group name	TNBS administration	Amount of sample to inject
1	Healthy control	✗	✗
2	TNBS only	✓	✗
3	Fraction A	✓	20 µg of LMW AcES fraction A in PBS
4	Fraction B	✓	20 µg of LMW AcES fraction B in PBS
5	Fraction C	✓	20 µg of LMW AcES fraction C in PBS
6	Fraction D	✓	20 µg of LMW AcES fraction D in PBS
7	Fraction E	✓	20 µg of LMW AcES fraction E in PBS

5.2.5 Material used for mice anaesthesia

The mice were fully anesthetized with a solution mixture of Ilium Ketamil® (Ketamine 100 mg/ml, Troy Laboratories Australia Pty Ltd) and Ilium Xilazil® (Xylazine 100 mg/ml, Troy Laboratories Australia Pty Ltd) in PBS (**table 20**). 200 µl of this solution mixture was injected intraperitoneally in every mouse that underwent colitis induction with TNBS.

Table 20: Anaesthetics used for anaesthesia and its duration

Ketamine 100 mg/ml	0.05 ml injection solution/100 g body weight
Xylazine 100 mg/ml	0.005 ml injection solution/100 g body weight
Duration of anaesthesia	Approximately 30 minutes

5.2.6 Sample injection

20 μg of fraction sample was to be injected intraperitoneally per mouse. Because of the needle dead volume, 100 μg was regarded the minimum amount of sample that had to be prepared per group with four mice. The volume that was injected per mouse was 200 μl. This means that the fraction volume containing 100 μg of peptide had to be diluted with a specific volume of high grade PBS to make up a final volume of 1000 μl. 500 μl of unfractionated LMW AcES was injected in each mouse of group 3 when the first batch of LMW AcES was tested.

5.2.7 Colitis induction

TNBS for colitis induction was purchased from Sigma Aldrich and for the administration, a 25 mg/ml TNBS solution in 45 % EtOH/water (*v*/*v*) was prepared by Dr Severine Navarro. Colitis was then induced by TNBS as previously described [35]. For the intrarectal injection of the TNBS/EtOH mixture, a 3,5-French, 38-cm, polyurethane catheter and a 1 ml disposable syringe was used. After filling the syringe with the TNBS/EtOH mixture, the catheter tip was lubricated with Viscotears® eye gel. The catheter was then inserted into the rectum of the mouse, which was hold by its tail, and 100 μl of the TNBS/EtOH mixture was administered to the colon. Ultimately, the mouse was held by its tail for 30 seconds, enabling the mixture to distribute evenly in the colon.

5.2.8 Sacrifice and dissection

On day 3 after the colitis induction with the TNBS/EtOH enema, the mice were sacrificed using carbon dioxide in a closed system, and then dissected. The abdomen was sprayed with EtOH/H_2O (70:30 *v*/*v*) and a laparotomy was performed with a longitudinal incision to open the abdominal cavity [35]. Fat and cecum ware placed to the side and the colon was removed entirely. After measuring the colon's length with a ruler, it was opened longitudinally and washed in PBS to remove the stool.

5.2.9 Macroscopic Evaluation

The normal mouse colon is divided into three sections, an ascending, a transverse and a descending colon [57]. Mucosal folds are transverse in the upper parts of the colon and

longitudinal in the descending colon [57]. A light microscope was used to examine the cleaned colons for signs of inflammation and formation of connective tissue between the colon and adjacent visceral organs (adhesions), degree of ulcerations, wall thickness, oedema and impaired intestinal motility were considered signs of inflammation. The severity was determined by a macroscopic scoring system where the parameters were graded (0 = normal to 4 = most severe) as described before [41].

5.3 LC/MS of fractions C and E

The LC/MS system consisted of:

- Shimadzu CBM20A system controller
- Shimadzu Pump LC20AD solvent delivery unit
- Shimadzu SIL20AC Autosampler
- Shimadzu CTO20A Column oven
- Shimadzu SUBCvp Subcontroller
- C18 HPLC column
- AB Sciex Triple TOF 5600 System mass spectrometer with Analyst software

3.00 µl of sample was injected and the flow rate was set to 0.0008 ml/minute.

Liquid chromatography method: 1 % buffer B for 5 minutes, linear ramping to 40 % buffer B over 25 minutes, linear ramping to 80 % buffer B over 5 minutes, holding at 80 % buffer B for 5 minutes, ramping back to 1 % buffer B over 0.1 minute and holding at 1 % buffer B for 10 minutes.

5.4 NMR spectroscopy of fraction C

1D ^{1}H NMR spectrum of fraction C was recorded on a Bruker 600 Mhz spectrometer at 298 K. The sample was dissolved in 450 µl H_2O and 50 µl D_2O.

5.5 Peptide synthesis

5.5.1 Deprotection for Fmoc chemistry

The ring system of the Fmoc-group of a protected amino acid (Fmoc-Xaa, **15**) has electron withdrawing properties, which means that the hydrogen on carbon-9 is acidic and can be removed via β-elimination by a weak base (**figure 52**) [8]. The secondary amine piperidine (**16**) is commonly used for this deprotonation and induces an electron shift that ruptures the molecule [8]. The result of this reaction is the deprotected amino acid (Xaa, **18**), carbon dioxide (CO_2) and a dibenzofulvene (**17**) intermediate [8]. Piperidine reacts further with the dibenzofulvene intermediate to form the fulvene-piperidine adduct (**19**) [8].

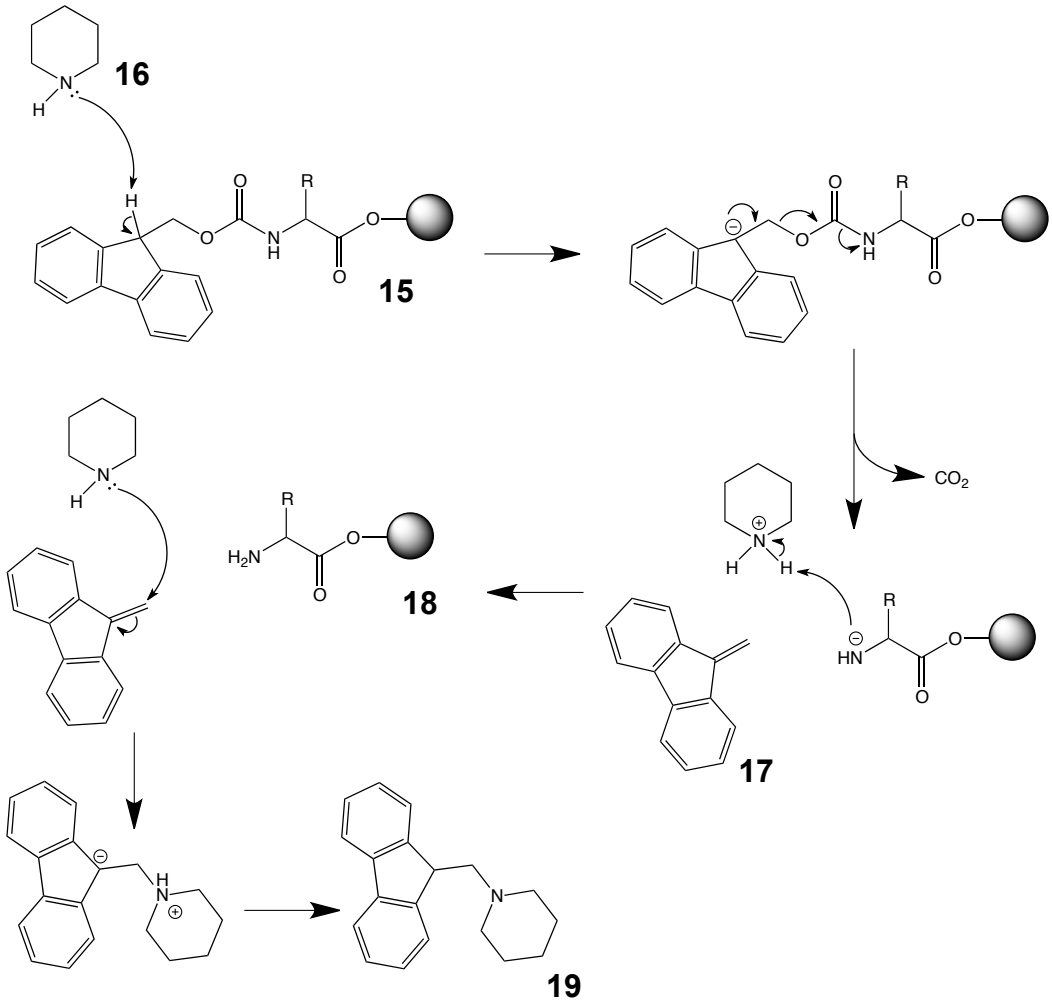

Figure 52: Deprotection step by step; (**15**) Fmoc-Xaa, (**16**) piperidine, (**17**) Dibenzofulvene, (**18**) Deprotected Xaa, (**19**) Fulvene-piperidine adduct

5.5.2 Peptide bond formation from HBTU- and HCTU-mediated reactions

In this thesis, either *O*-(6-benzotriazol-1-yl)-*N*,*N*,*N*',*N*'-tetramethyluronium hexafluorophosphate (HBTU) or *O*-(6-chlorobenzotriazol-1-yl)-*N*,*N*,*N*',*N*'-tetramethyluronium hexafluorophosphate (HCTU) was used as coupling reagent.

Deprotonation by DIPEA (**20**) generates the carboxylate anion (**22**) of the Fmoc-protected amino acid (**21**) (**figure 53**). The carboxylate anion is now able to attack the coupling reagent (**23**), resulting in the formation of the *O*-acyl-uronium cation (**24**). Two different pathways for the formation of a new peptide bond that yields the elongated peptide (**27**) are now possible. Either, the *O*-acyl-uronium cation is attacked by the N-terminal amino group of the resin-bound peptide (**25**) and forms the peptide bond directly, or, it reacts with the benzotriazolyloxy anion (**26**) to construct a benzotriazolyl ester (**28**), which has to be aminolyzed in a second step in order to elongate the peptide. Additionally to tetramethyl urea (**29**), that is released in both pathways of the reaction with the *O*-acyl-uronium cation, pathway B also leads to the release of hydroxybenzotriazole (**30**) in the second step [8].

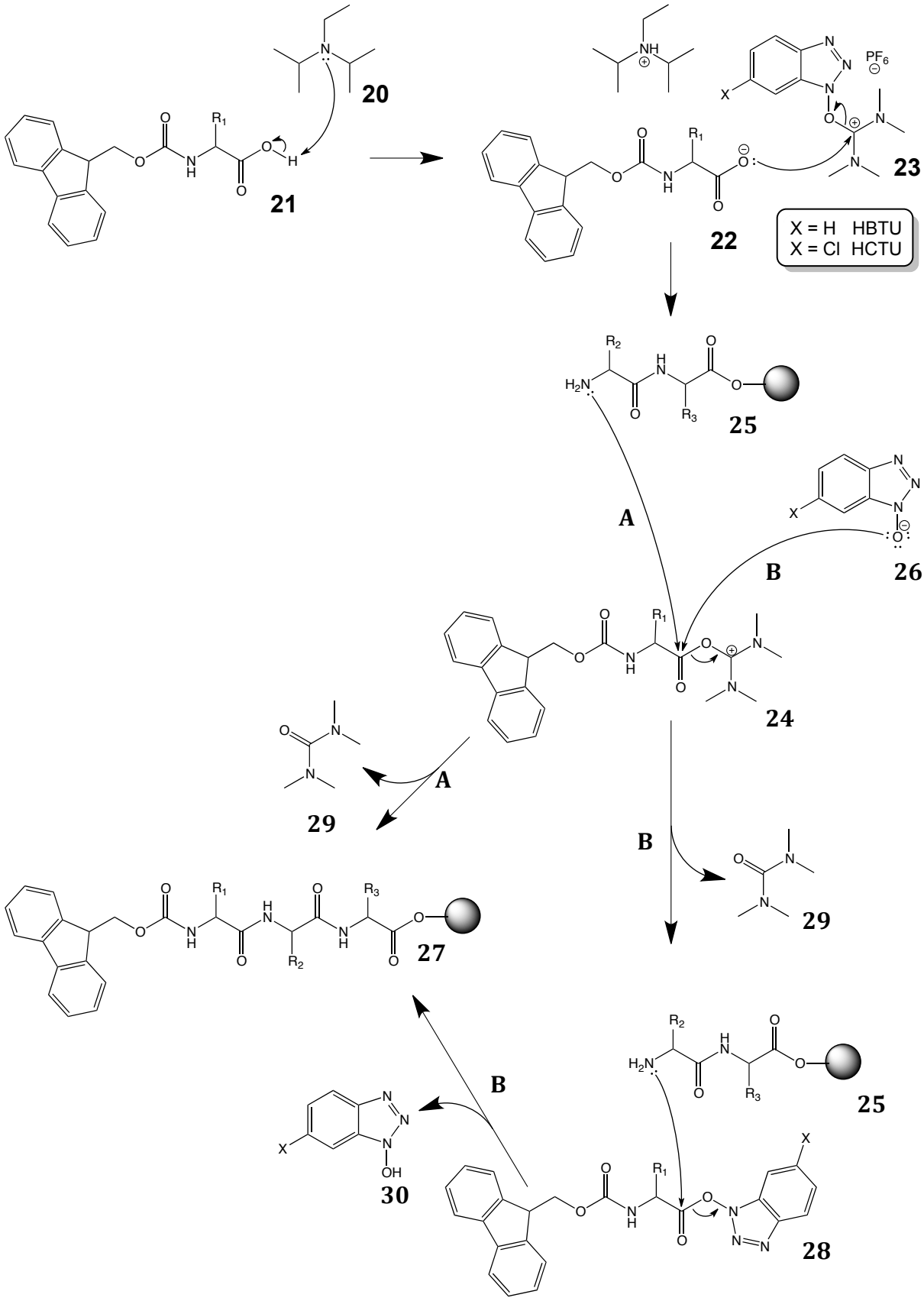

Figure 53: Formation of a new peptide bond; (**20**) DIPEA, (**21**) Fmoc-Xaa, (**22**) carboxylate anion of Fmoc-Xaa, (**23**) coupling reagent, (**24**) *O*-acyl-uronium cation, (**25**) resin-bound peptide, (**26**) benzotriazolyloxy anion, (**27**) elongated peptide, (**28**) benzotriazolyl ester, (**29**) tetramethyl urea, (**30**) hydroxybenzotriazole

5.5.3 The ninhydrin test

The purpose of the ninhydrin test is to determine the yield of a coupling reaction by quantifying unreacted primary amines in the sample [58]. A small resin aliquot (3 – 5 mg) is taken out of the reaction vessel, washed with 50/50 methanol (MeOH)/dichloromethane (DCM), dried until the resin has a sandy appearance, transferred to a test tube and weighed. Then, 2 drops of 76 % w/w phenol, 4 drops of 0.2 mM potassium cyanide in pyridine, and 2 drops of 0.28 M ninhydrin in EtOH are added to the resin. As a control, the reagents in the same amounts are also added to a test tube containing no resin. After incubating both tubes at 100 °C for 5 minutes, 2.8 ml of EtOH/H_2O (60:40 v/v) is added. The resin is allowed to settle and the control solution is used to zero the spectrophotometer. Finally, the absorbance of the sample is measured. Usually, the absorbance is measured at 570 nm, but in this thesis λ = 580 nm was used. Ninhydrin (**31**) reacts with the amino group of a bound residue (**32**), generating the Schiff's base (**33**) (**figure 54**). Shift of the double bond (**34**) and subsequent hydrolysis yields the aldehyde (**35**) and another amine (**36**) that reacts with a second molecule of ninhydrin to finally give an anion, Ruhemann's purple (**38**) which is in equilibrium with its tetraoxo form (**37**) [8]. Ruhemann's purple is the chromophore with absorbance maxima at 410 and 570 nm [58]. The percentage coupling yield can then be calculated using following formula:

$$\%\ coupling\ yield = 100\ \% \cdot \left(1 - \left(\frac{200 \cdot A_{580}}{SV \cdot mass\ of\ resin}\right)\right)$$

where A_{580} is the absorbance measured at 580 nm and SV is the substitution value of the residue in mmol/g. A coupling yield above 99.6 % is desirable, but not always achievable.

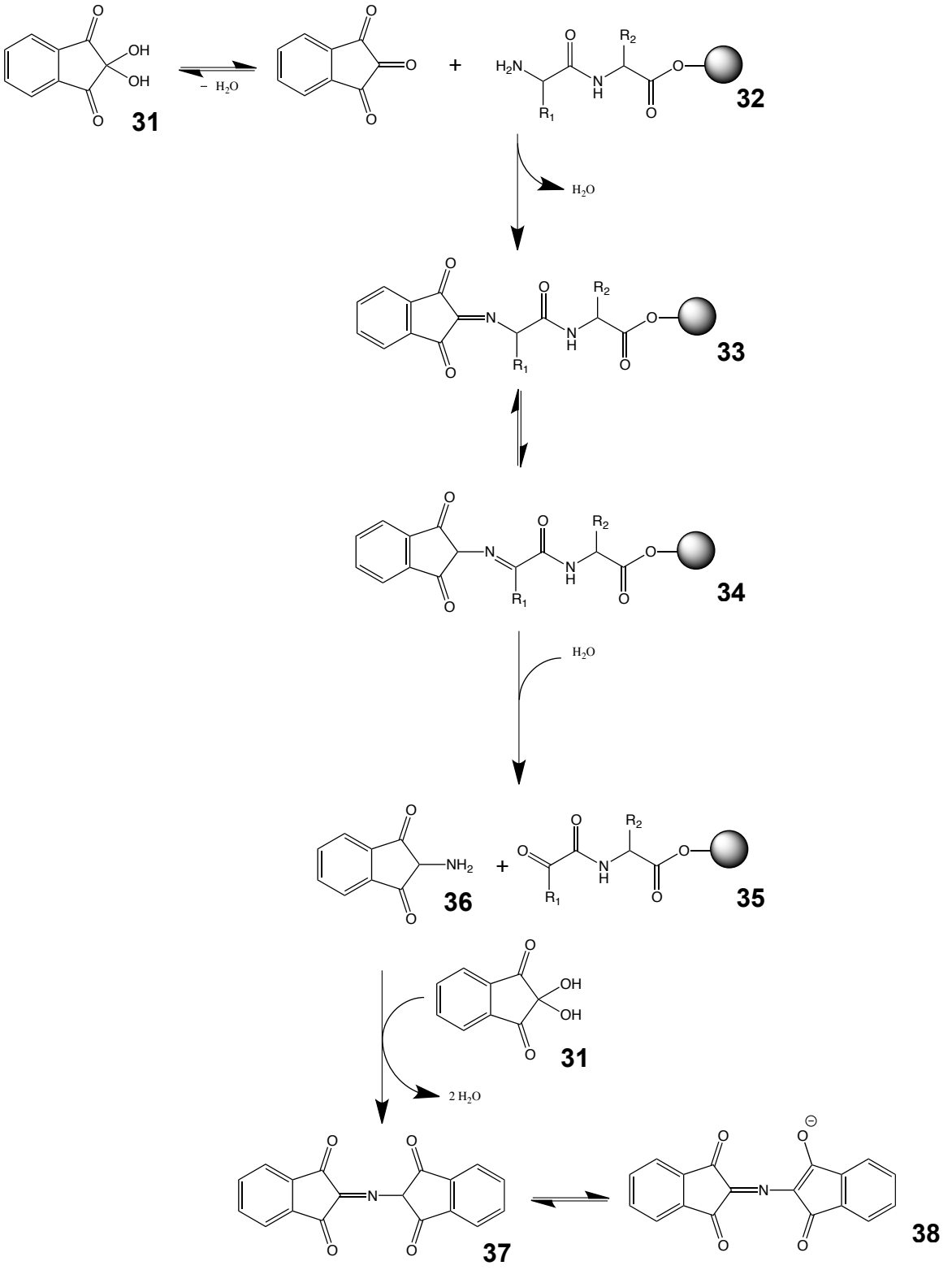

Figure 54: Reactions of the ninhydrin test; (**31**) ninhydrin, (**32**) peptide bound residue, (**33**) Schiff's base, (**34**) shift of the double bond, (**35**) aldehyde, (**36**) amine, (**37**) tetraoxo form, (**38**) Ruhemann's purple

5.5.4 Native chemical ligation via the formation of a C-terminal acylurea moiety

Initially, the Fmoc group on the Rink Amide MBHA resin (**39**) is removed with piperidine yielding the deprotected resin (**40**) (**figure 55**). Fmoc-Dbz is then loaded onto the resin (**41**) using HBTU and DIPEA, before it is deprotected with piperidine and standard Fmoc SPPS is applied to elongate the peptide chain (**42**). The last residue has to be protected by base stable, but acid labile, protecting groups; the α-amino group of the last residue is therefore derivatized with a Boc group [42]. When chain assembly is complete, acylation by 4-nitrophenyl chloroformate (**43**) and treatment with DIPEA results in the formation of the resin bound peptide-Nbz (**44**) [42]. Cleavage with TFA yields the free peptide-Nbz (**45**), which forms a thioester (**47**) when reacting with MPAA (**46**) at pH 7 [42]. Finally, the thiol group of a Cys residue at the N-terminus of the peptide (**48**) to be ligated to the thioester peptide attacks the α-carbonyl giving a new thioester (**49**) [59]. A spontaneous rearrangement leads to the formation of the final ligation product (**50**) with a normal peptide bond [59].

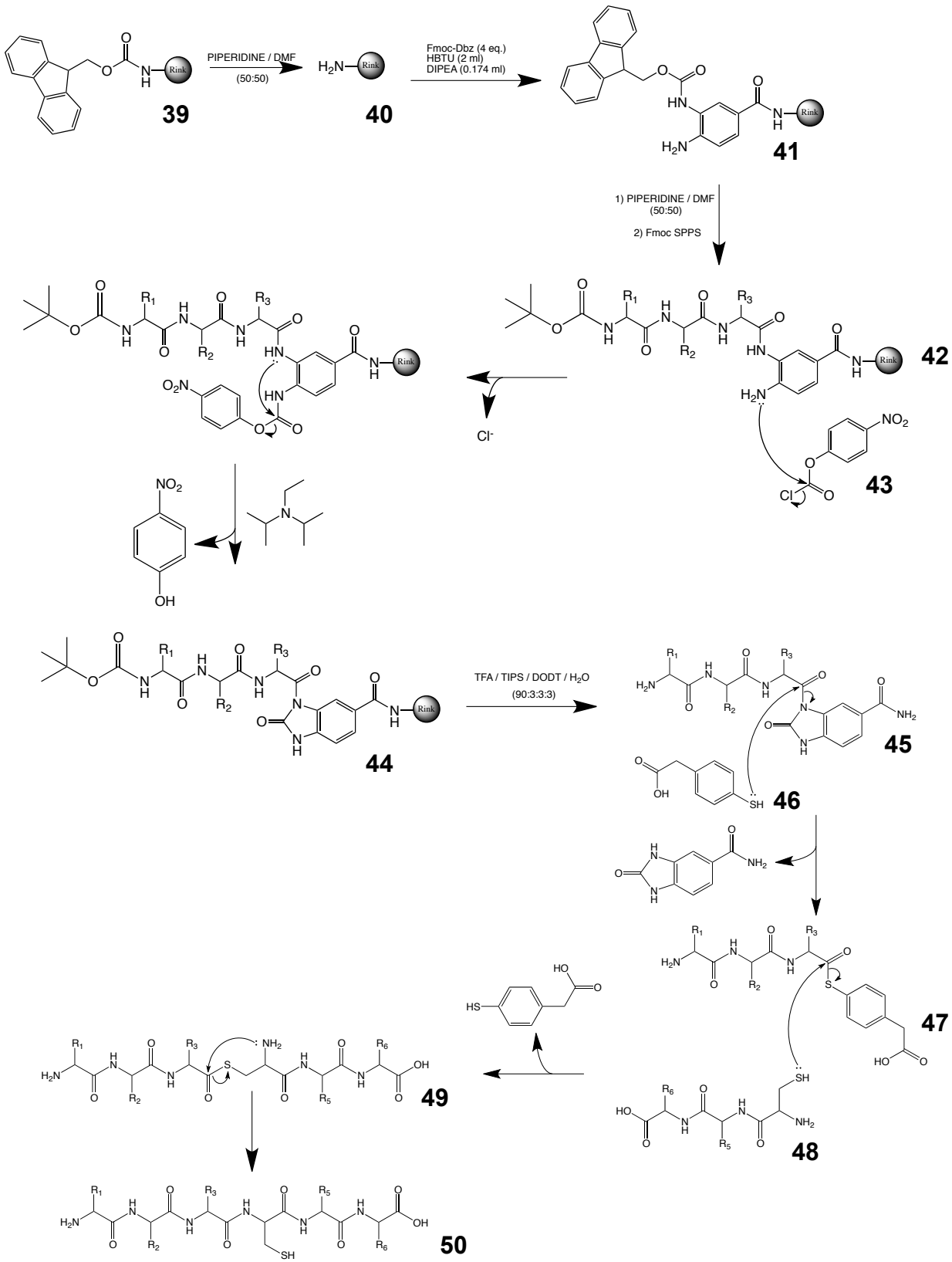

Figure 55: Native chemical ligation via the formation of a C-terminal acylurea functionality; (**39**) Rink Amide MBHA resin, (**40**) deprotected resin, (**41**) Fmoc-Dbz loaded resin, (**42**) peptide with Dbz, (**43**) 4-nitrophenyl chloroformate, (**44**) resin-bound peptide-Nbz, (**45**) peptide-Nbz, (**46**) MPAA, (**47**) thioester, (**48**) peptide with C-terminal Cys-residue, (**49**) new thioester, (**50**) ligation product

5.5.5 Native chemical ligation via the formation of a peptide hydrazide

In this thesis, 2-chlorotrityl chloride resin (**51**) was used as a solid support for the peptide hydrazide (**53**) (**figure 56**). Loading of the hydrazide group onto the resin (**52**) is achieved by treating it with a mixture of hydrazine hydrate, DIPEA and *N*,*N*-Dimethylformamide (DMF). Standard Fmoc-SPPS and a subsequent cleavage provide the final peptide hydrazide (**53**) [49]. Oxidation with $NaNO_2$ at a low pH results first in the formation of the peptide azide (**54**), which is then transformed to a thioester (**47**) when MPAA (**46**) is introduced in the next step [49]. Finally, the thiol group of a Cys-residue at the N-terminus of the peptide (**48**) to be ligated to the thioester peptide attacks the α-carbonyl giving a new thioester (**49**) [59]. A spontaneous rearrangement leads to the formation of the final ligation product (**50**) with a normal peptide bond [59].

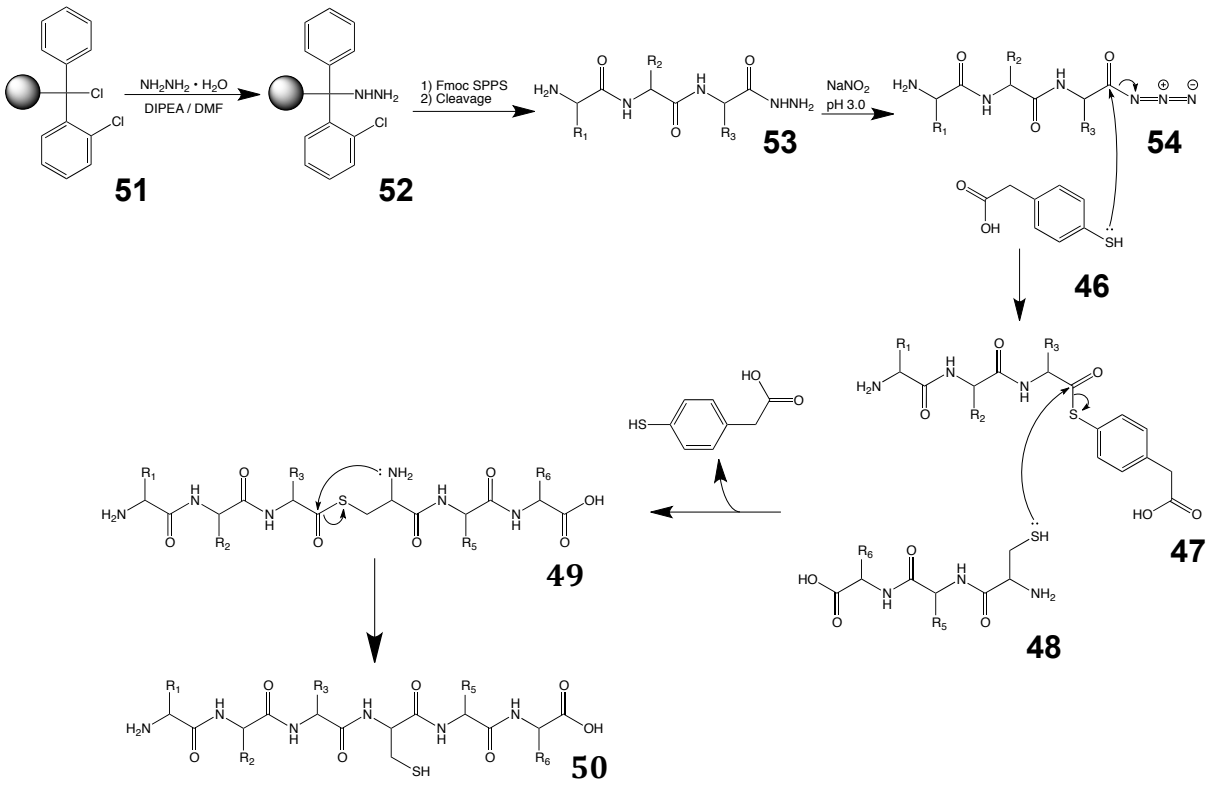

Figure 56: Native chemical ligation via the formation of the a peptide hydrazide; (**51**) 2-chlorotrityl chloride resin, (**52**) resin loaded with a hydrazide group, (**53**) peptide hydrazide, (**54**) peptide azide, (**46**) MPAA, (**47**) thioester, (**48**) peptide with C-terminal Cys-residue, (**49**) new thioester, (**50**) ligation product

5.5.6 Synthesis of Name 2

5.5.6.1 Synthesis of Name2 N-terminus

482 mg (0.25 mmol scale) of Rink Amide MBHA resin (GL Biochem (Shanghai) Ltd, China) was transferred to a reaction vessel and swollen in DMF for 0.5 hour. The resin was deprotected with piperidine/DMF (50:50 *v*/*v)* twice for 1 minute and washed thoroughly with DMF to remove piperidine and the liberated Fmoc group. 4 equivalents of Fmoc-Dbz, 2 ml of 0.5 M HBTU in DMF and 0.174 ml of DIPEA were added to the reaction vessel, mixed thoroughly and allowed to react for 19 hours and 45 minutes in order to load the resin. Ninhydrin test revealed a poor coupling yield (86.4 %), therefore the loading was repeated twice the two subsequent days. After the successful loading (coupling yield: 99.6 %), the remaining residues were coupled using 4 equivalents of the respective amino acid, 2 ml of 0.5 M HBTU in DMF and 0.174 ml of DIPEA. The last residue was glutamine with a Boc group for protection of the α-amino group and a xanthenyl (Xan) group for side chain protection. Couplings were checked by ninhydrin test and test cleavages were conducted to monitor the synthesis. After complete assembly of the linear peptide chain, the resin was washed with DCM and 10 ml of 4-nitrophenyl chloroformate in DCM (100 mg of 4-nitrophenyl chloroformate in 10 ml DCM) was added to the reaction vessel and allowed to react for 1 hour at 23 °C. The solution was then removed by vacuum filtration and the resin was washed three times with DCM and three times with DMF. In the next step 10 ml of DIPEA/DMF (10:90 *v*/*v*) was added to the reaction vessel and allowed to stand for 15 minutes before it was removed by vacuum filtration. Finally the resin was washed five times with DMF, five times with DCM and dried under nitrogen. A total of 1.924 g of peptidyl resin was obtained and 400 mg was taken out for cleavage. The peptide was cleaved from the resin for 2 hours at 23 °C using 50 ml of TFA/TIPS/DODT/H_2O (90:3:3:3 *v*/*v*/*v*/*v*). After a while, the cleavage mixture remained slightly yellow, which is indicative of free trityl protecting groups. Therefore, an additional 0,5 ml of TIPS was added to scavenge these remaining groups. Most of the TFA was removed using a rotary evaporator and the crude peptide was washed with cold diethyl ether and extracted with buffer A/buffer B (50:50 *v*/*v*). The peptide crude was then lyophilized overnight. Crude peptide was purified by RP-HPLC using a preparative column (250 x 22 mm, 300 Å pore size, 10 µm

particle size) and a 1 % gradient of buffer B. ESI-MS was used to identify the fractions containing the peptide. Analytical RP-HPLC of both crude and fractions were run.

5.5.6.2 Synthesis of Name2 C-terminus

2-Chlorotrityl chloride resin (Merck Schuchardt OHG, Germany) was used for the manual synthesis of the Name2 C-terminus. 214 mg of resin (0.25 mmol scale; substitution value: 1.3 mmol/g) were transferred to a reaction vessel and swollen in DCM for 0.5 hour. In order to load the resin with the first residue, 2 equivalents of Fmoc-Cys and 8 equivalents DIPEA were dissolved in DCM, added to the reaction vessel and allowed to react. After 2 hours the solution was removed by vacuum filtration and the reaction vessel was rinsed with DCM before another 2 equivalents of Fmoc-Cys and 8 equivalents of DIPEA in DCM were added and allowed to react for 2 hours. To cap unreactive sites the resin was treated with DCM/MeOH/DIPEA (17:2:1 *v*/*v*/*v*), then washed with DCM and DMF [8]. Removal of the Fmoc group was achieved by treatment with piperidine/DMF (50:50 *v*/*v)* twice for 1 minute and washing with DMF. 4 equivalents of the respective Fmoc protected amino acid were dissolved in 2 ml of coupling reagent and 0.174 ml of DIPEA before the mixture was added to the reaction vessel. For this synthesis, 0.5 M HCTU in DMF was used for the first coupling, and if additional couplings of that residue were necessary, 0.5 M HBTU in DMF was used as coupling reagent. Couplings were checked by ninhydrin test and test cleavages were conducted to monitor the synthesis. After complete chain assembly, the N-terminal Fmoc group was removed with piperidine/DMF (50:50 *v*/*v)* (2 x 1 minute); the resin was washed with DMF and DCM and then dried under nitrogen. The peptide was cleaved from the resin for 2 hours at 23 °C using 50 ml of TFA/TIPS/DODT/H_2O (90:3:3:3). Most of the TFA was removed using a rotary evaporator and the crude peptide was washed with cold diethyl ether and extracted with buffer A/buffer B (50:50 *v*/*v*). The peptide crude was lyophilized overnight. Crude peptide was purified by RP-HPLC using a preparative column (250 x 22 mm, 300 Å pore size, 10 µm particle size) and a 1 % gradient of buffer B. ESI-MS was used to identify the fractions containing the peptide. Analytical RP-HPLC of both crude and fractions were run.

5.5.6.3 Native chemical ligation of Name2

The ligation between the N-terminus and the C-terminus part of Name 2 was attempted twice and both times a ligation buffer containing 6 M Gn · HCl and 0.2 M Na_2HPO_4 was used.

1. Attempt:

MPAA (169.52 mg) and TCEP · HCl (29.52 mg) were transferred to a scintillation vial containing 5 ml of ligation buffer, giving a MPAA concentration of 0.202 M and a TCEP · HCl concentration of 0.0206 M. The pH was adjusted to 7.0 with 2 M sodium hydroxide (NaOH), but the amount NaOH added was too much, so the pH ended up at 7.91. Name2 N-terminus (3.98 mg) and Name2 C-terminus (1.98) mg were transferred to an eppendorf tube, and 0.5 ml of ligation buffer was added to the tube to dissolve the peptides. The mixture was allowed to react for 21 hours at 23 °C. 0.1 ml was taken out of the reaction mixture to run a LC/MS. The remaining reaction mixture was diluted with 1.5 ml of buffer A before it was loaded onto a preparative column (250 x 22 mm, 300 Å pore size, 10 µm particle size) to be purified by RP-HPLC using a 1 % gradient of buffer B. The fractions were analysed by ESI-MS.

2. Attempt:

MPAA (33.87 mg, 0.201 M) and TCEP · HCl (5.80 mg, 0.0202 M) were transferred to a 3 ml HPLC vial. 1 ml of ligation buffer was added and the pH was raised to 6.98 with concentrated NaOH. The mixture was degassed by bubbling nitrogen into the mixture through a long needle while the vial was sealed with a septum. Then, 15.33 mg of Name2 N-terminus and 9.30 mg of Name2 C-terminus were dissolved in the ligation buffer before the reaction mixture was degassed one more time under nitrogen and allowed to react for approximately 24 hours. The next day, 1 ml of 4 % TFA was added in order to precipitate some of the MPAA and the mixture was transferred to a scintillation vial and filled up with buffer A (ca. 20 ml), filtered and loaded onto a preparative column (250 x 21,20 mm, 300 Å pore size, 10 µm particle size) to be purified by RP-HPLC using a 1 % gradient of buffer B. The fractions were analysed by ESI-MS and the fraction containing the ligation product was analysed by RP-HPLC and lyophilized.

5.5.6.4 Folding of Name2

For the folding of Name 2, a trial oxidation with eight different conditions was conducted with a peptide concentration of 0.5 mg/ml in eppendorf tubes at 23 °C:

1. 0.1 ml PBS
2. 0.1 ml 0.1 M NH_4HCO_3
3. 0.1 ml PBS/propan-2-ol (50:50)
4. 0.1 ml NH_4HCO_3/propan-2-ol (50:50)
5. 0.1 ml PBS, 2 mM GSH and 0.2 mM GSSG
6. 0.1 ml 0.1 M NH_4HCO_3, 2 mM GSH and 0.2 mM GSSG
7. 0.1 ml PBS/propan-2-ol (50:50), 2 mM GSH and 0.2 mM GSSG
8. 0.1 ml NH_4HCO_3/propan-2-ol (50:50), 2 mM GSH and 0.2 mM GSSG

After 24 hours, the folding mixtures were analysed by RP-HPLC using an analytical column (250 x 4.6 mm, 300 Å pore size, 5 µm particle size) and a 1 % gradient of buffer B. Condition 5 was found not only to give the highest peak of the major product but also the best peak height ratio between the major product and the other products in the mixture. 1.91 mg of reduced Name 2 was then oxidised in 10 ml of PBS containing 2 mM GSH and 0.2 mM GSSG for 24 hours at 23 °C. The oxidation mixture was purified by RP-HPLC using a semi-preparative column (250 x 10 mm, 300 Å pore size, 5 µm particle size) and a 1 % gradient of buffer B. ESI-MS was used to identify the fraction with the correct mass and that fraction was lyophilized overnight. The oxidised peptide was analysed by 1D ^1H NMR on a Bruker 600 Mhz spectrometer.

5.5.6.5 NMR spectroscopy of Name2

The peptide was dissolved in 450 µl H_2O and 50 µl D_2O. 1D, TOCSY and NOESY proton spectra were recorded on a BRUKER 600 Mhz spectrometer at 298 K with a mixing time of 150 ms. To characterise slowly exchanging protons, the peptide was dissolved in D_2O and 1D ^1H, TOCSY, NOESY and ^1H – ^{13}C HSQC spectra were recorded on a BRUKER 900 Mhz spectrometer. The HSQC was run at natural abundance. The sequential assignment was performed as previously described [43]. NOE peak volumes in the NOESY spectra were translated into distance restraints with the appropriate pseudoatom corrections

using the program CYANA. Backbone dihedral angle restraints were derived from $^{3}J_{H\alpha,HN}$ coupling constants measured directly from 1D spectra. Additional backbone restraints including Ψ angles were derived from Talos+, which compares observed chemical shifts with reported chemical shifts from known structures in the protein data bank (PDB). Intraresidue NOE and $^{3}J_{H\alpha\text{-}H\beta}$ coupling patterns derived from ECOSY were used in assigning X^{1} angle conformation of the side chains. The structure was calculated by using torsion angle dynamics within the CYANA software. Fifty structures were calculated and the 15 lowest energy structures were retained for analysis. Structures were visualised with MOLMOL.

5.5.7 Synthesis of Acan1

5.5.7.1 Synthesis of Acan1 N-terminus as a peptide hydrazide

192 mg (0.25 mmol scale, substitution value: 1,3 mmol/g) of 2-chlorotrityl chloride resin (Merck Schuchardt OHG, Germany) was swollen for 30 minutes in 25 ml of DMF and cooled at 0 °C in a round bottom flask [60]. A mixture of DIPEA (0.131 ml, 0.75 mmol), hydrazine hydrate (0.121 ml, 2.5 mmol) and DMF (1 ml) was added drop by drop and the suspension was stirred for 30 minutes at 23 °C. This step was repeated for another 30 minutes. The resin was then filtered in a reaction vessel, washed with DMF, water, DMF, MeOH and diethyl ether. Standard manual Fmoc-SPPS was applied for chain elongation. Amino acids were coupled using 2 ml of 0.5 M HBTU in DMF or 0.5 M HCTU in DMF and 0.174 ml of DIPEA. For deprotection piperidine/DMF (50:50) was used and couplings were checked by ninhydrin test. After chain assembly was complete, a final deprotection with piperidine/DMF (50:50 *v/v)* (1 x 1 minute and 1 x 5 minutes) was carried out and the resin was washed with DMF and DCM before it was dried under nitrogen. The peptidyl resin (336 mg) was cleaved with 50 ml TFA/TIPS/DODT/H_2O (90:3:3:3 *v/v/v/v*) for 2 hours at 23 °C. Most of the TFA was evaporated and the solution was washed with diethyl ether and extracted with buffer A/buffer B (50:50). The peptide crude was lyophilized and purified by RP-HPLC using a preparative column (250 x 22 mm, 300 Å pore size, 10 µm particle size) and a 1 % gradient of buffer. Fractions were analysed by ESI-MS.

5.5.7.2 Synthesis of Acan 1 C-terminus

480 mg (0.25 mmol scale) of Rink Amide MBHA resin (GL Biochem (Shanghai) Ltd, China) was swollen in DMF for 0.5 hour in a reaction vessel. The resin was then transferred to a CS 336X automated synthesiser (C S Bio Co., USA) that carried out the deprotection of the resin (with piperidine/DMF (20:80 *v*/*v*) and the peptide elongation using Fmoc protected amino acids, 0.5 M HBTU in DMF and 1 M DIPEA in DMF. The synthesiser also accomplished the final deprotection of the N-terminal residue. Every residue was coupled once and when chain assembly was complete, the peptidyl resin was washed with DMF by the synthesiser, then transferred to a reaction vessel to be washed with DCM and dried under nitrogen. 379 mg of peptidyl resin was cleaved at 23 °C for 2 hours using 50 ml of TFA/TIPS/DODT/H_2O (90:3:3:3 *v*/*v*/*v*/*v*). The majority of TFA was evaporated under pressure; peptide crude was precipitated with diethyl ether, extracted with buffer A/buffer B (50:50 *v*/*v*) and lyophilized overnight. 73 mg of peptide crude was purified by RP-HPLC with a preparative column (250 x 22 mm, 300 Å pore size, 10 µm particle size) using a 1 % gradient of buffer B. Fractions were analysed by ESI-MS.

5.5.7.3 Ligation of Acan 1 using a peptide hydrazide

The pH of 1 ml of buffer containing 6 M Gn · HCl and 0.2 M Na_2HPO_4 was adjusted to 2.83 using 32 % HCl. 5.11 mg Acan1 C-terminus and 6.24 mg of Acan1 N-terminus peptide hydrazide were dissolved in the buffer and held at –10 °C, 0.1 ml of 0.2 M $NaNO_2$ solution was added drop by drop and stirred. After 20 minutes 0.5 ml of 0.2 M MPAA in neutral buffer (6 M Gn · HCl and 0.2 M Na_2HPO_4) was added to the ligation mixture, the pH was adjusted to 7.60 using concentrated NaOH and stirring was continued overnight. The next day, 0.2 ml was taken out of the ligation mixture and analysed by RP-HPLC using an analytical column (150 x 2.1 mm, 300 Å pore size, 5 µm particle size) and a method that started with 5 % buffer for 5 minutes and then a 2 % linear gradient of buffer B. Fractions were analysed by ESI-MS.

5.5.7.4 Synthesis of Acan1 N-terminus with a Dbz group

460 mg of Rink Amide MBHA (0.25 mmol scale) was swollen for 30 minutes in a reaction *v*essel, deprotected with piperidine/DMF (50:50 *v*/*v*) twice for 1 minute, and loaded with Fmoc-Dbz. 4 equivalents of Fmoc-Dbz was activated with 2 ml of 0.5 M HBTU in DMF and 0.174 ml DIPEA and transferred to the reaction vessel. The loading was repeated three times and checked by ninhydrin test. The resin was then transferred to a CS 336X automated synthesiser (C S Bio Co., USA), which carried out the chain elongation using piperidine/DMF (20:80 *v*/*v*) for deprotection, 4 equivalents of Fmoc amino acids, 0.5 M HBTU in DMF and 1 M DIPEA in DMF for activation. The last residue was glutamine with a Boc group for protection of the α-amino group and a Xan group for side chain protection. Arginines were coupled twice. After the chain assembly was complete, the peptidyl resin was washed with DMF and DCM before it was dried under nitrogen. A test cleavage was performed to check if the synthesis was successful. 397 mg of peptidyl resin was swollen in DCM for 45 minutes before 100 mg of 4-nitrophenyl chloroformate in 10 ml DCM was added and allowed to react for 85 minutes. The resin was washed with DCM and DMF; 10 ml of DIPEA/DMF (10:90 *v*/*v*) was added and removed by vacuum filtration after 30 minutes. After washing the resin with DMF and DCM, it was dried under nitrogen. 397 mg of peptidyl resin was cleaved using 50 ml of TFA/TIPS/DODT/H_2O (90:3:3:3 *v*/*v*/*v*/*v*) for 2 hours at 23 °C. Most of the TFA was removed from the solution containing the peptide crude, which was then washed with diethyl ether and extracted with buffer A/buffer B (50:50). The peptide crude was lyophilized and purified by RP-HPLC using a preparative column (250 x 22 mm, 300 Å pore size, 10 µm particle size) and a 1 % gradient of buffer B. Fractions were analysed by ESI-MS.

407 mg of peptidyl resin was swollen in DCM for 45 minutes and activated with 5 equivalents of 4-nitrophenyl chloroformate (50.39 mg) in DCM for 85 minutes. The resin was washed with DCM and DMF before 5 ml of 0.5 M DIPEA in DMF was added and allowed to react for 15 minutes. Washes with DMF and DCM were carried out before the resin was dried under nitrogen. 20 ml of TFA/TIPS/DODT/H_2O (90:3:3:3 *v*/*v*/*v*/*v*) was used to cleave the peptide from the resin at 23 °C (2 hours). Most of the TFA was removed from the solution containing the peptide crude, which was then washed with diethyl ether and extracted with buffer A:buffer B (50:50). The peptide crude was

lyophilized and purified (60 mg) by RP-HPLC using a preparative column (250 x 21,20 mm, 300 Å pore size, 10 µm particle size) and a 1 % gradient of buffer B. Fractions were analysed by ESI-MS.

*5.5.7.5 Ligation of Acan1**

The pH of 1 ml of ligation buffer containing 6 M Gn · HCl, 0.2 M Na_2HPO_4, 0.201 M MPAA and 0.0209 M TCEP · HCl was adjusted from 4.31 to 6.81 using concentrated NaOH. The mixture was degassed under nitrogen for 10 minutes before 11.37 mg of Acan1* N-terminus and 9.40 mg of Acan1 C-terminus were added and the degassing under nitrogen was conducted for another 10 minutes. The ligation mixture was stirred at 23 °C and allowed to react for at least 24 hours. 1 ml of 4 % TFA was added to the mixture, diluted with buffer A (final volume: ca. 20 ml) and loaded on a preparative RP-HPLC column (250 x 22 mm, 300 Å pore size, 10 µm particle size) to be purified using a 1 % gradient of buffer B. The fractions were analysed by ESI-MS.

*5.5.7.6 Folding of Acan1**

For the folding of Acan1*, a trial oxidation with eight different conditions was conducted with a peptide concentration of 0.5 mg/ml in eppendorf-tubes at 23 °C:

1. 0.1 ml PBS
2. 0.1 ml 0.1 M NH_4HCO_3
3. 0.1 ml PBS/propan-2-ol (50:50)
4. 0.1 ml NH_4HCO_3/propan-2-ol (50:50)
5. 0.1 ml PBS, 2 mM GSH and 0.2 mM GSSG
6. 0.1 ml 0.1 M NH_4HCO_3, 2 mM GSH and 0.2 mM GSSG
7. 0.1 ml PBS/propan-2-ol (50:50), 2 mM GSH and 0.2 mM GSSG
8. 0.1 ml NH_4HCO_3/propan-2-ol (50:50), 2 mM GSH and 0.2 mM GSSG

After 24 hours, the folding mixtures were analysed by RP-HPLC using an analytical column (250 x 4.6 mm, 300 Å pore size, 5 µm particle size) and a 1 % gradient of buffer B. Condition 2 was then used for an oxidation on a larger scale, so that 2.00 mg of reduced Acan1* were oxidised in 10 ml of 0.1 M NH_4HCO_3 for 24 hours at 23 °C. The

oxidation mixture was purified by RP-HPLC using a semi-preparative column (250 x 10 mm, 300 Å pore size, 5 µm particle size) and a 1 % gradient of buffer B. ESI-MS was used to identify the fraction with the correct mass and that fraction was lyophilized overnight.

*5.5.7.7 NMR spectroscopy of Acan1**

1D ^{1}H NMR spectrum of fraction C was recorded on a Bruker 600 Mhz spectrometer at 298 K. The peptide was dissolved in 450 µl H_2O and 50 µl D_2O.

5.5.7.8 Ligation of Acan 1

The pH of 1 ml of ligation buffer containing 6 M Gn · HCl, 0.2 M Na_2HPO_4, 0.199 M MPAA and 0.0205 M TCEP · HCl was adjusted from 4.48 to 7.02 using concentrated NaOH. After degassing for 10 minutes, 1.00 mg of Acan 1 N-terminus and 1.29 mg of Acan 1 C-terminus were dissolved in 0.2 ml of ligation buffer before it was degassed for an additional 10 minutes. The ligation mixture was stirred at 23 °C and allowed to react for at least 24 hours. 0.2 ml of 4 % TFA was added to the mixture, diluted with buffer A (final volume: ca. 20 ml) and loaded on a semi-preparative RP-HPLC column (250 x 10 mm, 300 Å pore size, 5 µm particle size) to be purified using a 1 % gradient of buffer B. The fractions were analysed by ESI-MS.

5.5.8 Equipment

Liquid chromatography:

Preparative, semi-preparative and analytical RP-HPLC was performed using a Shimadzu Prominence HPLC system that consisted of:

- Shimadzu Prominence DGU-20A5 degasser
- Shimadzu Prominence LC-20AT solvent delivery unit
- Shimadzu Prominence CBM-20A system controller
- Shimadzu Prominence SPD-20A UV/VIS detector
- Lab solutions software

Preparative columns:

- GRACE VYDAC HPLC Columns C18 218TP1022 (250 x 22 mm, 300 Å pore size, 10 µm particle size)
- Phenomenex Jupiter C18 (250 x 21.20 mm, 300 Å pore size, 10 µm particle size)

Semi-preparative column

- GRACE VYDAC HPLC Columns C18 218TP510 (250 x 10 mm, 300 Å pore size, 5 µm particle size)

Analytical columns:

- GRACE VYDAC HPLC Columns C18 218TP54 (250 x 4.6 mm, 300 Å pore size, 5 µm particle size)
- GRACE VYDAC Everest C18 238EV54 (250 x 4.6 mm, 300 Å pore size, 5 µm particle size)
- GRACE VYDAC HPLC Columns C18 218TP5215 (150 x 2.1 mm, 300 Å pore size, 5 µm particle size)

Mass spectrometry:

An AB Sciex API 2000 mass spectrometer with Analyst software was used for the experiments.

6. References

1. Lehninger, A.L., Nelson, D.L. & Cox, M.M. *Lehninger principles of biochemistry*, Edn. 5th. (W.H. Freeman, New York; 2008).
2. Liskamp, R.M.J., Rijkers, D.T.S., Kruijtzer, J.A.W. & Kemmink, J. Peptides and Proteins as a Continuing Exciting Source of Inspiration for Peptidomimetics. *ChemBioChem* **12**, 1626-1653 (2011).
3. Bellmann-Sickert, K. & Beck-Sickinger, A.G. Peptide drugs to target G protein-coupled receptors. *Trends in Pharmacological Sciences* **31**, 434-441 (2010).
4. Sato, A.K., Viswanathan, M., Kent, R.B. & Wood, C.R. Therapeutic peptides: technological advances driving peptides into development. *Current opinion in biotechnology* **17**, 638-642 (2006).
5. Rowland, M., Tozer, T.N. & Rowland, M. *Clinical pharmacokinetics and pharmacodynamics : concepts and applications*, Edn. 4th. (Lippincott William & Wilkins, Philadelphia; 2009).
6. Ripka, A.S. & Rich, D.H. Peptidomimetic design. *Current opinion in chemical biology* **2**, 441-452 (1998).
7. Merrifield, R.B. SOLID PHASE PEPTIDE SYNTHESIS .1. SYNTHESIS OF A TETRAPEPTIDE. *J. Am. Chem. Soc.* **85**, 2149-& (1963).
8. Benoiton, N.L. *Chemistry of peptide synthesis*. (Taylor & Francis, Boca Raton; 2006).
9. Murphy, K., Travers, P., Walport, M. & Janeway, C. *Janeway's immunobiology*. (Garland Science, New York; 2011).
10. Abbas, A.K., Lichtman, A.H. & Pillai, S. *Cellular and molecular immunology*, Edn. 7th. (Saunders/Elsevier, Philadelphia; 2012).
11. Davidson, A. & Diamond, B. Autoimmune diseases. *The New England journal of medicine* **345**, 340-350 (2001).
12. Jacobson, D.L., Gange, S.J., Rose, N.R. & Graham, N.M.H. Epidemiology and Estimated Population Burden of Selected Autoimmune Diseases in the United States. *Clinical Immunology and Immunopathology* **84**, 223-243 (1997).
13. Graham, K.L. & Utz, P.J. Sources of autoantigens in systemic lupus erythematosus. *Current opinion in rheumatology* **17**, 513-517 (2005).
14. Yurasov, S., Wardemann, H., Hammersen, J., Tsuiji, M., Meffre, E., Pascual, V. & Nussenzweig, M.C. Defective B cell tolerance checkpoints in systemic lupus erythematosus. *The Journal of experimental medicine* **201**, 703-711 (2005).
15. Kotzin, B.L. Systemic lupus erythematosus. *Cell* **85**, 303-306 (1996).
16. Tsokos, G.C. Systemic lupus erythematosus. *The New England journal of medicine* **365**, 2110-2121 (2011).
17. Stappenbeck, T.S., Rioux, J.D., Mizoguchi, A., Saitoh, T., Huett, A., Darfeuille-Michaud, A., Wileman, T., Mizushima, N., Carding, S., Akira, S., Parkes, M. & Xavier, R.J. Crohn disease: a current perspective on genetics, autophagy and immunity. *Autophagy* **7**, 355-374 (2011).
18. de Silva, N.R., Brooker, S., Hotez, P.J., Montresor, A., Engels, D. & Savioli, L. Soil-transmitted helminth infections: updating the global picture. *Trends in parasitology* **19**, 547-551 (2003).
19. McSorley, H.J. & Loukas, A. The immunology of human hookworm infections. *Parasite immunology* **32**, 549-559 (2010).
20. Hotez, P.J., Brooker, S., Bethony, J.M., Bottazzi, M.E., Loukas, A. & Xiao, S. Hookworm infection. *The New England journal of medicine* **351**, 799-807 (2004).

21. Allen, L.H. Anemia and iron deficiency: effects on pregnancy outcome. *The American journal of clinical nutrition* **71**, 1280S-1284S (2000).
22. Loukas, A. & Prociv, P. Immune responses in hookworm infections. *Clinical microbiology reviews* **14**, 689-703, table of contents (2001).
23. Williamson, A.L., Lustigman, S., Oksov, Y., Deumic, V., Plieskatt, J., Mendez, S., Zhan, B., Bottazzi, M.E., Hotez, P.J. & Loukas, A. Ancylostoma caninum MTP-1, an astacin-like metalloprotease secreted by infective hookworm larvae, is involved in tissue migration. *Infection and immunity* **74**, 961-967 (2006).
24. Segura, M., Su, Z., Piccirillo, C. & Stevenson, M.M. Impairment of dendritic cell function by excretory-secretory products: a potential mechanism for nematode-induced immunosuppression. *European journal of immunology* **37**, 1887-1904 (2007).
25. Smith, P., Fallon, R.E., Mangan, N.E., Walsh, C.M., Saraiva, M., Sayers, J.R., McKenzie, A.N., Alcami, A. & Fallon, P.G. Schistosoma mansoni secretes a chemokine binding protein with antiinflammatory activity. *The Journal of experimental medicine* **202**, 1319-1325 (2005).
26. Fujiwara, R.T., Cancado, G.G., Freitas, P.A., Santiago, H.C., Massara, C.L., Dos Santos Carvalho, O., Correa-Oliveira, R., Geiger, S.M. & Bethony, J. Necator americanus infection: a possible cause of altered dendritic cell differentiation and eosinophil profile in chronically infected individuals. *PLoS neglected tropical diseases* **3**, e399 (2009).
27. Moyle, M., Foster, D.L., McGrath, D.E., Brown, S.M., Laroche, Y., De Meutter, J., Stanssens, P., Bogowitz, C.A., Fried, V.A., Ely, J.A. & et al. A hookworm glycoprotein that inhibits neutrophil function is a ligand of the integrin CD11b/CD18. *The Journal of biological chemistry* **269**, 10008-10015 (1994).
28. Muchowski, P.J., Zhang, L., Chang, E.R., Soule, H.R., Plow, E.F. & Moyle, M. Functional interaction between the integrin antagonist neutrophil inhibitory factor and the I domain of CD11b/CD18. *The Journal of biological chemistry* **269**, 26419-26423 (1994).
29. Mulvenna, J., Hamilton, B., Nagaraj, S.H., Smyth, D., Loukas, A. & Gorman, J.J. Proteomics analysis of the excretory/secretory component of the blood-feeding stage of the hookworm, Ancylostoma caninum. *Molecular & cellular proteomics : MCP* **8**, 109-121 (2009).
30. Castaneda, O., Sotolongo, V., Amor, A.M., Stocklin, R., Anderson, A.J., Harvey, A.L., Engstrom, A., Wernstedt, C. & Karlsson, E. Characterization of a potassium channel toxin from the Caribbean Sea anemone Stichodactyla helianthus. *Toxicon : official journal of the International Society on Toxinology* **33**, 603-613 (1995).
31. Pennington, M.W., Mahnir, V.M., Khaytin, I., Zaydenberg, I., Byrnes, M.E. & Kem, W.R. An essential binding surface for ShK toxin interaction with rat brain potassium channels. *Biochemistry* **35**, 16407-16411 (1996).
32. Lin, C.S., Boltz, R.C., Blake, J.T., Nguyen, M., Talento, A., Fischer, P.A., Springer, M.S., Sigal, N.H., Slaughter, R.S., Garcia, M.L. & et al. Voltage-gated potassium channels regulate calcium-dependent pathways involved in human T lymphocyte activation. *The Journal of experimental medicine* **177**, 637-645 (1993).
33. Cahalan, M.D., Wulff, H. & Chandy, K.G. Molecular properties and physiological roles of ion channels in the immune system. *Journal of clinical immunology* **21**, 235-252 (2001).
34. Chi, V., Pennington, M.W., Norton, R.S., Tarcha, E.J., Londono, L.M., Sims-Fahey, B., Upadhyay, S.K., Lakey, J.T., Iadonato, S., Wulff, H., Beeton, C. & Chandy, K.G.

Development of a sea anemone toxin as an immunomodulator for therapy of autoimmune diseases. *Toxicon : official journal of the International Society on Toxinology* **59**, 529-546 (2012).
35. Scheiffele, F. & Fuss, I.J. Induction of TNBS colitis in mice. *Current protocols in immunology / edited by John E. Coligan ... [et al.]* **Chapter 15**, Unit 15 19 (2002).
36. Morris, G.P., Beck, P.L., Herridge, M.S., Depew, W.T., Szewczuk, M.R. & Wallace, J.L. Hapten-induced model of chronic inflammation and ulceration in the rat colon. *Gastroenterology* **96**, 795-803 (1989).
37. Neurath, M., Fuss, I. & Strober, W. TNBS-colitis. *International reviews of immunology* **19**, 51-62 (2000).
38. Strober, W. & Fuss, I.J. Proinflammatory Cytokines in the Pathogenesis of Inflammatory Bowel Diseases. *Gastroenterology* **140**, 1756-1767.e1751 (2011).
39. Monteleone, G., Biancone, L., Marasco, R., Morrone, G., Marasco, O., Luzza, F. & Pallone, F. Interleukin 12 is expressed and actively released by Crohn's disease intestinal lamina propria mononuclear cells. *Gastroenterology* **112**, 1169-1178 (1997).
40. Weaver, C.T., Hatton, R.D., Mangan, P.R. & Harrington, L.E. IL-17 family cytokines and the expanding diversity of effector T cell lineages. *Annual review of immunology* **25**, 821-852 (2007).
41. Menachem, Y., Trop, S., Kolker, O., Shibolet, O., Alper, R., Nagler, A. & Ilan, Y. Adoptive transfer of NK 1.1+ lymphocytes in immune-mediated colitis: a pro-inflammatory or a tolerizing subgroup of cells? *Microbes and Infection* **7**, 825-835 (2005).
42. Blanco-Canosa, J.B. & Dawson, P.E. An efficient Fmoc-SPPS approach for the generation of thioester peptide precursors for use in native chemical ligation. *Angewandte Chemie (International ed. in English)* **47**, 6851-6855 (2008).
43. Wüthrich, K. *NMR of proteins and nucleic acids*. (Wiley, New York; 1986).
44. Wishart, D.S., Bigam, C.G., Holm, A., Hodges, R.S. & Sykes, B.D. 1H, 13C and 15N random coil NMR chemical shifts of the common amino acids. I. Investigations of nearest-neighbor effects. *Journal of biomolecular NMR* **5**, 67-81 (1995).
45. Wishart, D.S., Sykes, B.D. & Richards, F.M. The chemical shift index: a fast and simple method for the assignment of protein secondary structure through NMR spectroscopy. *Biochemistry* **31**, 1647-1651 (1992).
46. Wishart, D.S. & Sykes, B.D. The 13C chemical-shift index: a simple method for the identification of protein secondary structure using 13C chemical-shift data. *Journal of biomolecular NMR* **4**, 171-180 (1994).
47. Tudor, J.E., Pallaghy, P.K., Pennington, M.W. & Norton, R.S. Solution structure of ShK toxin, a novel potassium channel inhibitor from a sea anemone. *Nature structural biology* **3**, 317-320 (1996).
48. Zikos, C., Livaniou, E., Leondiadis, L., Ferderigos, N., Ithakissios, D.S. & Evangelatos, G.P. Comparative evaluation of four trityl-type amidomethyl polystyrene resins in Fmoc solid phase peptide synthesis. *Journal of peptide science : an official publication of the European Peptide Society* **9**, 419-429 (2003).
49. Fang, G.M., Li, Y.M., Shen, F., Huang, Y.C., Li, J.B., Lin, Y., Cui, H.K. & Liu, L. Protein chemical synthesis by ligation of peptide hydrazides. *Angewandte Chemie (International ed. in English)* **50**, 7645-7649 (2011).
50. Talley, N.J., Abreu, M.T., Achkar, J.P., Bernstein, C.N., Dubinsky, M.C., Hanauer, S.B., Kane, S.V., Sandborn, W.J., Ullman, T.A. & Moayyedi, P. An evidence-based

systematic review on medical therapies for inflammatory bowel disease. *The American journal of gastroenterology* **106 Suppl 1**, S2-25; quiz S26 (2011).
51. Nicholls, R.J. Review article: ulcerative colitis--surgical indications and treatment. *Alimentary pharmacology & therapeutics* **16 Suppl 4**, 25-28 (2002).
52. Poggioli, G., Pierangeli, F., Laureti, S. & Ugolini, F. Review article: indication and type of surgery in Crohn's disease. *Alimentary pharmacology & therapeutics* **16 Suppl 4**, 59-64 (2002).
53. Hackeng, T.M., Griffin, J.H. & Dawson, P.E. Protein synthesis by native chemical ligation: expanded scope by using straightforward methodology. *Proceedings of the National Academy of Sciences of the United States of America* **96**, 10068-10073 (1999).
54. Andrushchenko, V.V., Vogel, H.J. & Prenner, E.J. Optimization of the hydrochloric acid concentration used for trifluoroacetate removal from synthetic peptides. *J. Pept. Sci.* **13**, 37-43 (2007).
55. Gutsmann, T., Schromm, A.B. & Brandenburg, K. The physicochemistry of endotoxins in relation to bioactivity. *International journal of medical microbiology : IJMM* **297**, 341-352 (2007).
56. Smith, P.K., Krohn, R.I., Hermanson, G.T., Mallia, A.K., Gartner, F.H., Provenzano, M.D., Fujimoto, E.K., Goeke, N.M., Olson, B.J. & Klenk, D.C. Measurement of protein using bicinchoninic acid. *Analytical biochemistry* **150**, 76-85 (1985).
57. Hedrich, H.J. & Bullock, G.R. *The laboratory mouse*. (Elsevier Academic Press, Amsterdam ; Boston; 2004).
58. Sarin, V.K., Kent, S.B.H., Tam, J.P. & Merrifield, R.B. Quantitative monitoring of solid-phase peptide synthesis by the ninhydrin reaction. *Analytical biochemistry* **117**, 147-157 (1981).
59. Dawson, P.E., Muir, T.W., Clark-Lewis, I. & Kent, S.B. Synthesis of proteins by native chemical ligation. *Science (New York, N.Y.)* **266**, 776-779 (1994).
60. Zheng, J.S., Tang, S., Guo, Y., Chang, H.N. & Liu, L. Synthesis of cyclic peptides and cyclic proteins via ligation of peptide hydrazides. *ChemBioChem* **13**, 542-546 (2012).

7. Appendix

7.1 Analytical HPLC of fractions

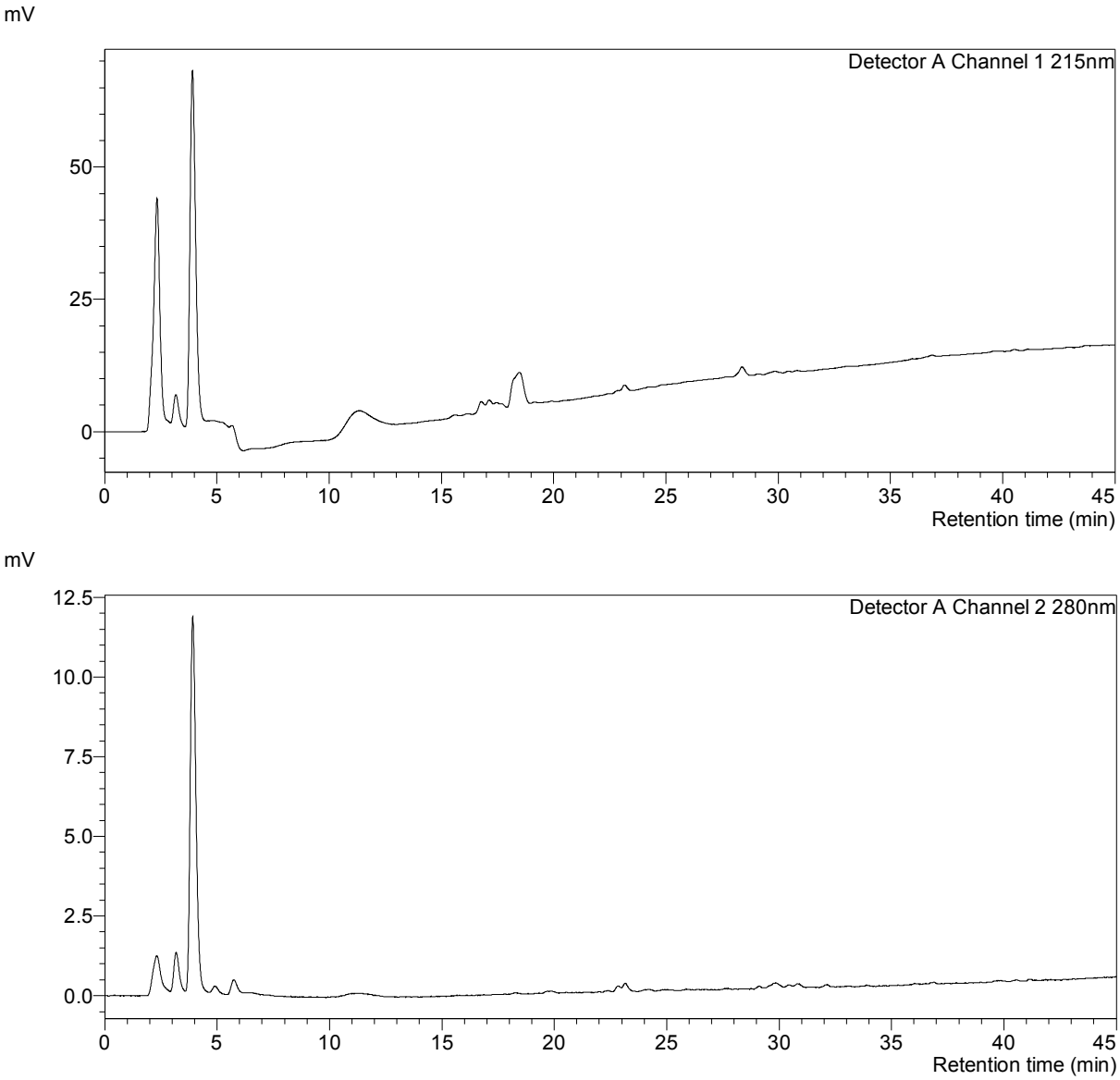

Figure A1: Analytical RP-HPLC chromatogram of fraction A with absorbance detection at 215 and 280 nm

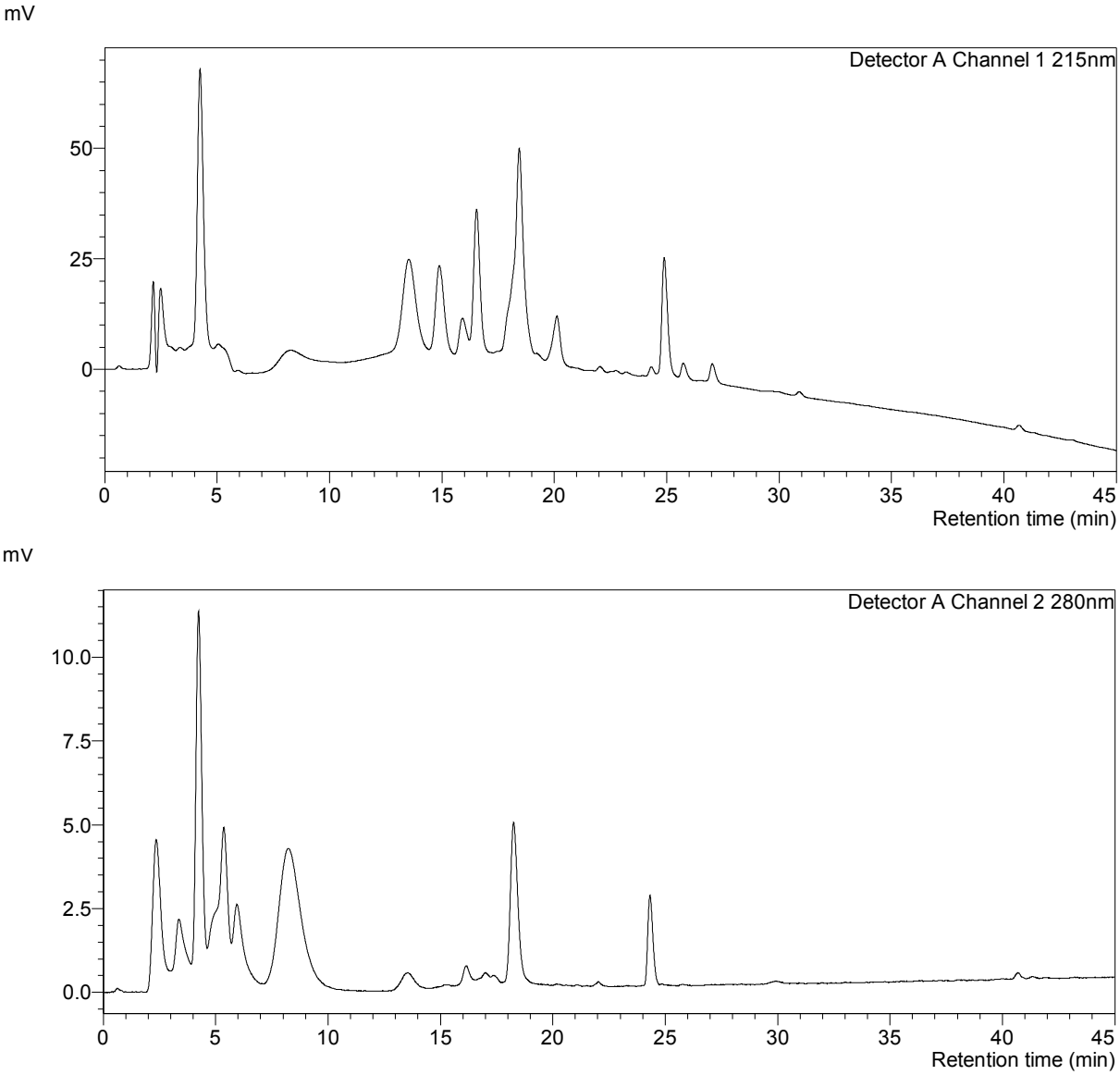

Figure A2: Analytical RP-HPLC chromatogram of fraction B with absorbance detection at 215 and 280 nm

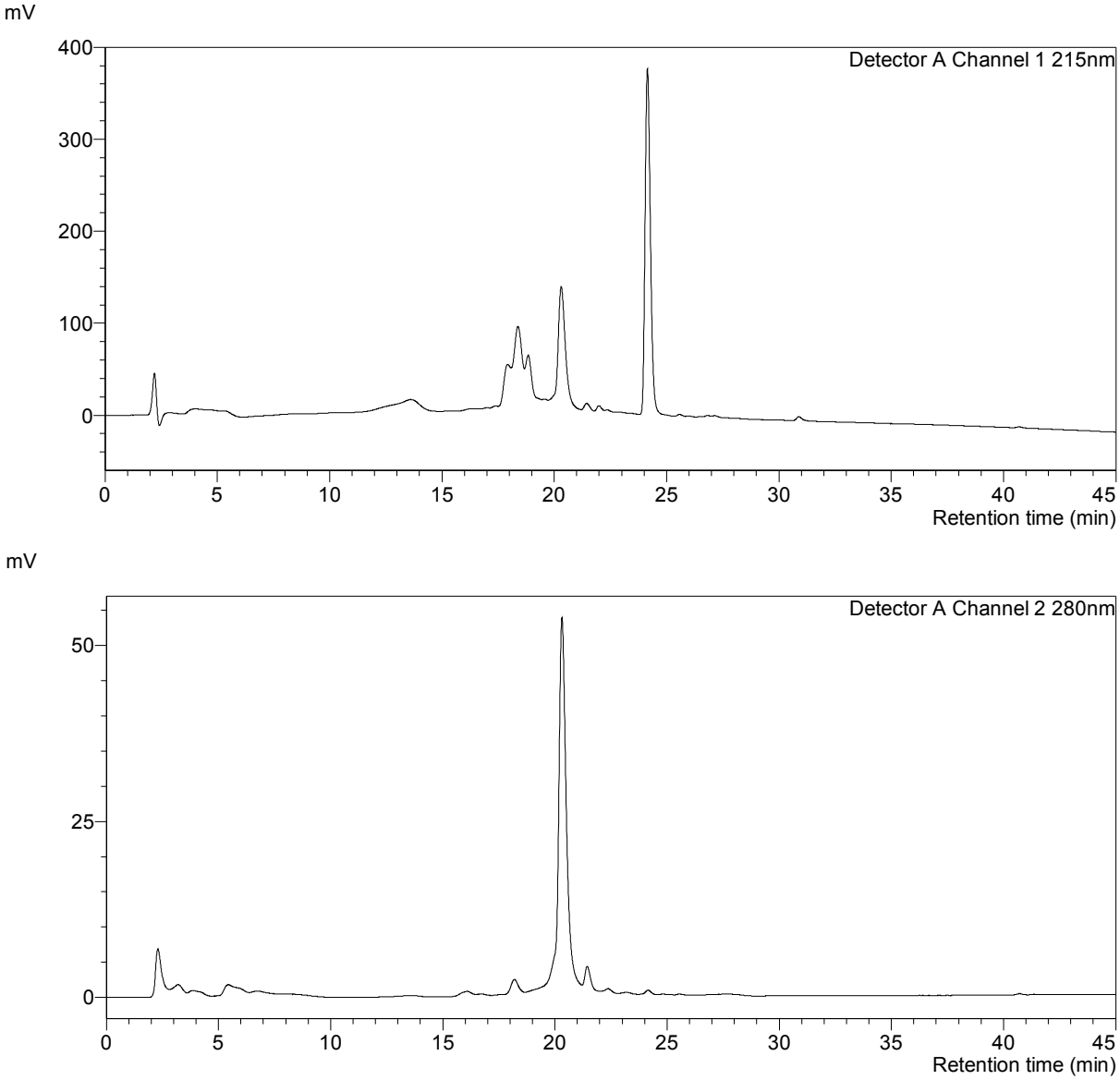

Figure A3: Analytical RP-HPLC chromatogram of fraction C with absorbance detection at 215 and 280 nm

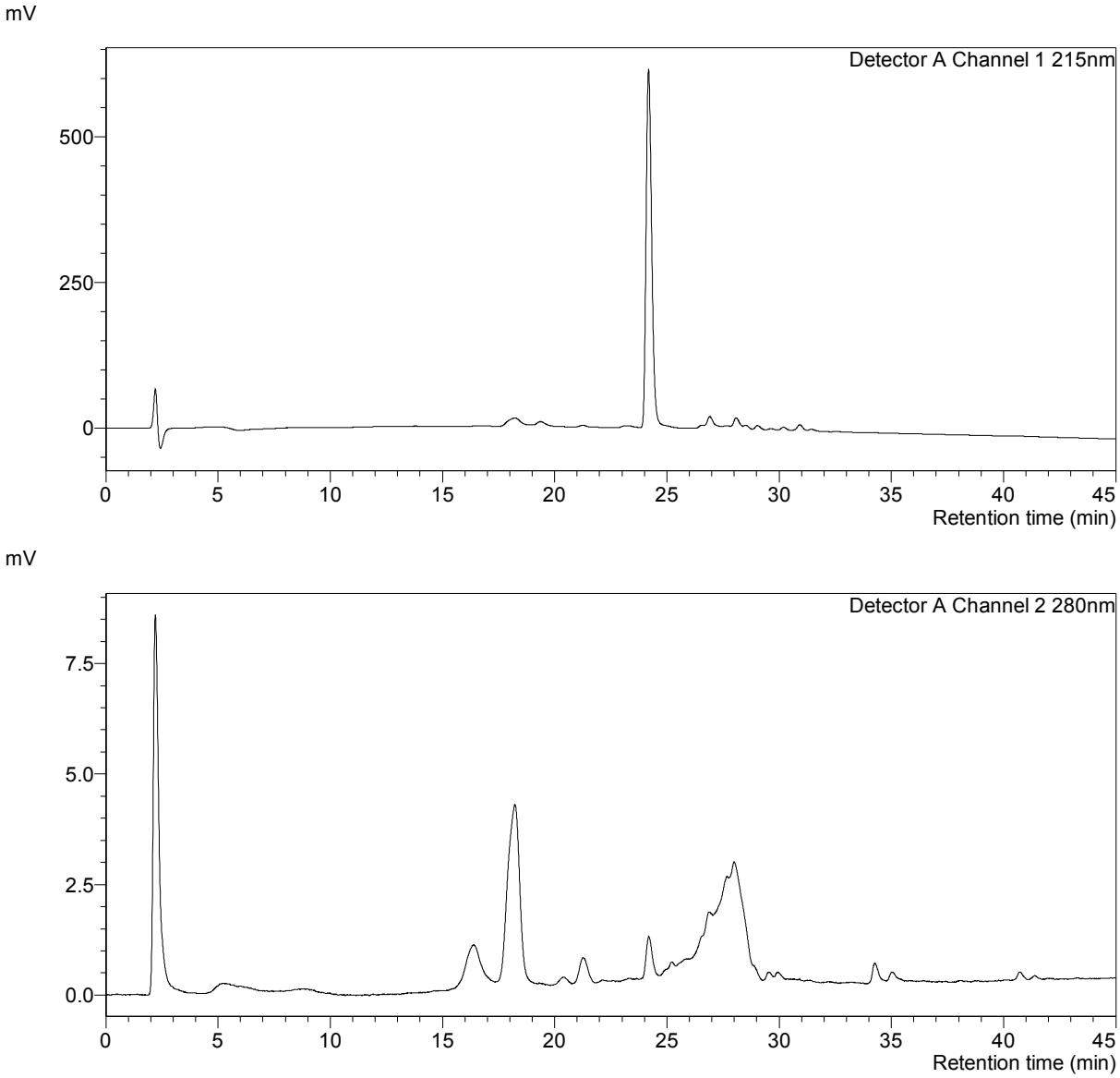

Figure A4: Analytical RP-HPLC chromatogram of fraction D with absorbance detection at 215 and 280 nm

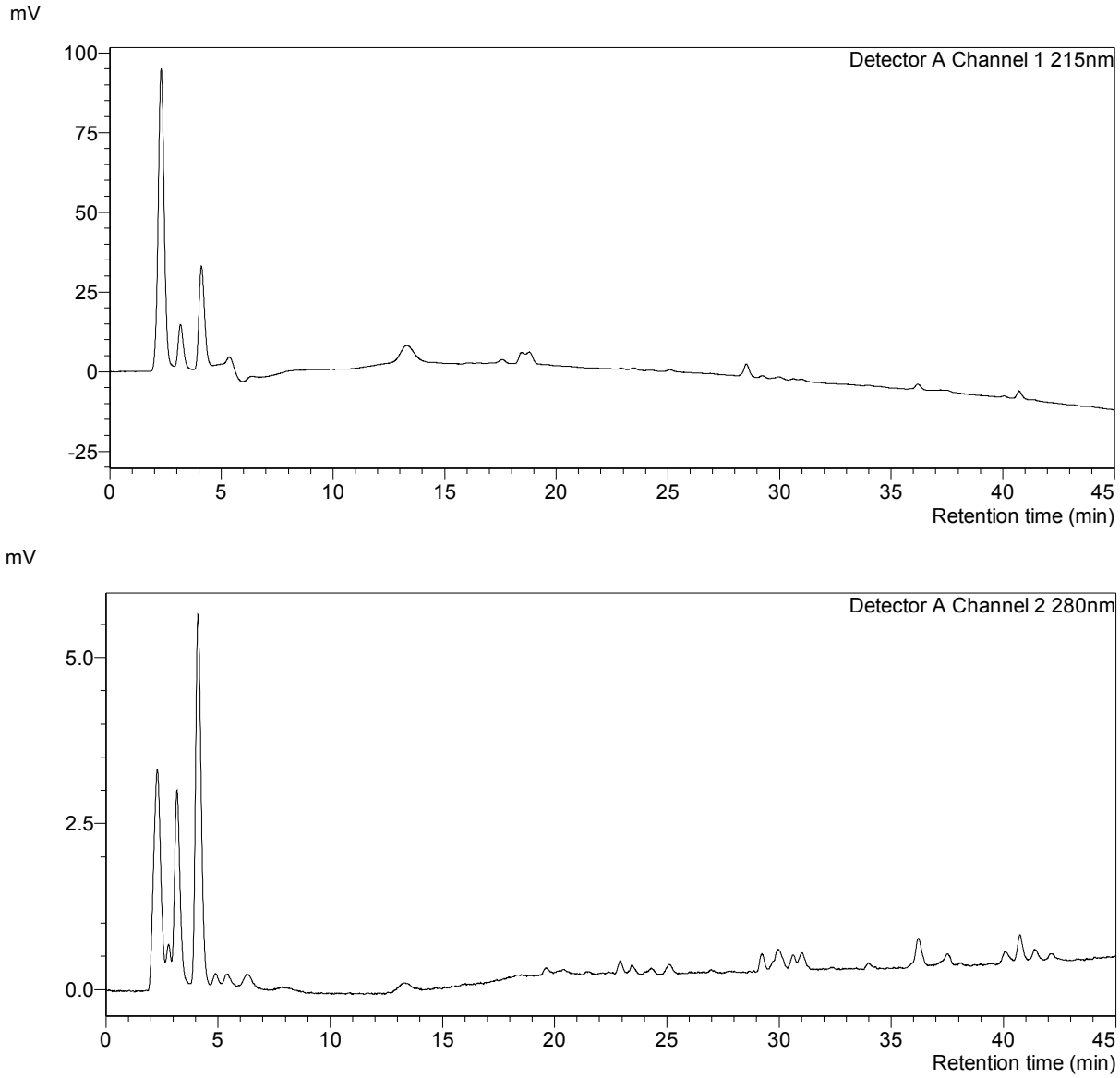

Figure A5: Analytical RP-HPLC chromatogram of fraction E with absorbance detection at 215 and 280 nm

7.2 LC/MS of fraction E

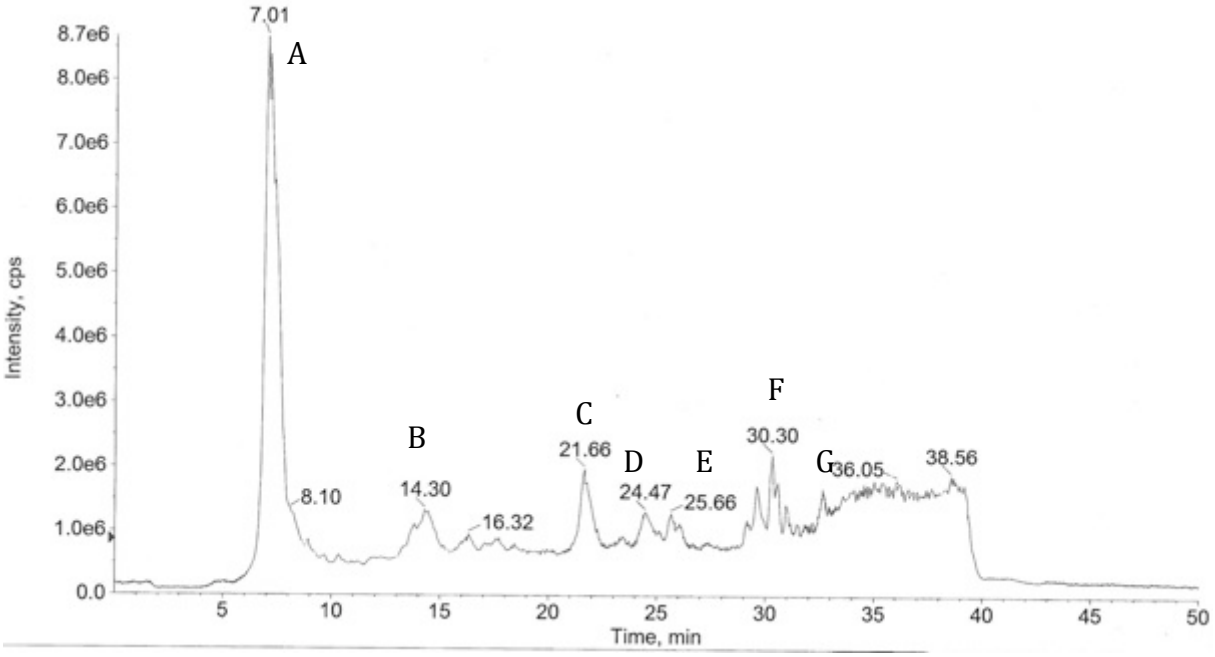

Figure A6: RP-HPLC chromatogram from the LC/MS analysis of fraction E

7.3 ESI-MS

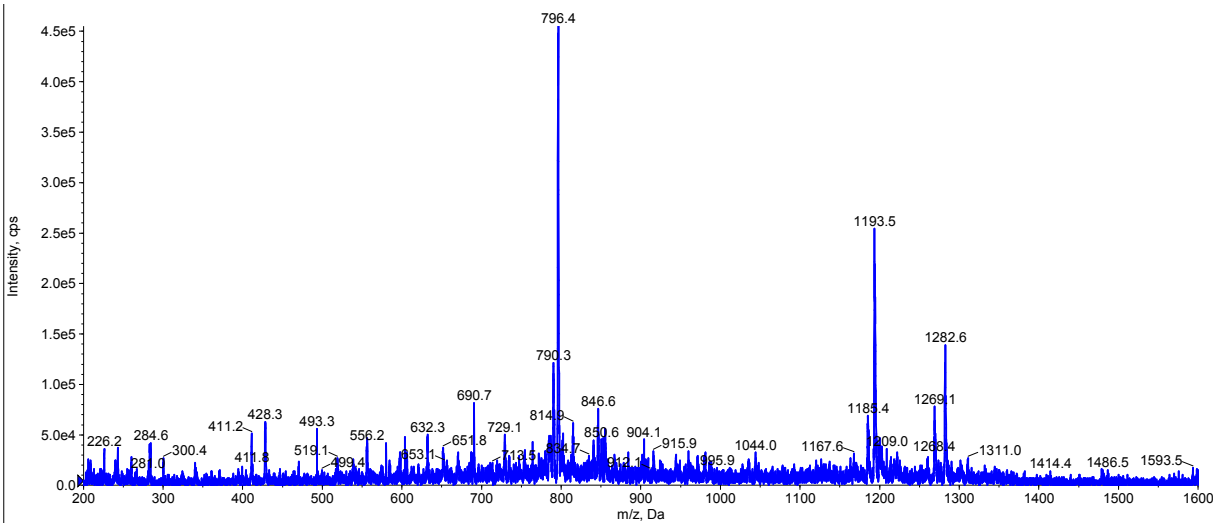

Figure A7: ESI-MS of Name2 N-terminus peptide crude

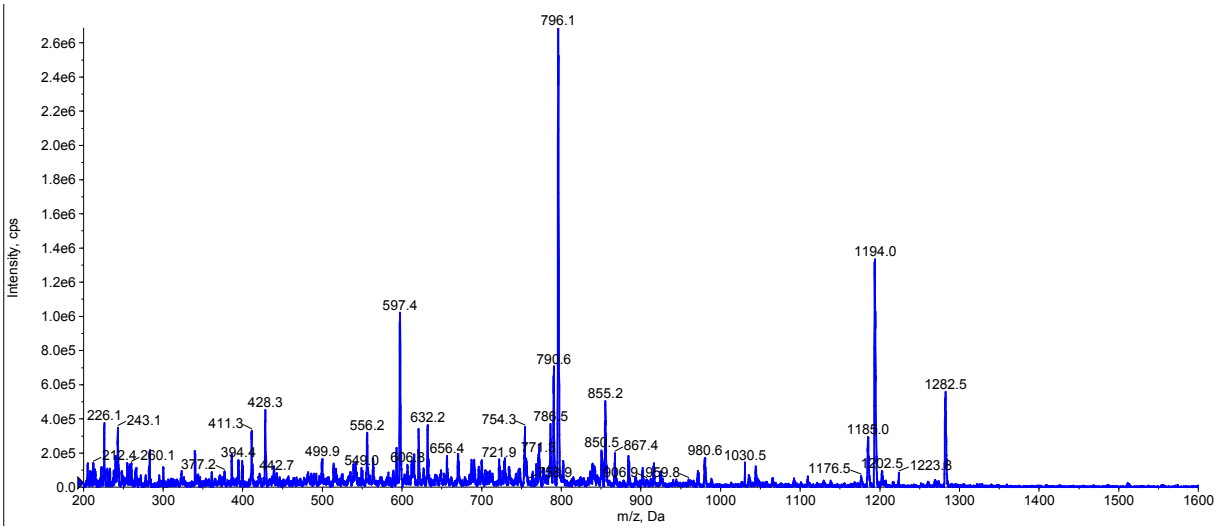

Figure A8: ESI-MS of purified Name2 N-terminus

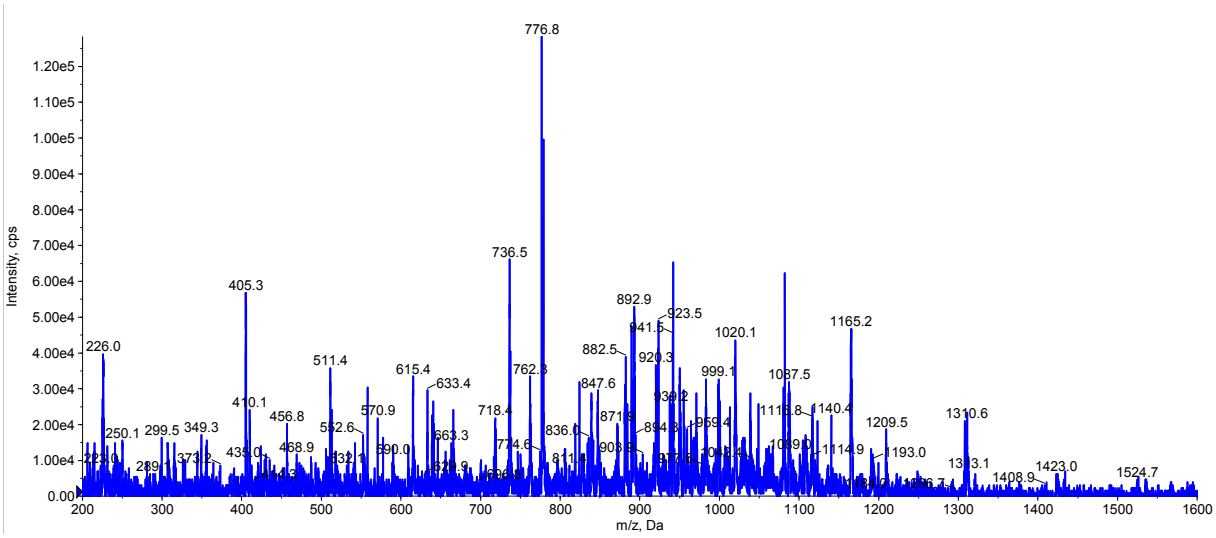

Figure A9: ESI-MS of Name2 C-terminus peptide crude

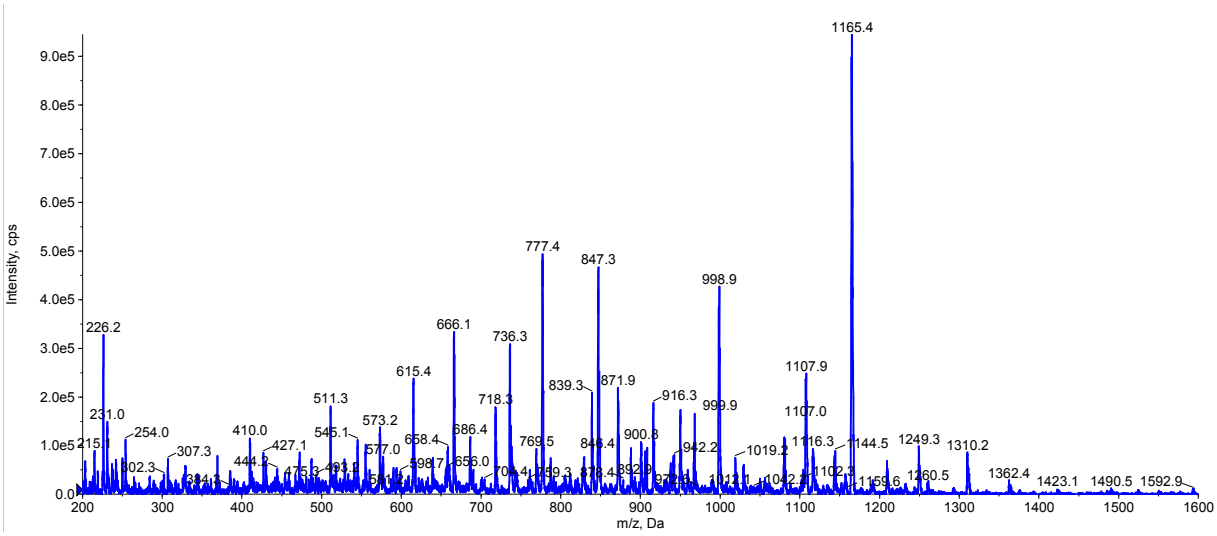

Figure A10: ESI-MS of purified Name2 C-terminus

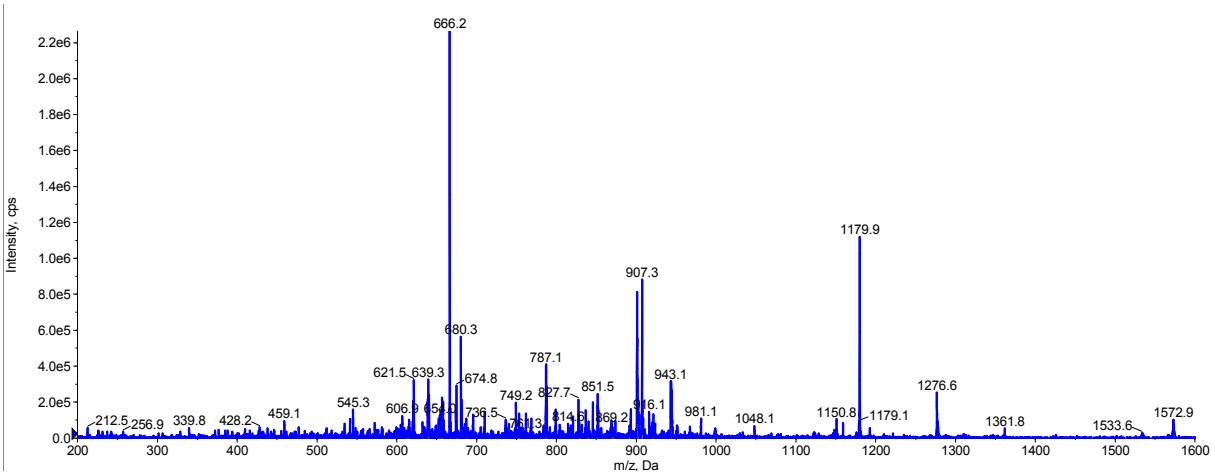

Figure A11: ESI-MS that confirmed the presence of the correct ligation product – 1. ligation attempt

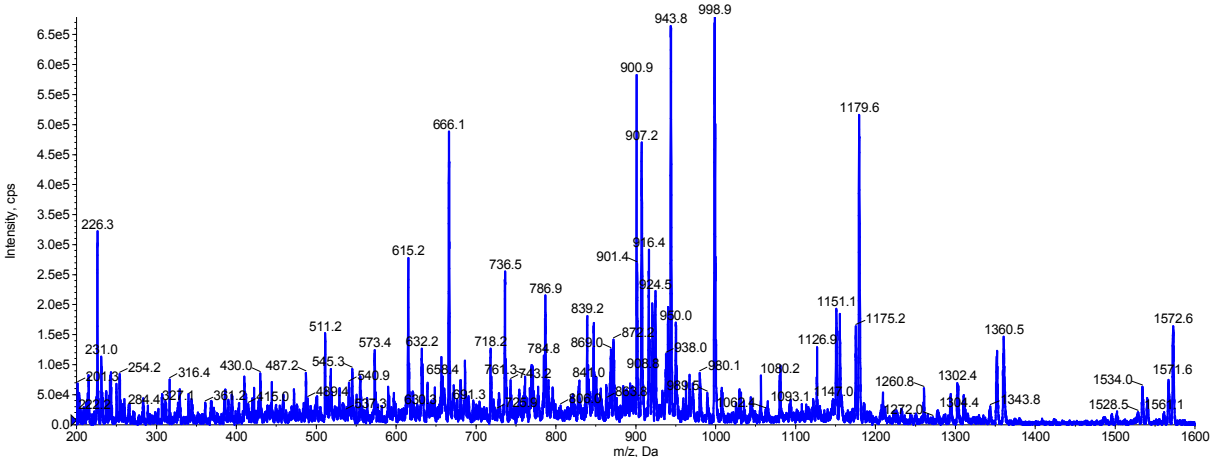

Figure A12: ESI-MS of the fraction containing Name2 – 2. ligation attempt

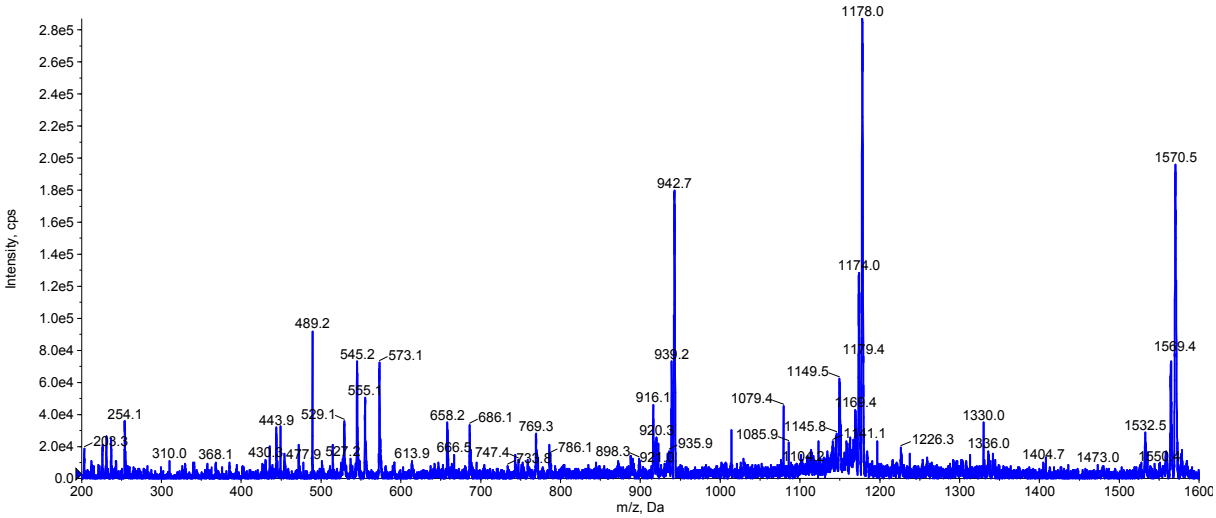

Figure A13: ESI-MS of oxidised Name2

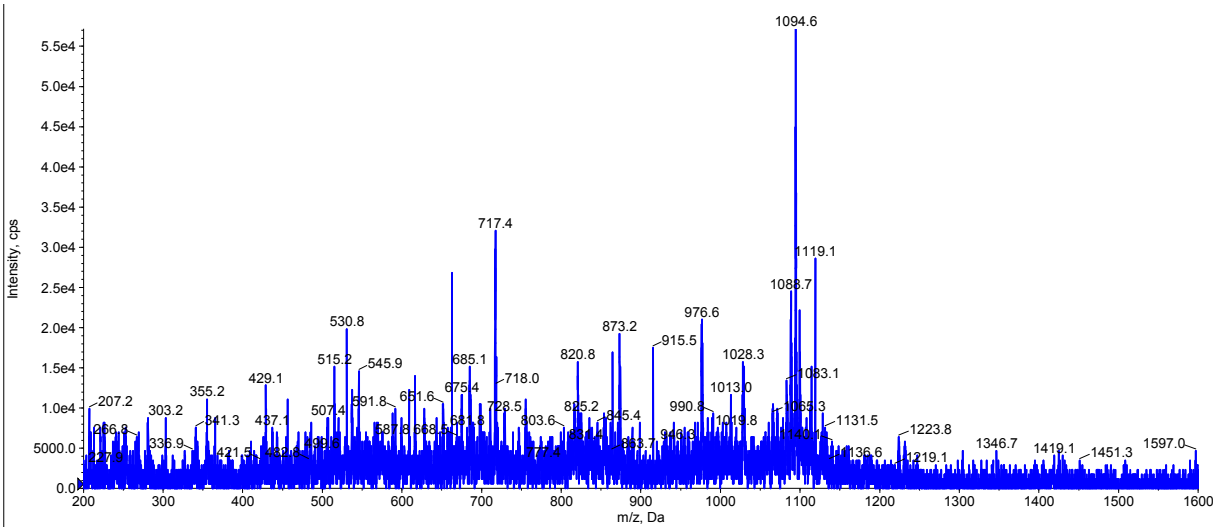

Figure A14: ESI-MS of crude Acan1 N-terminus hydrazide

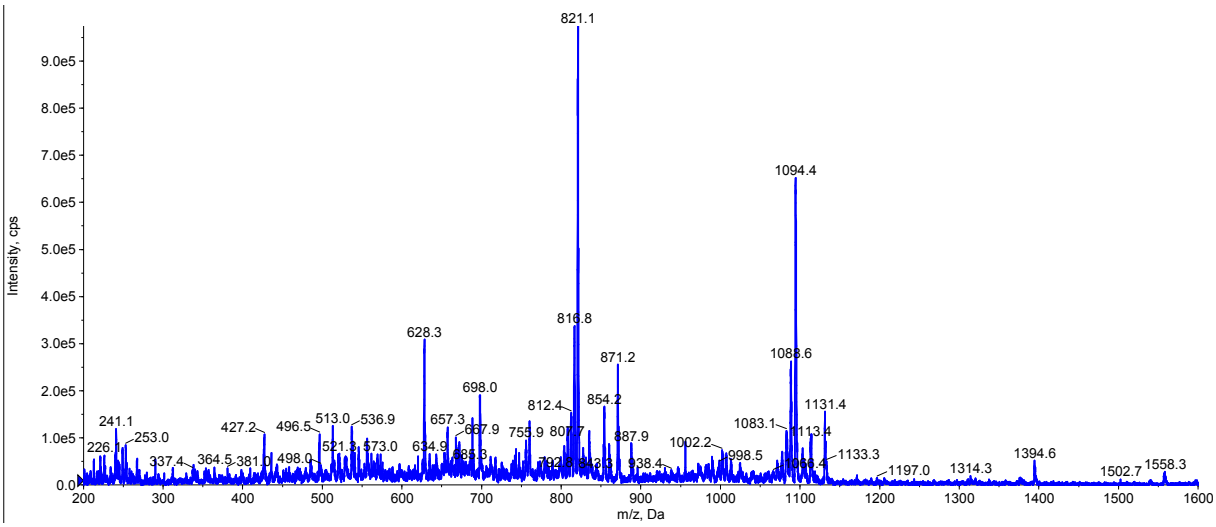

Figure A15: ESI-MS of purified Acan1 N-terminus peptide hydrazide

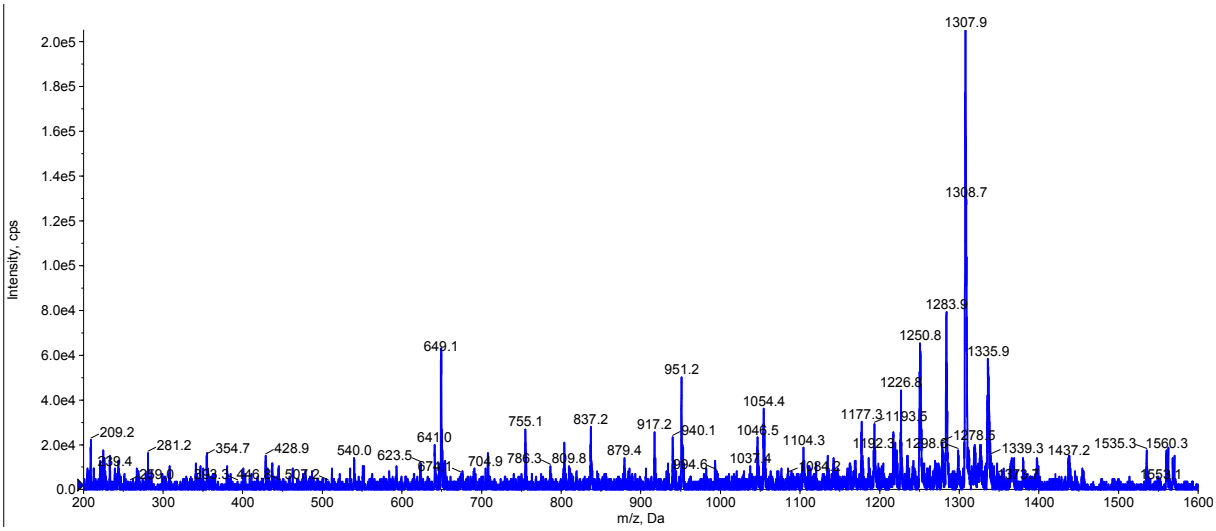

Figure A16: ESI-MS of Acan1 C-terminus peptide crude

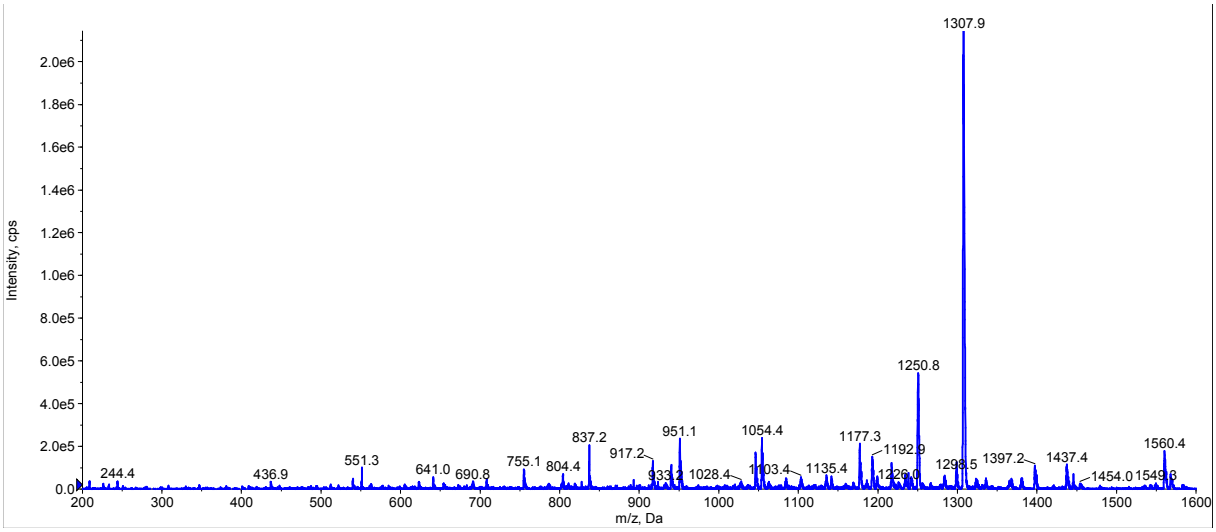

Figure A17: ESI-MS of purified Acan1 C-terminus

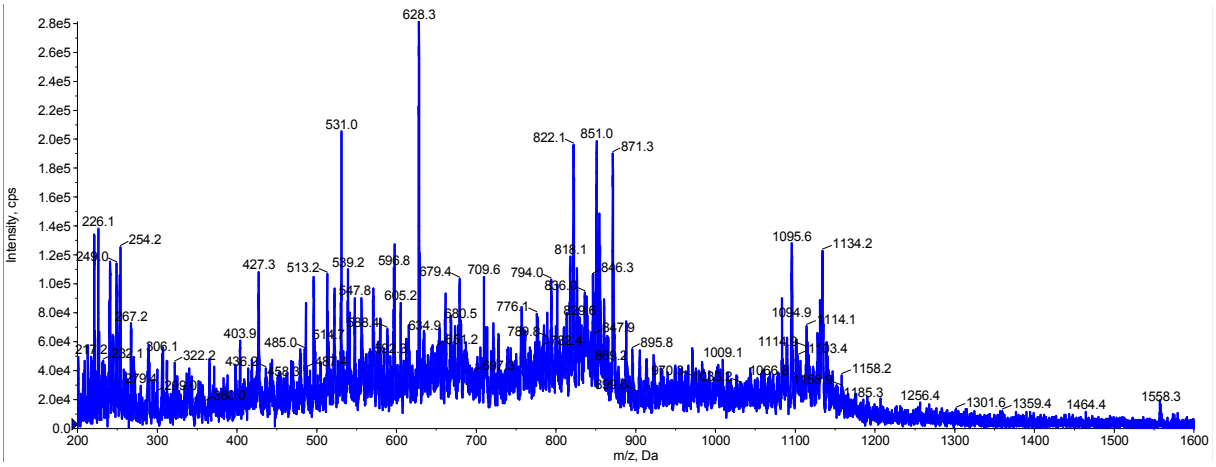

Figure A18: ESI-MS of a test cleavage of Acan1 N-terminus right after the synthesis

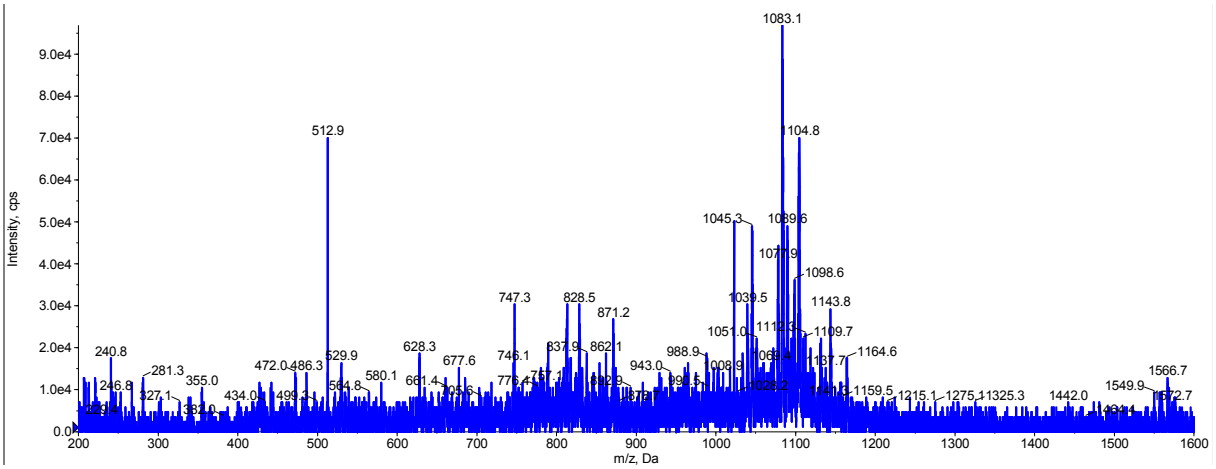

Figure A19: ESI-MS of the peptide crude after activation and cleavage of the first batch of Acan1 N-terminus peptidyl resin

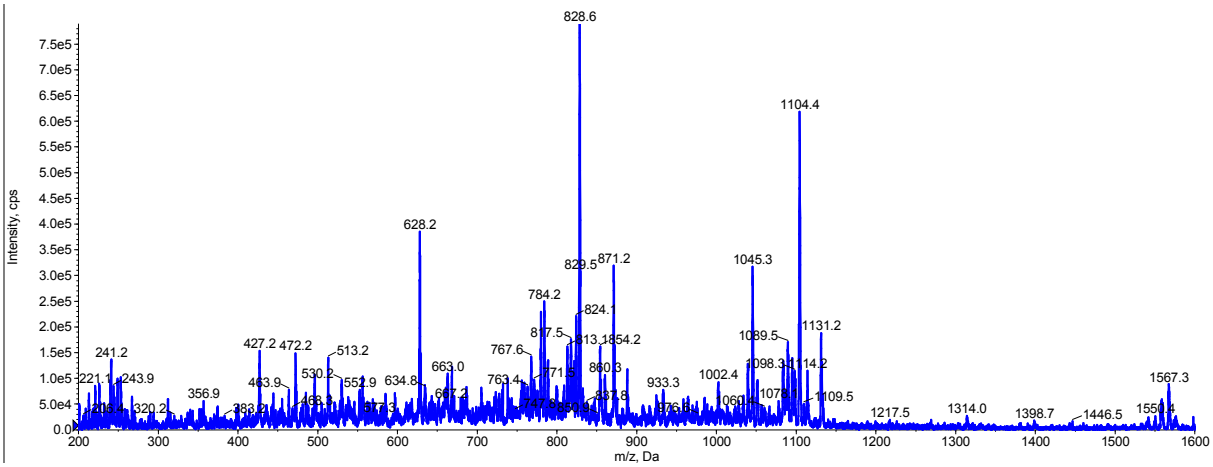

Figure A20: ESI-MS of a fraction containing the by-product peptide-Nbz (1. batch)

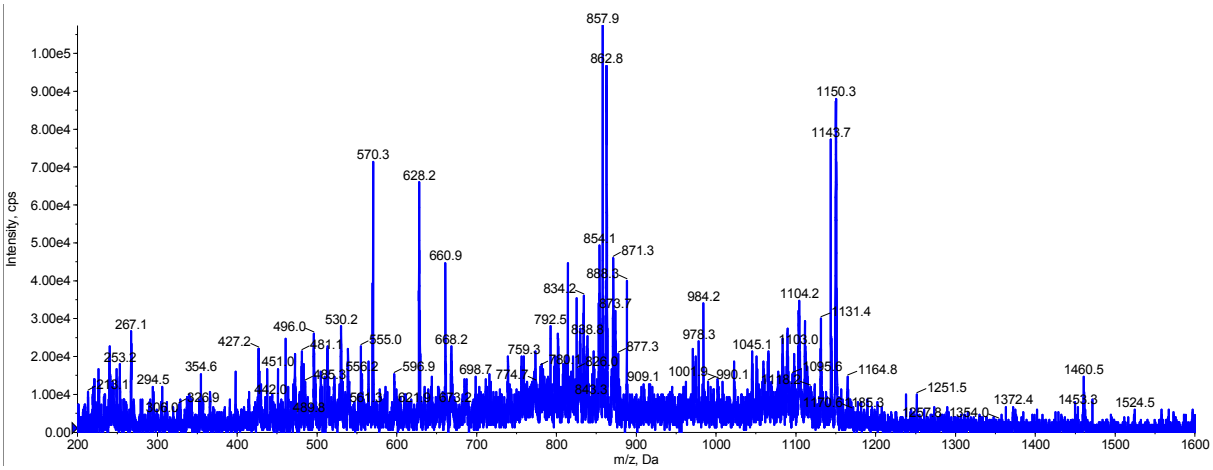

Figure A21: ESI-MS of the fraction containing the correct Acan1 N-terminus peptide-Nbz (1. batch)

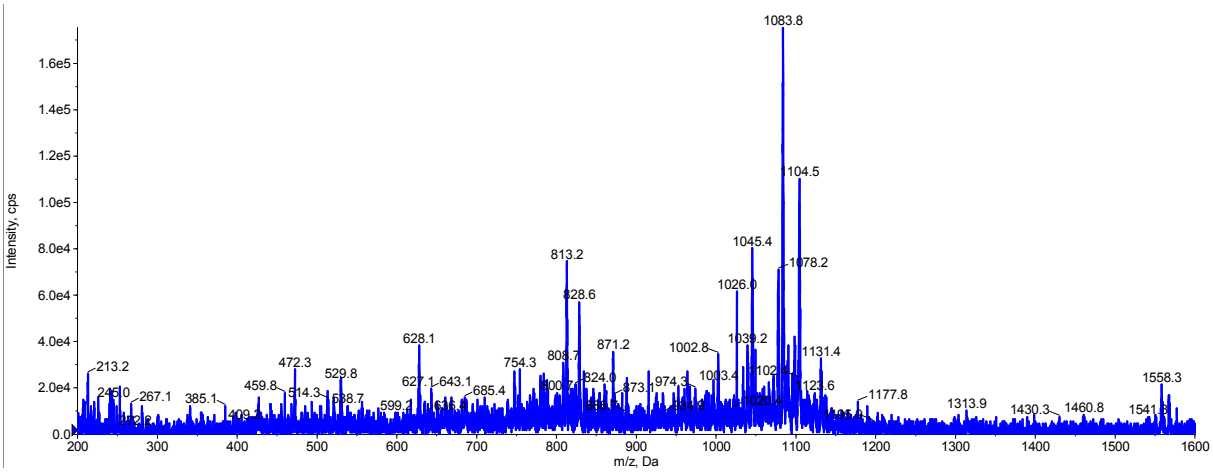

Figure A22: ESI-MS of the peptide crude after activation and cleavage of the second batch of Acan1 N-terminus peptidyl resin

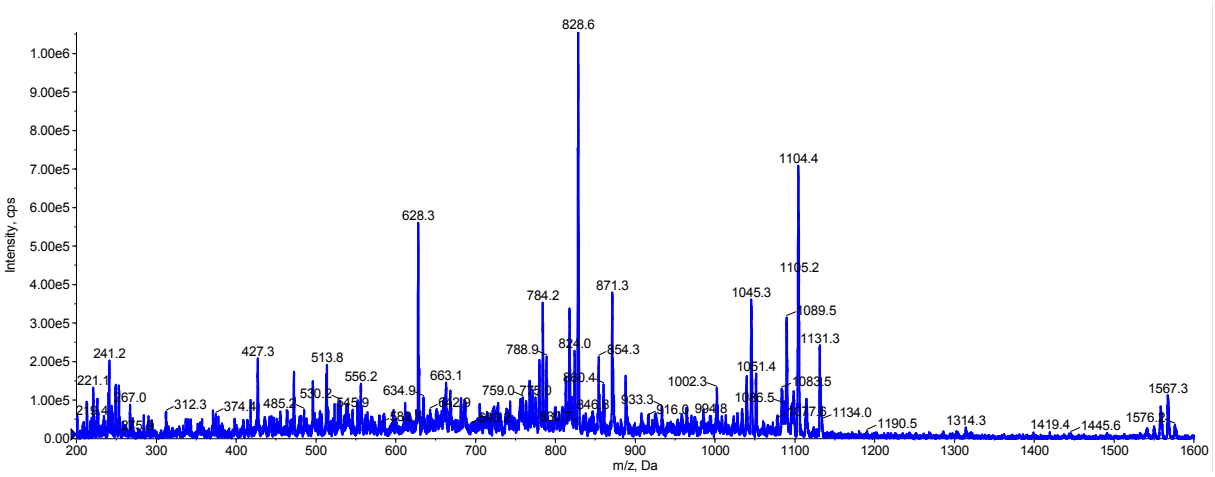

Figure A23: ESI-MS of a fraction containing the by-product peptide-Nbz (2. Batch)

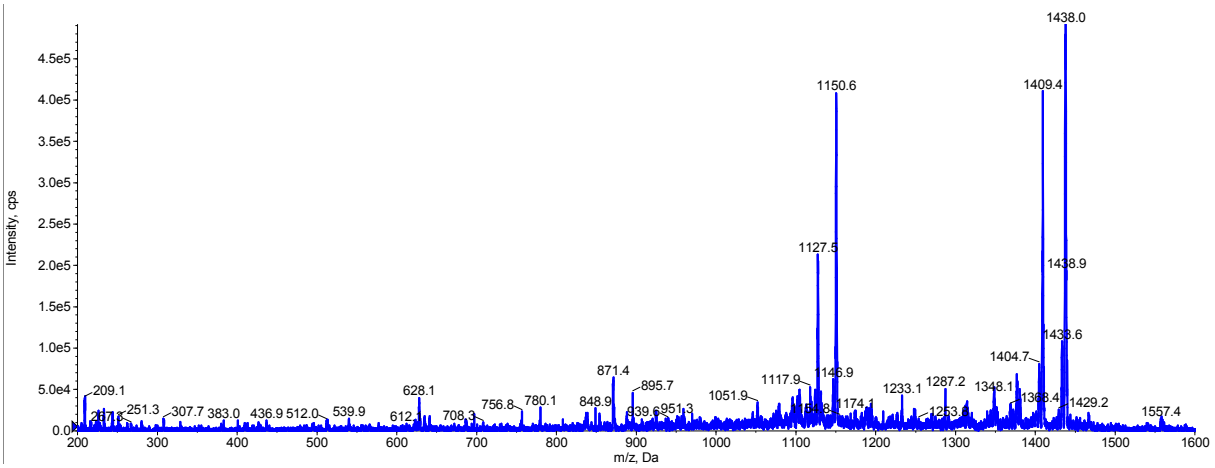

Figure A24: ESI-MS of fraction 37

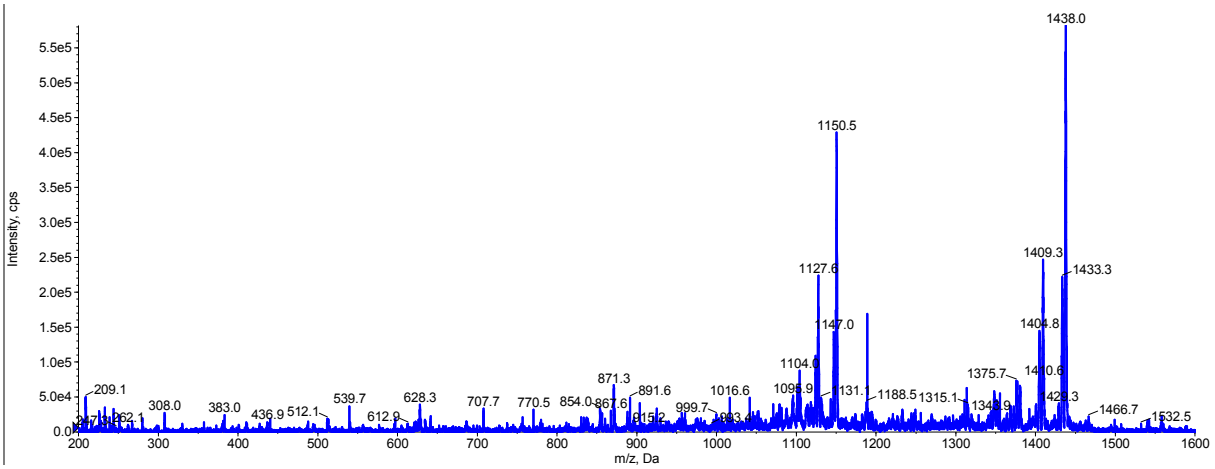

Figure A25: ESI-MS of fraction 38

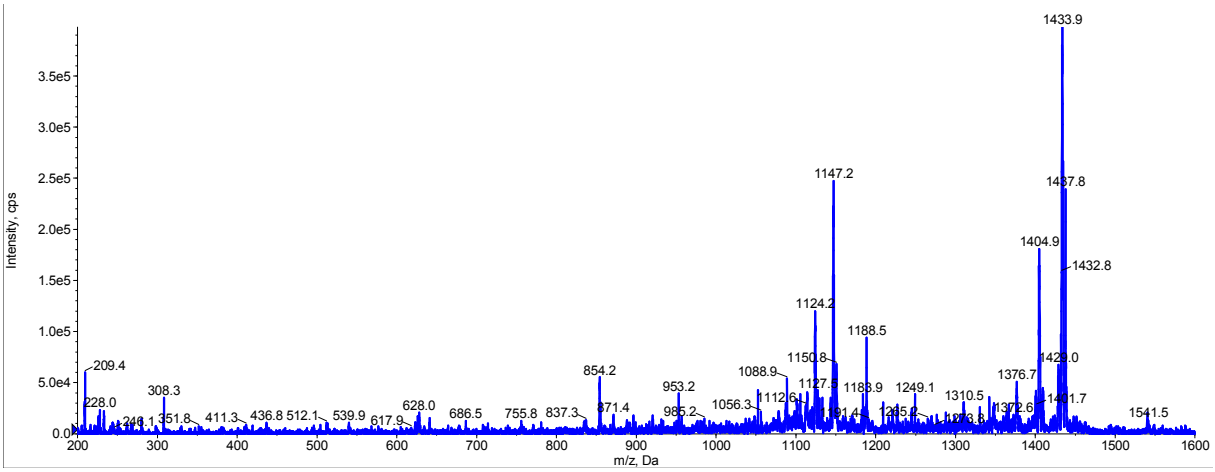

Figure A26: ESI-MS of fraction 39

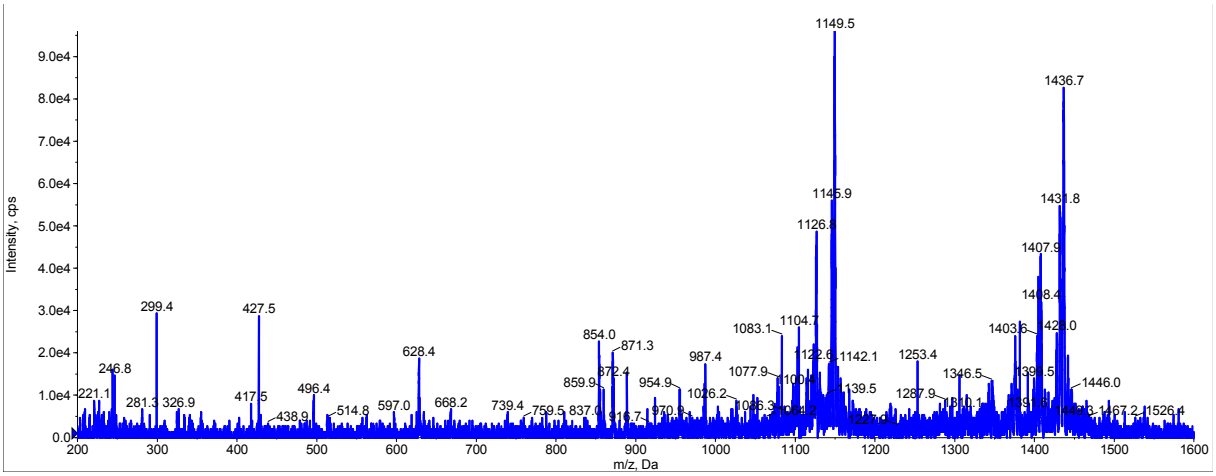

Figure A27: ESI-MS of fraction 9 from the oxidation of Acan1*

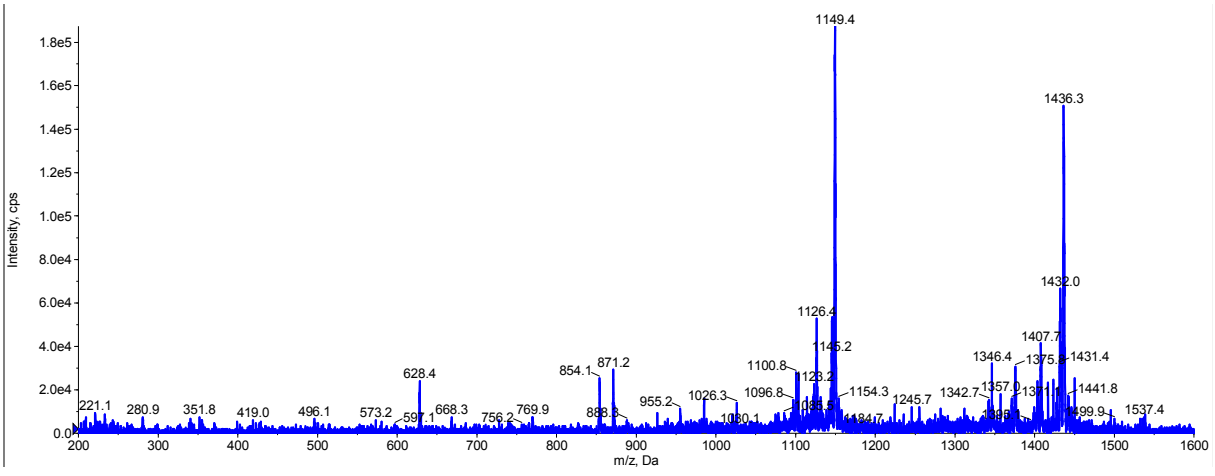

Figure A28: ESI-MS of fraction 10 from the oxidation of Acan1*

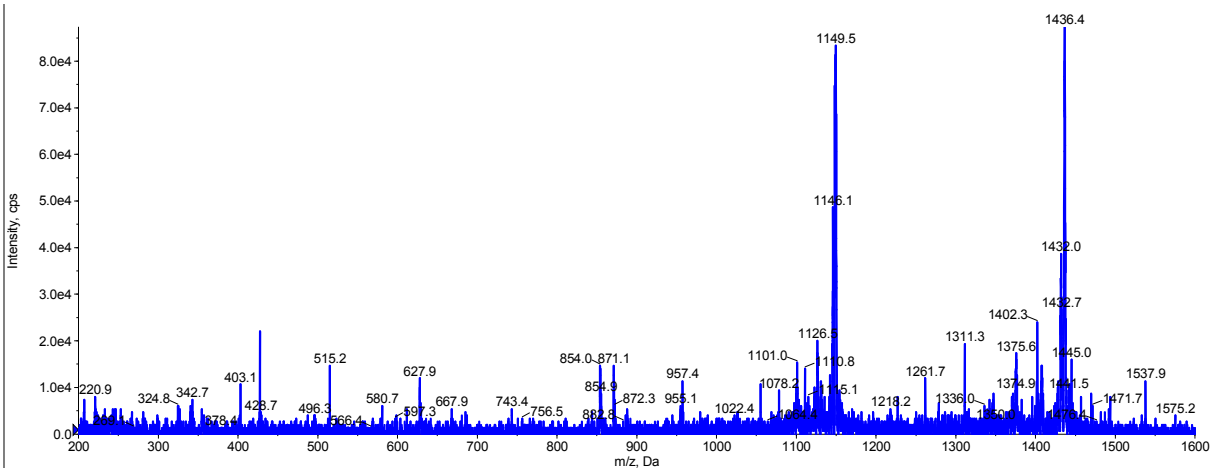

Figure A29: ESI-MS of fraction 11 from the oxidation of Acan1*